Synthesis of Pyrido[2,1-α]isoindoles *via* Palladium-Catalyzed Carbonylation and 1,3-Dipolar Cycloaddition with Benzyne

Karina S. Wong

A thesis submitted to McGill University in partial fulfillment of the requirements of the degree of Master of Science

Department of Chemistry

McGill University

Montreal, Quebec, Canada

H3A 0B8

December 2024

Abstract

Nitrogen-containing heterocycles are important structures in organic chemistry. This feature is driven in part by their broad presence in pharmaceuticals. The majority of therapeutic drugs currently in the market contains at least one nitrogen-heterocycle. An example of these are fused ring nitrogen heterocycles. These products are commonly synthesized through intramolecular cyclization or annulation reactions, and as such face challenges related to the build up of the appropriately substituted precursor for cyclization, which can limit their accessibility. One avenue to address this issue is to employ 1,3-dipolar cycloaddition reactions with benzyne. Chapter 1 provides a brief overview of routes to prepare benzyne and its usefulness in 1,3-dipolar cycloadditions.

Chapter 2 describes our development of a new method to synthesize pyrido[2,1-α]isoindoles, a 6:5:6 fused heterocyclic ring system, *via* the palladium-catalyzed carbonylative coupling of imines, 2-bromopyridines, and *o*-trimethylsilylaryl triflates. Mechanistic insights suggest the reaction proceeds *via* the *in situ* formation of 2-pyridyl acyl chloride electrophiles, which react with the imines to produce mesoionic pyridine-based 1,3-dipoles. Subsequent cycloaddition of *in situ* generated arynes results in the formation of pyrido[2,1-α]isoindoles. Overall, this transformation offers a one-pot, mild, and modular approach to synthesize highly functionalized pyrido[2,1-α]isoindoles.

Résumé

Les hétérocycles azotés jouent un rôle central dans l'industrie pharmaceutique et se retrouvent dans la majorité des médicaments thérapeutiques actuellement disponibles. Parmi ceux-ci, on y retrouve les hétérocycles azotés à cycles fusionnés. Ils sont habituellement synthétisés par cyclisations intramoléculaires ou réactions d'annulation, des méthodes à usage limité puisque la synthèse des précurseurs est souvent fastidieuse et requiert plusieurs étapes de préparation. Une approche alternative pour surmonter ces défis réside dans l'utilisation des cycloadditions 1,3-dipolaires avec le benzyne. Le premier chapitre présente une introduction concise sur les méthodes de génération du benzyne et de son utilité dans les cycloadditions 1,3-dipolaires.

Le deuxième chapitre démontre le développement d'une nouvelle méthode de synthèse de pyrido[2,1-α]isoindoles, un système de cycles fusionnés (6:5:6), réalisée *via* un couplage carbonylatif catalysé au palladium entre des imines, des 2-bromopyridines, et des triflates de *o*-triméthylsilylaryles. L'analyse mécanistique suggère que la réaction passe par la formation *in situ* d'électrophiles de type chlorure de 2-pyridylacyle, qui réagissent ensuite avec les imines pour produire des 1,3-dipôles mésoioniques à base de pyridine. La cycloaddition qui s'ensuit avec les intermédiaires de benzyne générés *in situ* permet la formation de pyrido[2,1-α]isoindoles. Cette transformation constitue ainsi une approche en une étape qui est modulaire pour la synthèse de pyrido[2,1-α]isoindoles hautement fonctionnalisés.

Acknowledgements

I would like to thank my supervisor, Prof. Bruce Arndtsen, for his invaluable guidance throughout the writing of this thesis and my manuscript, and for his insightful advice during group meetings, which has greatly contributed to my development of skills that I will carry forward in my career.

I am also thankful to my committee members, Prof. Jean-Philip Lumb and Prof. Youla Tsantrizos, as well as my reviewer, Prof. Scott Bohle for their constructive feedback. Additionally, I extend my appreciation to Dr. Alexander Wahba, Dr. Nadim Saadeh, and Dr. Hatem Titi for their assistance with product characterizations.

I am especially grateful to my colleagues, who have also become cherished friends: Cuihan Zhou, Meijing Jiang, Ming Tam, Anthony Labelle, José Zgheib, Yiyang Ma, and Yiram Kim. Thank you for making my time here both memorable and enjoyable, for supporting me academically and personally, and for sharing countless insightful research discussions over tea.

I owe my deepest thanks to my parents for their love, support, and encouragement, and to my rabbit and "research assistant," Rudy, whose presence has been a source of serotonin and peace throughout this journey.

Lastly, I dedicate this thesis to my late maternal grandfather who exemplified stoicism, hard work, and perseverance.

Table of Contents

Abstract **2**
Résumé **3**
Acknowledgements **4**
Table of Contents **5**
List of Schemes **7**
List of Figures **9**
List of Tables **9**
List of Abbreviations **10**
Contributions of Co-Authors **13**
Chapter 1 – Introduction **14**
1.1 Perspective 14
1.2 Benzyne Generation 17
1.3 Benzyne 1,3-Dipolar Cycloadditions in Heterocycle Synthesis 20
1.3.1 Cycloaddition of Benzyne with Cyclic 1,3-Dipoles 22
1.3.1.1 Reactions with Sydnones (1,2,3-Oxadiazolium-5-Olates) *22*
1.3.1.2 Reactions with 1,2,4-Triazolium-3-Olates *28*
1.3.1.3 Reactions with 1,2,3,4-Tetrazolium-5-Thiolates *30*
1.3.1.4 Reactions with Münchnones (1,3-Oxazolium-5-Olates) *32*
1.3.1.5 Reactions with Thioisomünchnones (1,3-Thiazolium-4-Olates) *35*
1.3.1.6 Reactions with 1,3-Dithiolium-4-Olates *39*
1.4 Overview of the Thesis 41
1.5 References 42
Chapter 2 – Design of a Modular, Palladium-Catalyzed Carbonylative Synthesis of Pyrido[2,1-α]isoindoles *via* Benzyne 1,3-Dipolar Cycloaddition **54**
2.1 Preface 54
2.2 Introduction 54

2.3 Results and Discussion 56
2.4 Conclusions 62
2.5 Supporting Information 63
2.5.1 General Considerations 63
2.5.2 Supplementary Tables and Figures 64
2.5.3 General Experimental Procedures 65
2.5.3.1 Reaction Development for a One-Step Synthesis of Pyrido[2,1-α]isoindoles (Table 2.3.1, entries 1-7 and 10 and Table 2.5.1) *65*
2.5.3.2 Reaction Development for a One-Pot Synthesis of Pyrido[2,1-α]isoindoles (Table 2.3.1, entries 8-9). *66*
2.5.3.3 Typical Procedure for the Synthesis of Pyrido[2,1-α]isoindoles (Tables 2.3.2). . *67*
2.5.3.4 Typical Isolation of Pyrido[2,1-α]isoindoles Under an Inert Atmosphere *68*
2.5.4 Characterization Data of Pyrido[2,1-α]isoindoles (Table 2.3.2) 69
2.5.5 Crystallographic Data 78
2.5.6 References 84
Chapter 3 – Conclusions 89
Appendix I. NMR Spectra of Pyrido[2,1-α]isoindoles in Chapter 2 90

List of Schemes

Scheme 1.1.1. Cycloaddition of acyclic and mesoionic 1,3-dipoles with dipolarophiles to form neutral 5-membered heterocycles. 14
Scheme 1.1.2. Classification of 1,3-dipolar cycloadditions based on HOMO-LUMO interactions between the 1,3-dipole and dipolarophile. 15
Scheme 1.1.3. FDA-approved small drug molecules with nitrogen-based heterocycles. 16
Scheme 1.1.4. Examples of 1,3-dipolar cycloaddition with benzyne with acyclic (left) and mesoionic (right) dipoles to form fused heterocyclic systems. 17
Scheme 1.2.1. Earliest evidence of aryne intermediates *via* dehydrohalogenation of haloarenes. 18
Scheme 1.2.2. Isotope-labelling experiment confirming the existence of a benzyne intermediate. 18
Scheme 1.2.3. Benzyne generation *via* metal-halogen exchange-elimination. 19
Scheme 1.2.4. Benzyne generation *via* thermal decomposition. 19
Scheme 1.2.5. Benzyne generation *via* oxidation. 19
Scheme 1.2.6. Benzyne generation *via* fluoride-induced 1,2-elimination. 20
Scheme 1.3.1. The first reported use of an aryne as a dipolarophile in the 1,3-dipolar cycloaddition of benzyne with diazoacetic ester. 21
Scheme 1.3.2. 1,3-Dipolar cycloaddition of benzyne with acyclic 1,3-dipoles to form various heterocycles. 21
Scheme 1.3.3. Conventional synthesis of Sydnones. 22
Scheme 1.3.4. The first example of a 1,3-dipolar cycloaddition of benzyne and a Sydnone. 22
Scheme 1.3.5. Synthesis of 2,3-disubstituted indazoles from a) 1-aminobenzotriazole and b) *o*-trimethylsilylaryl triflates. 23
Scheme 1.3.6. Low regioselectivity in cycloaddition of unsymmetrical benzynes with Sydnones. 24
Scheme 1.3.7. Thiazolidine-based Sydnone functioning as a masked 1,3-dipole for subsequent [3+2] cycloaddition. 24
Scheme 1.3.8. Regioselective, silyl group controlled benzyne cycloaddition with a 3,4-disubstituted Sydnone. 25
Scheme 1.3.9. Cycloaddition of polyaromatic Sydnones with arynes to form pyrazole-containing helicenes. 26

Scheme 1.3.10. Sydnone-benzyne cycloaddition to form Niraparib. 27
Scheme 1.3.11. The first synthetic methods to prepare substituted 1,2,4-triazolium-3-olates. 28
Scheme 1.3.12. The synthesis of 1,4-diphenyl-1,2,4-triazol-3-one *via* the 1,3-dipolar cycloaddition of *N*-phenylsydnone with phenyl isocyanate. 29
Scheme 1.3.13. Synthesis of 1,2,4-triazolium-3-olates from other mesoionic 1,3-dipoles. 29
Scheme 1.3.14. 1,3-Dipolar cycloaddition of 1,4-diphenyl-1,2,4-triazolium-3-olate with different benzyne precursors..... 30
Scheme 1.3.15. 1,3-Dipolar cycloaddition of electron-rich amine-substituted 1,2,4-triazolium-3-olate with benzyne. 30
Scheme 1.3.16. Synthesis of 2,3-diaryltetrazolium-5-thiolates from diarylthiocarbazones. 31
Scheme 1.3.17. 1,3-Dipolar cycloaddition of dipolarophiles with Type B mesoionic rings. 31
Scheme 1.3.18. 1,3-Dipolar cycloaddition of 1,2,3,4-tetrazolium-5-thiolates with benzyne to form 2-phenylazobenzothiazole..... 32
Scheme 1.3.19. Advances in synthetic methods to form Münchnones. 33
Scheme 1.3.20. First example of the synthesis of isoindoles and epiminoanthracenes through Münchnone [3+2] cycloaddition with 1-aminobenzotriazole. 33
Scheme 1.3.21. Münchnone-benzyne [3+2] cycloaddition to form isoindoles and epiminoanthracenes..... 34
Scheme 1.3.22. Münchnone-benzyne [3+2] cycloaddition to selectively form isoindoles. 35
Scheme 1.3.23. Synthesis of thioisomünchnones and polycyclic derivatives. 36
Scheme 1.3.24. Effect of 5-substituent on the regiospecificity of the 1,3-dipolar cycloaddition thioisomünchnones with DMAD. 37
Scheme 1.3.25. Effect of 3-substituent on the regiospecificity of the 1,3-cycloaddition thioisomünchnones with methyl propiolate. 38
Scheme 1.3.26. 1,3-Dipolar cycloaddition of thioisomünchnone with benzyne under thermal and photochemical conditions. 39
Scheme 1.3.27. Synthetic methods to form 1,3-dithiolium-4-olates. 39
Scheme 1.3.28. Synthesis of diphenylbenzo[*c*]thiophen *via* benzyne 1,3-dipolar cycloaddition with a 1,3-dithiolium-4-olate. 40
Scheme 1.3.29. Formation of polyaromatic benzo[*c*]thiophens from 1,3-dipolar cycloaddition of *o*-trimethylsilylaryl triflates and 1,3-dithiolium-4-olates. 40

Scheme 2.5.1. One-step synthesis of pyrido[2,1-α]isoindole 2a with *in situ* formed benzyne..... 65
Scheme 2.5.2. Two-step synthesis of pyrido[2,1-α]isoindole 2a. 67

List of Figures

Figure 2.2.1. Carbonylative formation of 1,3-dipoles and benzyne cycloaddition routes to pyrido[2,1-α]isoindole synthesis. 55
Figure. 2.3.1. Crystal structure of 2c. 61
Figure 2.3.2. Proposed reaction mechanism of pyrido[2,1-α]isoindole formation. 62
Figure 2.5.1. *In situ* ^{1}H NMR analysis of reaction (Table 2.3.1, entry 8)..... 65
Figure 2.5.2. ORTEP diagram of 2c with the numbering scheme adopted. Ellipsoid drawn at 50% probability level. 78
Figure 2.5.3. Intermolecular interactions within the crystal lattice of 2c: C-H/π (3.705 Å) between C12-H and the pyrido[2,1-α]isoindole core; H-bonding (3.528 Å) between the *p*-OCH_3 group and C2-H. 79

List of Tables

Table 2.3.1. Development of a palladium-catalyzed synthesis of pyrido[2,1-α]isoindoles..... 57
Table 2.3.2. Modulation of imines, bromopyridines, and arynes in pyrido[2,1-α]isoindole synthesis. 59
Table 2.5.1. Palladium catalyst development for a one-step synthesis of pyrido[2,1-α]isoindoles. 64
Table 2.5.2. Crystal data and structure refinement for 2c. 79
Table 2.5.3. Fractional Atomic Coordinates ($\times 10^4$) and Equivalent Isotropic Displacement Parameters ($Å^2 \times 10^3$) for 2c. U_{eq} is defined as 1/3 of the trace of the orthogonalised U_{IJ} tensor.. 80
Table 2.5.4. Anisotropic Displacement Parameters ($Å^2 \times 10^3$) for 2c. The Anisotropic displacement factor exponent takes the form: $-2\pi^2[h^2a^{*2}U_{11}+2hka^*b^*U_{12}+\ldots]$. 81
Table 2.5.5. Bond Lengths for 2c. 81
Table 2.5.6. Bond Angles for 2c. 82
Table 2.5.7. Hydrogen Atom Coordinates ($Å \times 10^4$) and Isotropic Displacement Parameters ($Å^2 \times 10^3$) for 2c. 83

Table 2.5.8. Atomic Occupancy for 2c. 83

List of Abbreviations

Å	Ångstrom
Ac_2O	Acetic anhydride
ADP	Adenosine diphosphate
APCI	Atmospheric pressure chemical ionization
Ar	Aryl
atm	Atmosphere
Bn	Benzyl
Boc	Tert-butoxycarbonyl
br	Broad
Bu	Butyl
°C	Degrees Celsius
C_6H_6	Benzene
Cat.	Catalysis/catalyst
CCDC	Cambridge Crystallographic Data Centre
CV	Column volume
d	Doublet
dba	Dibenzylideneacetone
DCM	Dichloromethane
dd	Doublet of doublets
ddd	Doublet of doublets of doublets
ddt	Doublet of doublet of triplets
DFT	Density functional theory
DMAD	Dimethyl acetylenedicarboxylate
DPEphos	Bis[(2-diphenylphosphino)phenyl] ether
dppe	1,2-Bis(diphenylphosphino)ethane
dq	Doublet of quartets
dt	Doublet of triplets

E	Energy
EDG	Electron donating group
ESI	Electrospray ionization
Et_2O	Diethylether
EtOH	Ethanol
EWG	Electron withdrawing group
FDA	Food and Drug Administration
hept	Heptet
HMPA	Hexamethylphosphoramide
HOMO	Highest occupied molecular orbital
hr	Hour
HRMS	High resolution mass spectrometry
hv	Light
i-Pr	isopropyl
J	Coupling constant
JohnPhos	(2-Biphenyl)di-tert-butylphosphine
LUMO	Lowest occupied molecular orbital
m	Multiplet
m/z	Mass-to-charge ratio
Me	Methyl
mg	Miligram
MHz	Megahertz
Min	Minute
mL	Mililitre
mmol	Milimole
mol	Mole
NaOEt	Sodium ethoxide
NBS	N-Bromosuccinimide
NfF	Nonafluorobutanesulfonyl fluoride
NIS	N-Iodosuccinimide
NMR	Nuclear magnetic resonance

[O]	Oxidation
OAc	Acetate
OEt	Ethoxy
ORTEP	Oak Ridge Thermal-Ellipsoid Plot Program
OTBS	Tert-butyldimethylsilyl ether
OTf	Trifloromethanesulfonate
OTs	Toluenesulfonyl
p	Pentet
Ph	Phenyl
ppm	Parts per milion
p-Tol	para-Toluene
q	Quartet
RT	Room temperature
s	Singlet
sext	Sextet
t	Triplet
TBAF	Tetrabutylammonium fluoride
t-Bu	Tert-butyl
t-BuOH	Tert-butanol
td	Triplet of doublets
THF	Tetrahydrofuran
TMS	Trimethylsilyl
TOF	Time-of-flight
TS	Transition state
tt	Triplet of triplets
UV	Ultraviolet
Xantphos	4,5-Bis(diphenylphosphino)-9,9-dimethylxanthene
δ	Chemical shift
Δ	Heat

Contributions of Co-Authors

The thesis is comprised of three chapters. Chapter 1 is an introduction describing general ways of generating benzyne and 1,3-dipolar cycloadditions of acyclic and cyclic 1,3-dipoles with benzyne to form benzo-fused 5-membered heterocycles. Chapter 2 is a published manuscript (*Chem. Comm.*, 2025, DOI: 10.1039/D4CC06483F) and describes the palladium-catalyzed carbonylative synthesis of pyrido[2,1-α]isoindoles *via* benzyne 1,3-dipolar cycloaddition. Dr. Mohammad Ghanbari carried out research in our lab that preliminarily showed the use of the pyridine-based 1,3-dipole to undergo cycloaddition with benzyne. However, all experiments described in this chapter, including the use of palladium catalysis, the reaction development, and structural diversifications were performed by me under the supervision of Dr. Bruce Arndtsen for the completion of the degree of Master of Science in chemistry. My supervisor, Dr. Bruce Arndtsen assisted in the editing of this thesis.

Chapter 1 – Introduction

1.1 Perspective

Dating back to the late nineteenth century, 1,3-dipolar cycloadditions offer one of the most versatile strategies for the synthesis of 5-membered heterocycles.[1,2] The term "1,3-dipole" refers to a compound with a zwitterionic resonance structure across three atoms, i.e. *a*-*b*-*c*, where atom *a* has an incomplete octet and is positively charged, atom *b* is neutral, and atom *c* has a lone pair and is negatively charged. Mesoionic 1,3-dipoles are a specific class of 1,3-dipole that incorporate the zwitterionic structure into an often aromatic ring with multiple resonance structures. A dipolarophile, *D*-*E*, is a double or triple bond-containing molecule that is the other component in these reactions. A 1,3-dipolar cycloaddition is defined as the combination of a 1,3-dipole and a dipolarophile to form a neutral 5-membered ring.[3,4] In the case of mesoionic 1,3-dipoles, cycloaddition with the dipolarophile often forms a neutral 5-membered heterocycle *via* the elimination of a small molecule, *d*-*e*-*f*, through cycloreversion after the initial cycloadduct is formed (Scheme 1.1.1).[5,6]

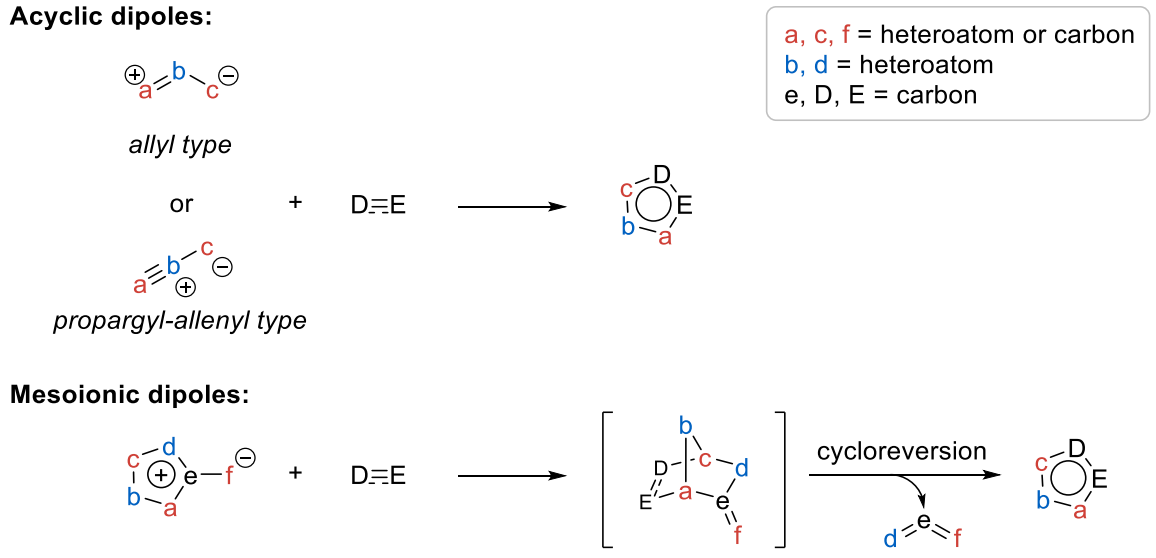

Scheme 1.1.1. Cycloaddition of acyclic and mesoionic 1,3-dipoles with dipolarophiles to form neutral 5-membered heterocycles.

The interaction between a 1,3-dipole and dipolarophile is classified based on HOMO-LUMO orbital energies of the two components as a way to understand influences on cycloaddition reaction rates (Scheme 1.1.2).[7] Type 1 interactions occur between the high-lying filled orbital

(HOMO: highest occupied molecular orbital) of electron-rich 1,3-dipoles and the low-lying empty orbital (LUMO: lowest unoccupied molecular orbital) of electron-deficient dipolarophiles. Decreasing the difference in HOMO-LUMO energies between the two cycloaddition partners, such as with substituents, accelerate the reaction. Type 2 interactions occur between 1,3-dipoles and dipolarophiles of similar orbital energies that would favour the concurrent interaction of the HOMO and LUMO of the 1,3-dipole with the LUMO and HOMO of the dipolarophile, respectfully. Type 3 interactions are the opposite of Type 1 in that the fastest reactions occur between electron-deficient 1,3-dipoles and electron-rich dipolarophiles.

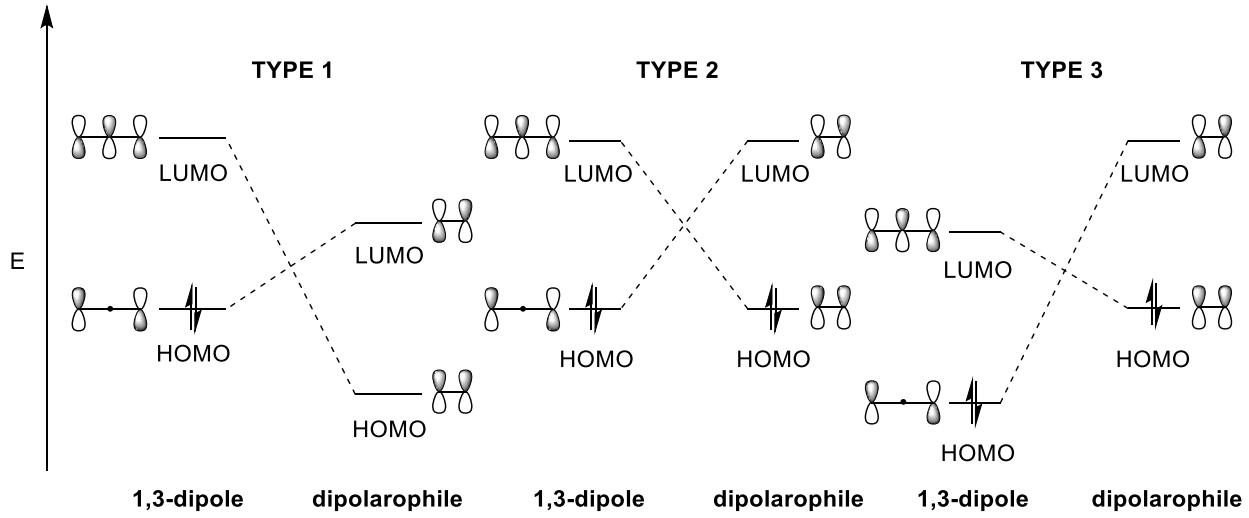

Scheme 1.1.2. Classification of 1,3-dipolar cycloadditions based on HOMO-LUMO interactions between the 1,3-dipole and dipolarophile.

1,3-Dipolar cycloaddition reactions with nitrogen-containing 1,3-dipoles provide a convergent method to prepare N-containing heterocycles. Heterocycles are fundamental structures in several fields in chemistry, most notably in pharmaceuticals.[8] Therapeutic drugs containing heterocycles have been on the rise for several decades. Many of these are nitrogen-based heterocycles. Over the last decade, 82% of FDA-approved small drug molecules contained at least one nitrogen heterocycle, an increase of 23% since the 1930s.[9,10] Nearly half of these drugs contain a 5-membered ring, and among these, fused-ring nitrogen heterocyclic systems have seen a substantial increase in use over time (Scheme 1.1.3).

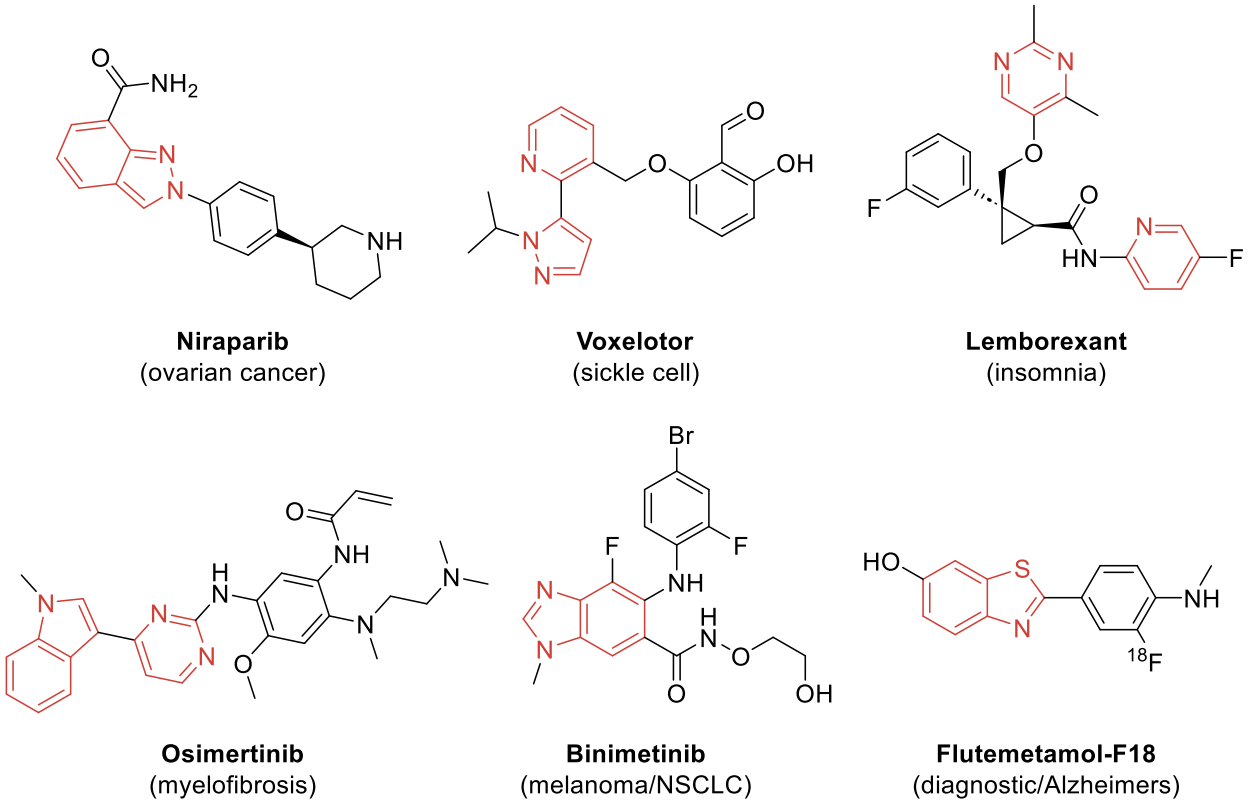

Scheme 1.1.3. FDA-approved small drug molecules with nitrogen-based heterocycles.

Fused heterocyclic systems are synthesized through different approaches including the intramolecular cyclization of linear precursors, annulation reactions, and cycloadditions.[11,12] One useful route to these molecules is *via* 1,3-dipolar cycloadditions with benzyne. Since their discovery, benzynes have evolved into a key building block in organic chemistry with applications in a wide range of reactions, including nucleophilic additions, pericyclic reactions, transition metal-catalyzed reactions, and σ-bond insertions.[13–15] The utility of benzyne in the synthesis of fused heterocycles has been thoroughly demonstrated through numerous examples of 1,3-dipolar cycloadditions involving both acyclic (also conventionally referred to as "linear") and cyclic 1,3-dipoles.[13,15–19] Examples of these fused systems include the synthesis of benzotriazoles, benzisoxazolines, indazoles, isoindoles, and benzo[c]thiophenes, as depicted in Scheme 1.1.4.

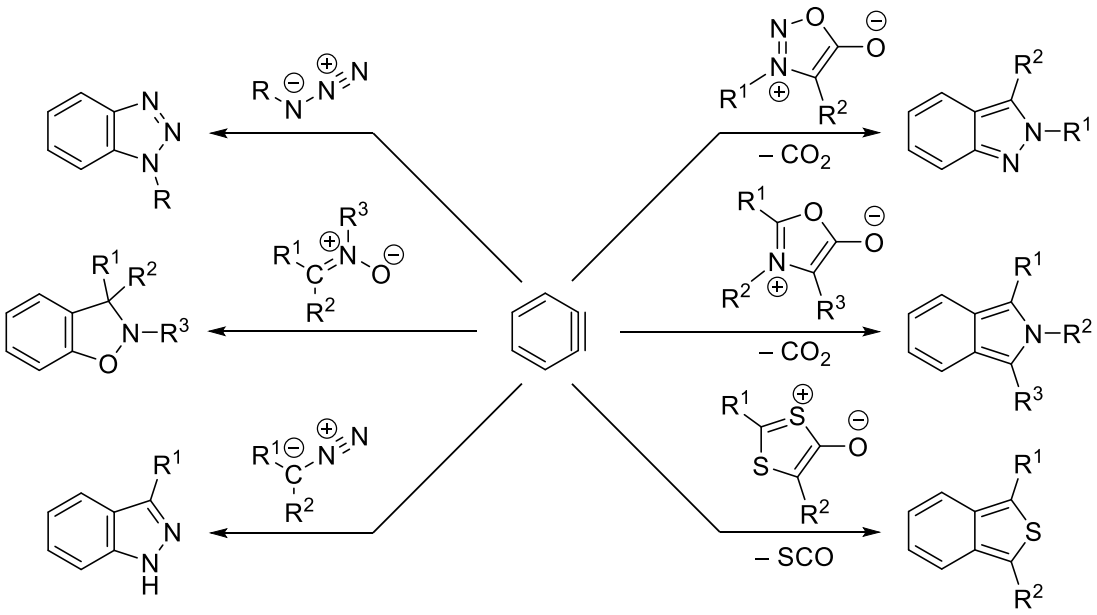

Scheme 1.1.4. Examples of 1,3-dipolar cycloaddition with benzyne with acyclic (left) and mesoionic (right) 1,3-dipoles to form fused heterocyclic systems.

This chapter covers an overview of benzyne, its methods of generation (Section 1.2) and its use in 1,3-dipolar cycloadditions as a route to form fused heterocycles (Section 1.3).

1.2 Benzyne Generation

The first reported generation of an aryne can be traced to 1864 in the work of Fittig on the reaction of bromobenzene and sodium, which formed biphenyl (Scheme 1.2.1a).[20] The concept of a triple bond within an aromatic system was not suspected until 1902 when Stoermer and Kahlert proposed the possibility of an aryne intermediate in their analogous reaction between 3-bromobenzofuran and sodium ethoxide (Scheme 1.2.1b).[21] The existence of arynes, specifically benzyne, was confirmed in 1953 by Roberts through his pioneering work using ^{14}C-labelling experiments. The reaction of chlorobenzene with potassium amide in liquid ammonia produced an equal mixture of two aniline products – one with ^{14}C on the α-carbon and the other on the β-carbon, demonstrating functionalization on either triple bond carbon of the *in situ* generated benzyne intermediate (Scheme 1.2.2).[22–24]

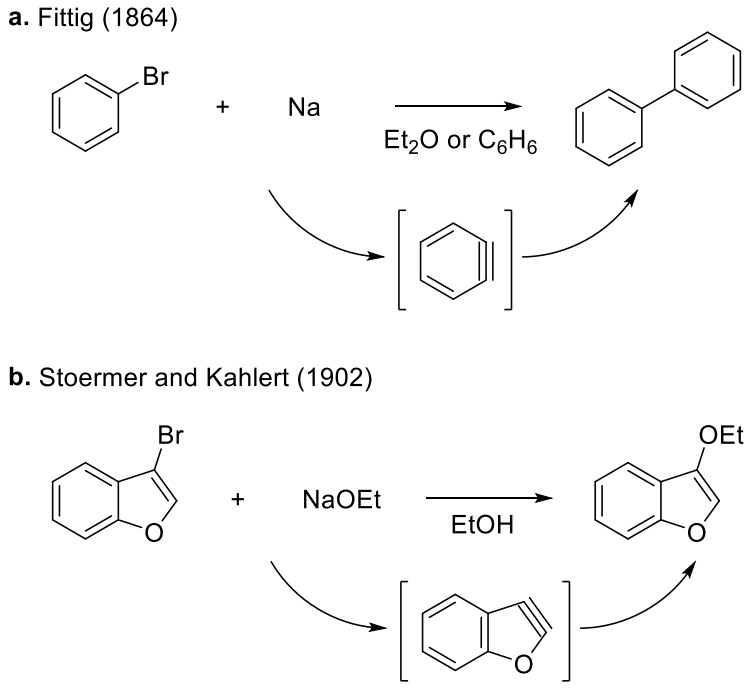

Scheme 1.2.1. Earliest evidence of aryne intermediates *via* dehydrohalogenation of haloarenes.

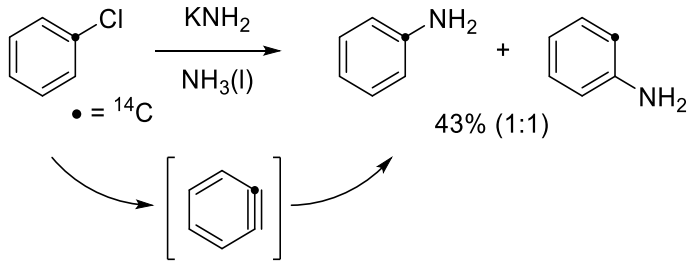

Scheme 1.2.2. Isotope-labelling experiment confirming the existence of a benzyne intermediate.

Building on this early strategy of dehydrohalogenating haloarenes with strong bases to form benzyne, others reported the metal-halogen exchange-elimination of *o*-dihaloarenes or *o*-haloaryl triflates/tosylates using metals like magnesium, lithium, lithium-mercury amalgam, or organometallic reagents (Scheme 1.2.3).[25–29] The use of strong bases often makes this approach incompatible with reactive functional groups. However, undesired nucleophilic addition can be avoided in part with sterically encumbered bases such as lithium 2,2,6,6-tetramethylpiperidide (LiTMP) and lithium diadamantylamide (LDAM).[30,31]

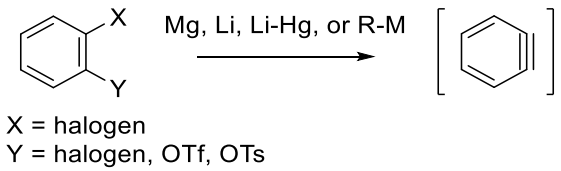

Scheme 1.2.3. Benzyne generation *via* metal-halogen exchange-elimination.

Benzyne generation through thermal decomposition of precursors was later developed, including the decomposition of benzenediazonium-2-carboxylate, which releases N_2 and CO_2.[32,33] Although the temperatures required for decomposition are relatively low (40 – 60°C), a significant drawback of this method is the explosive nature of the diazonium precursor. An alternative precursor with the same disadvantage is benzo[*d*][1,2,3]thiadiazole 1,1-dioxide, which decomposes at lower temperatures to release N_2 and SO_2.[34] Similarly, diphenyliodonium-2-carboxylate can serve as a precursor, but it requires thermolysis at 160°C to over 200°C (Scheme 1.2.4).[35,36] Soon after, another approach was reported involving the oxidation of 1-aminobenzotriazole with lead tetraacetate or nickel peroxide.[37,38] Other oxidants, such as *N*-halosuccinimides, have also been employed (Scheme 1.2.5).[39]

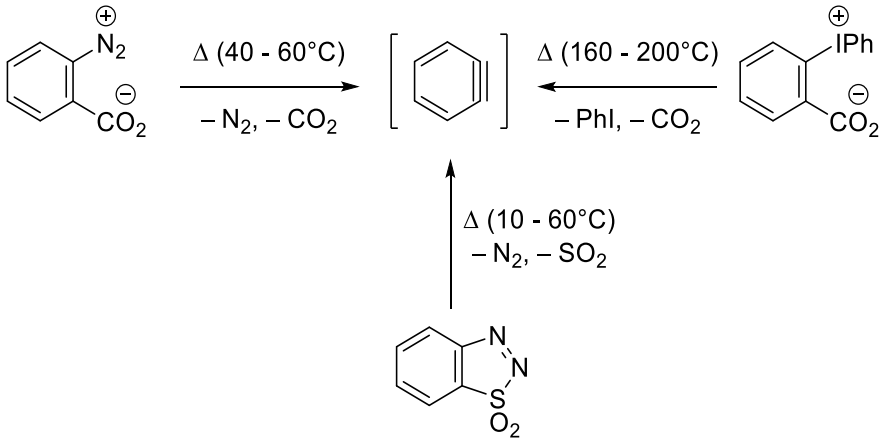

Scheme 1.2.4. Benzyne generation *via* thermal decomposition.

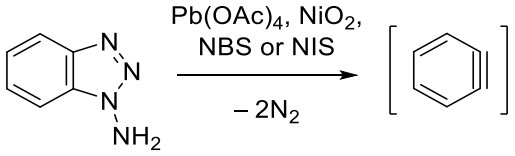

Scheme 1.2.5. Benzyne generation *via* oxidation.

Up until the early 1980s, methods for generating benzyne typically relied on strong bases, explosive precursors, and oxidative conditions, all of which restricted their compatibility with reactive functional groups. It was not until 1983 that Kobayashi developed a milder method using *o*-trimethylsilylphenyl triflate, which undergoes a fluoride-induced removal of the silyl group followed by the elimination of the triflate leaving group under ambient conditions (Scheme 1.2.6).[40] In addition to the mild reaction conditions, an attractive aspect of this approach stems from the slow and controlled rate in which the benzyne intermediate is formed. The solubility of the fluoride source in the chosen solvent system can help maintain a low concentration of benzyne throughout the reaction, which can be useful for enhancing reaction selectivity in many systems. Interestingly, Kobayashi's work went largely unrecognized by the chemistry community for nearly 15 years. However, based on the more recent recognition of this approach, publications on benzyne have increased substantially over the past two decades, enabling chemists to explore and expand the range of transformations that benzyne can partake in – demonstrating this method's significant impact on modern aryne chemistry.[15,17,41–43]

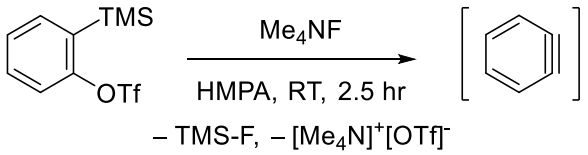

Scheme 1.2.6. Benzyne generation *via* fluoride-induced 1,2-elimination.

1.3 Benzyne 1,3-Dipolar Cycloadditions in Heterocycle Synthesis

1,3-Dipolar cycloadditions with benzyne can provide access to a wide range of benzo-fused heterocycles. The first use of benzyne as a dipolarophile was reported in 1961 by Huisgen and Knorr involving the reaction of benzyne, generated from the thermal decomposition of benzenediazonium-2-carboxylate, with diazoacetic ester to form the 1*H*-indazole product in 75% yield (Scheme 1.3.1).[44] Subsequent studies have demonstrated that many 1,3-dipoles can participate in cycloadditions with benzyne such as azides, nitrones, azomethine ylides, azomethine imines, nitrile imines, nitrile oxides, and pyridinium ylides (Scheme 1.3.2). In addition to acyclic 1,3-dipoles, cyclic mesoionic 1,3-dipoles have also been employed in benzyne cycloaddition. Examples of these latter are highlighted in the sections below.

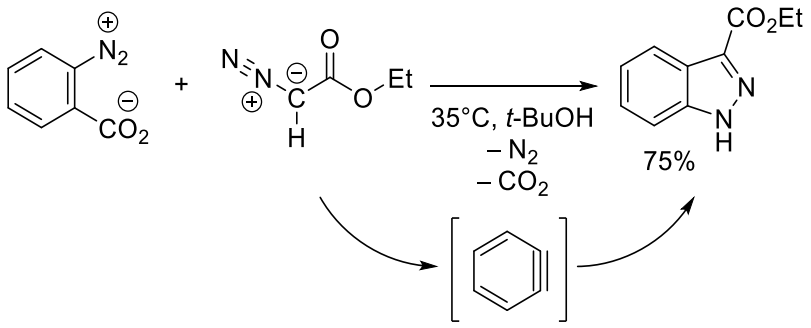

Scheme 1.3.1. The first reported use of an aryne as a dipolarophile in the 1,3-dipolar cycloaddition of benzyne with diazoacetic ester.

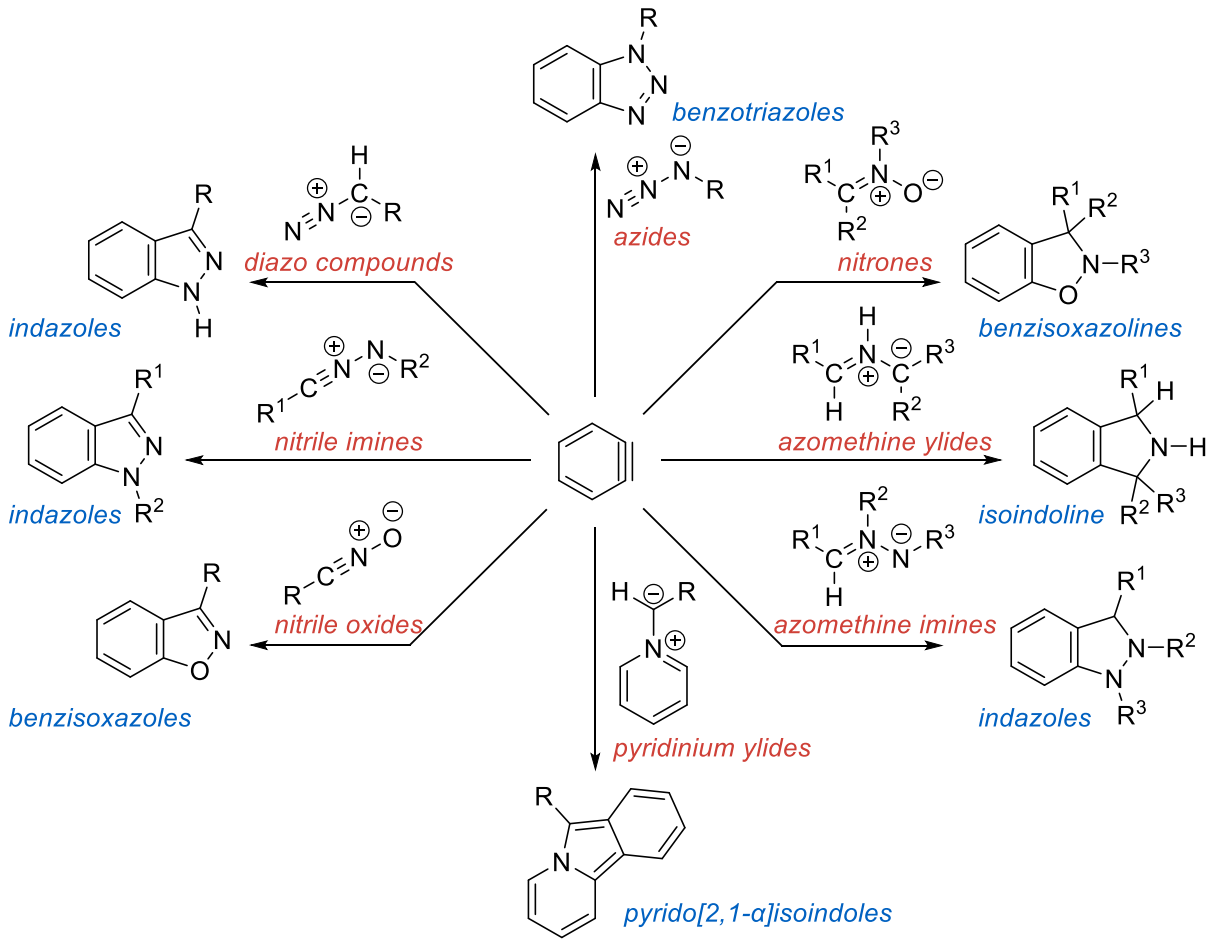

Scheme 1.3.2. 1,3-Dipolar cycloaddition of benzyne with acyclic 1,3-dipoles to form various heterocycles.

1.3.1 Cycloaddition of Benzyne with Cyclic 1,3-Dipoles

1.3.1.1 Reactions with Sydnones (1,2,3-Oxadiazolium-5-Olates)

Sydnones (1,2,3-oxadiazolium-5-olates) were first synthesized by Earl and Mackey in 1935 through the cyclodehydration of *N*-nitrosoglycine derivatives (Scheme 1.3.3).[45] This approach continues to be the most widely used method for the synthesis of these dipoles.[46,47] Since their discovery, these sometimes crystalline and stable molecules have been found to serve as components in medicinal compounds and, more commonly, exploited in cycloadditions for heterocycle synthesis.[48–51] An example of the latter is its cycloaddition with benzyne, first noted by Gotthardt, Huisgen, and Knorr, which leads to spontaneous cycloreversion to eliminate CO_2 and form indazoles (Scheme 1.3.4). The reaction employs benzenediazonium-2-carboxylate as benzyne precursor, which undergoes thermal CO_2 and N_2 loss in the presence of *N*-phenylsydnone.[52,53] As noted above, a non-isolable bicyclic cycloadduct is initially formed and undergoes cycloreversion to release CO_2, forming 2-phenyl-indazole in 49% yield.

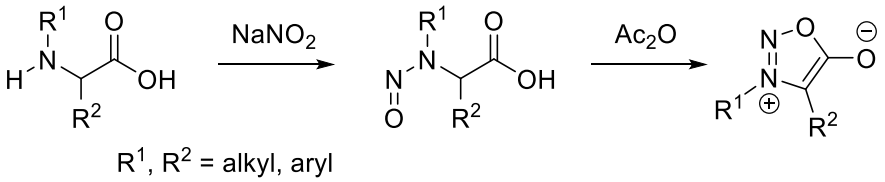

Scheme 1.3.3. Conventional synthesis of Sydnones.

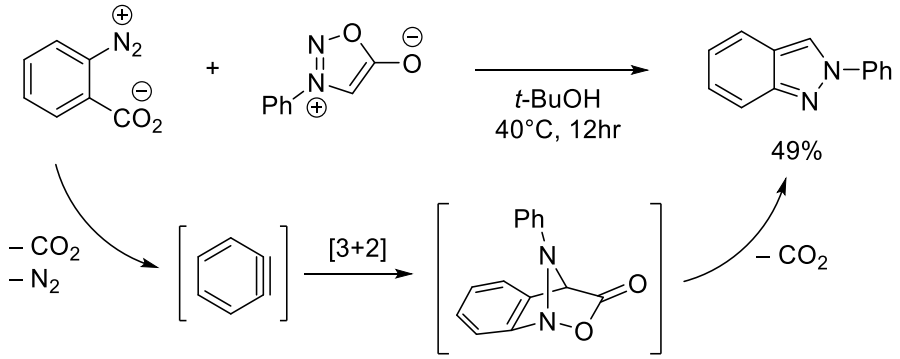

Scheme 1.3.4. The first example of a 1,3-dipolar cycloaddition of benzyne and a Sydnone.

This reaction was later studied by Kato who obtained a greater yield of the same 2-phenyl-indazole using 1-aminobenzotriazole as the benzyne precursor.[54] This reaction generates benzyne

under oxidative conditions with $Pb(OAc)_4$ *via* the elimination of 2 equivalents of N_2, and was used to form various 2,3-disubstituted indazoles (Scheme 1.3.5a).

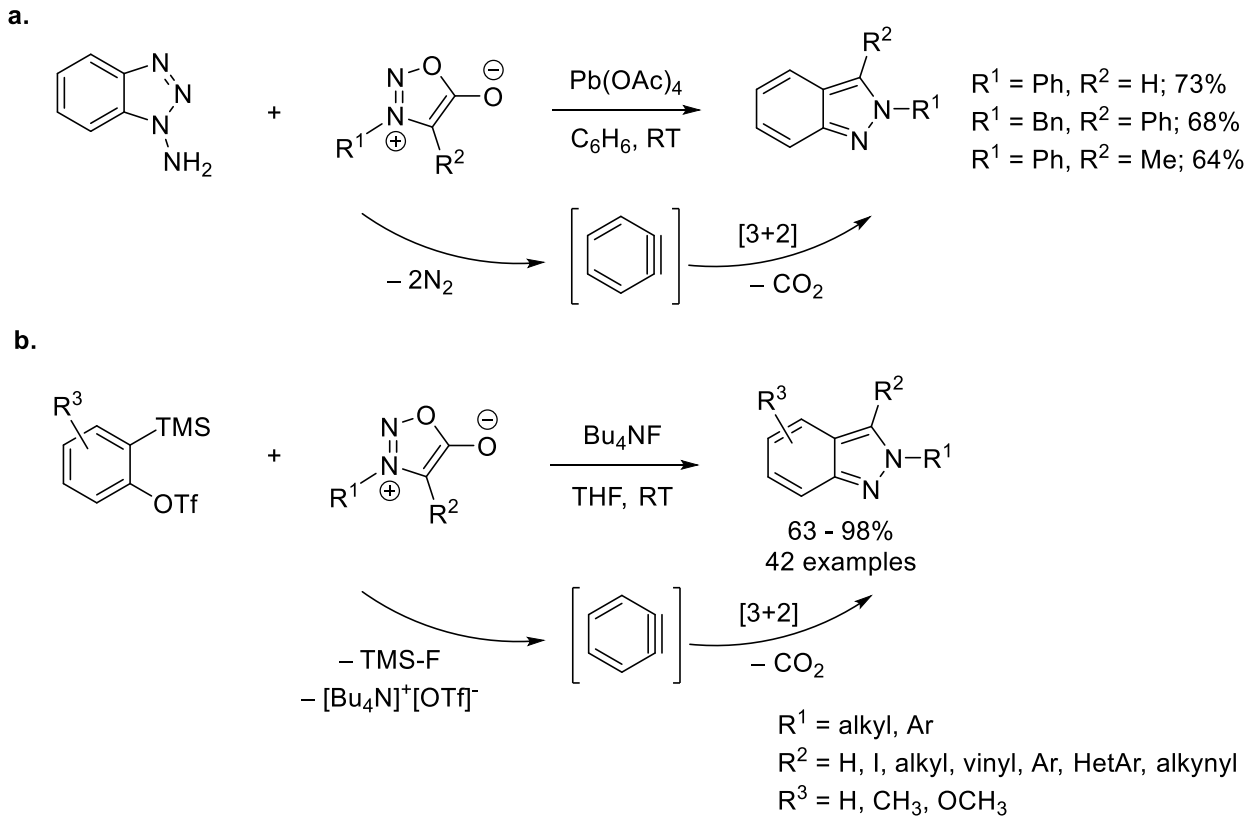

Scheme 1.3.5. Synthesis of 2,3-disubstituted indazoles from a) 1-aminobenzotriazole and b) *o*-trimethylsilylaryl triflates.

Larock and Shi showed how *o*-trimethylsilylaryl triflates can also serve as benzyne precursors in this chemistry.[55,56] Benzyne can be generated under mild conditions *via* this approach and was used to form a wide range of mono and polysubstituted indazoles in generally good to excellent yields (Scheme 1.3.5b). However, unsymmetrical benzyne precursors offered low regioselectivity despite attempts to create steric and electronic bias (Scheme 1.3.6). Studies on the frontier molecular orbitals (FMOs) of Sydnones suggest that either N2 or C4 can participate as the nucleophile in cycloadditions.[57–59] Hence, Sydnone cycloadditions with unsymmetrical alkynes typically do not afford high regioselectivity (*vide infra*).[60]

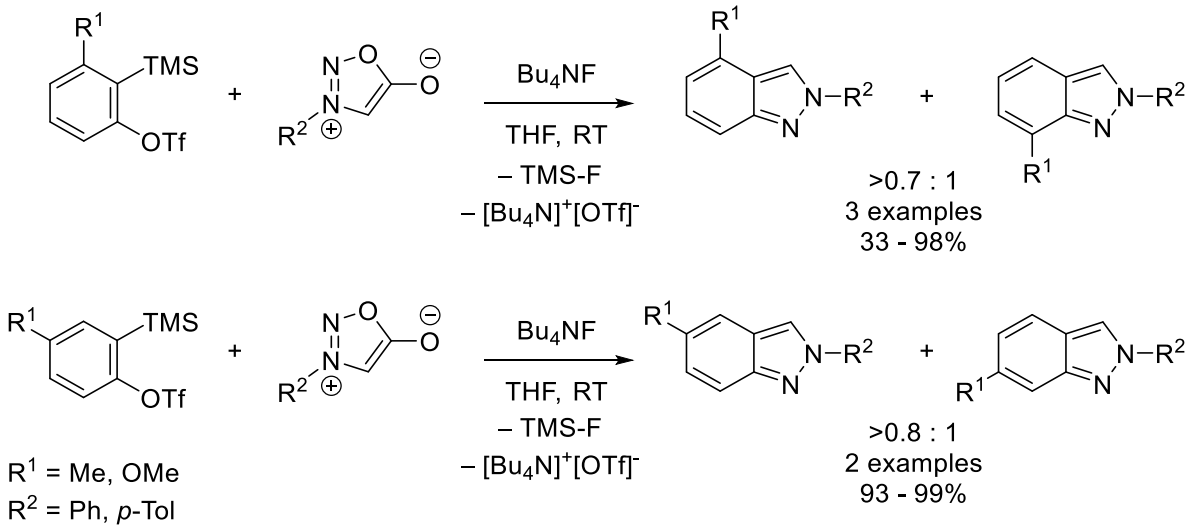

Scheme 1.3.6. Low regioselectivity in cycloaddition of unsymmetrical benzynes with Sydnones.

Melo has shown how benzyne cycloaddition can be combined with other subsequent 1,3-dipolar cycloaddition reactions. This exploits a thiazolidine-based Sydnone, where after benzyne cycloaddition, oxidation of the thiazolidine results in SO_2 deletion to form a zwitterionic benzodiazafulvenium methide. As such, the thiazolidine participated as a masked 1,3-dipole precursor for subsequent [3+2] cycloaddition with a maleimide (Scheme 1.3.7).[61]

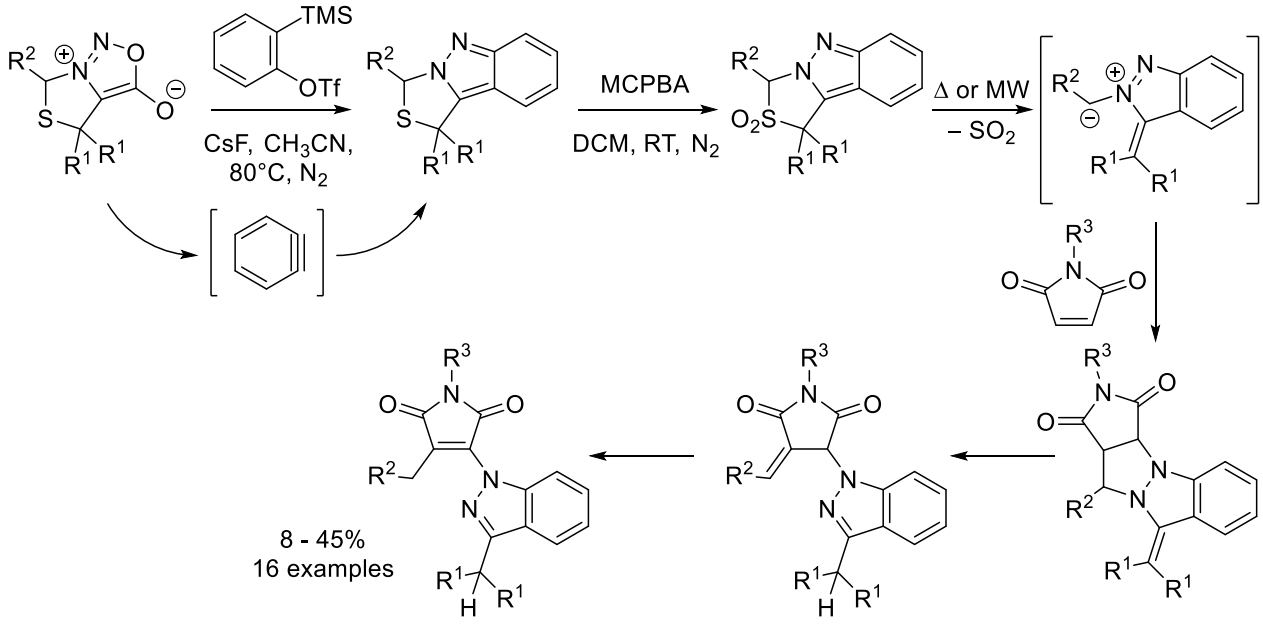

Scheme 1.3.7. Thiazolidine-based Sydnone functioning as a masked 1,3-dipole for subsequent [3+2] cycloaddition.

As noted above, regioselectivity can often be a challenge in benzyne-Sydnone cycloaddition, where presumably, in addition to the high benzyne reactivity, a mixture of both regioisomers is often observed with unsymmetrical benzyne precursors. However, Ikawa and Akai showed that regioselectivity in Sydnone-aryne cycloaddition can be obtained with a large trialkyl silyl group *ortho* to the aryne triple bond (Scheme 1.3.8). The reaction with *p*-methoxyphenyl 4-substituted N-phenyl Sydnone favours the less sterically hindered, distal product where the silyl group is furthest away from the *p*-methoxyphenyl group over the more hindered, proximal product. Interestingly, the more sterically encumbered Si(*t*-Bu)Me_2 gave lower selectivity than the $SiMe_3$ group.[62,63]

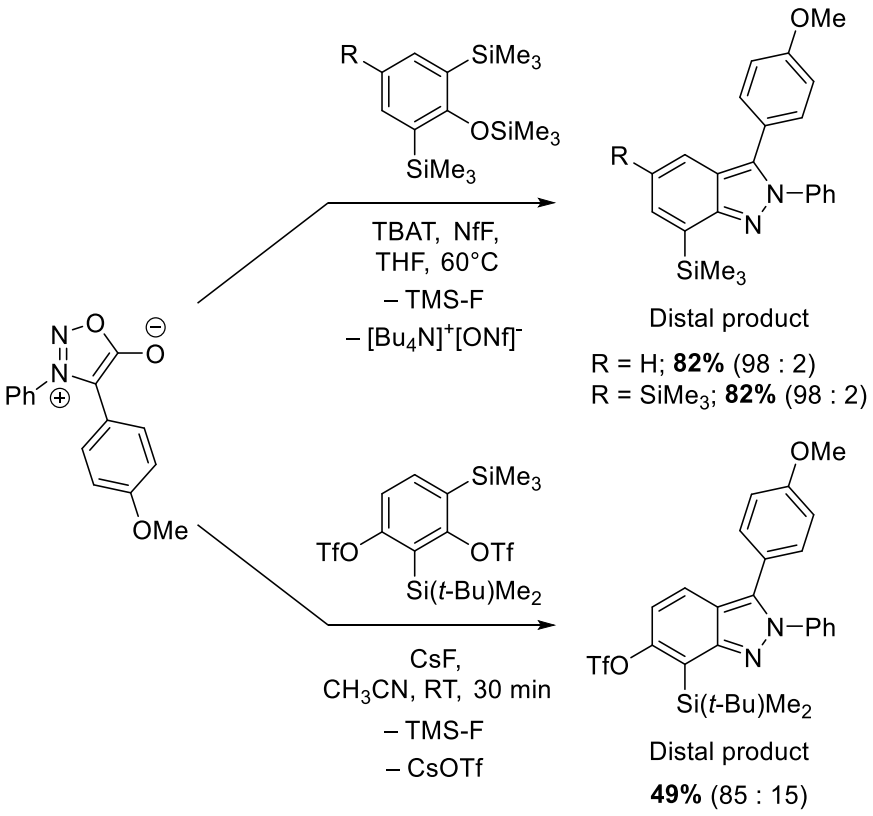

Scheme 1.3.8. Regioselective, silyl group-controlled benzyne cycloaddition with a 3,4-disubstituted Sydnone.

In addition to reaction development, benzyne cycloaddition with Sydnones has also been used in several applications. For example, helicenes possess chiroptical properties that make them attractive molecules in materials science.[64,65] The optoelectronic features of these molecules can be tuned by replacing carbon with heteroatoms in the core structure.[66,67] Audisio *et al.* developed

an efficient synthesis of pyrazole-containing helicenes *via* the [3+2] cycloaddition of polyaromatic Sydnones with 1,2-naphthalene- and 3,4-phenanthrene-derived arynes (Scheme 1.3.9).[68,69] Interesting selectivity was observed in the reaction, where the more sterically hindered, helical C-shaped product was favoured over the less hindered S-shaped isomer. DFT calculations revealed that two key factors contributed to the reaction favouring the formation of the helical, C-shaped isomer over the S-shaped isomer. It was found that the transition state (TS) that played the most important role in these reactions was at the initial cycloaddition step, during which aromatic stabilization took place. This included edge-to-face C–H···π interactions between an aromatic C–H bond of the aryne and the π system of the Sydnone as well as face-to-face π–π interactions, both contributing to the lowering of the activation barrier towards the C-shaped isomer. Primary orbital interactions also explain the regioselectivity. The FMOs involved in this system show that the larger coefficient in the HOMO of the Sydnone is on N2 and the larger coefficient in the LUMO of the aryne is on the "external" carbon of the triple bond. DFT-generated TS structures in the formation of the C-shaped isomer possessed near ideal primary orbital interactions i.e. the four bond-forming atoms are coplanar (0° dihedral angle), as opposed to distortions from coplanarity observed in the TS to form the S-isomer.

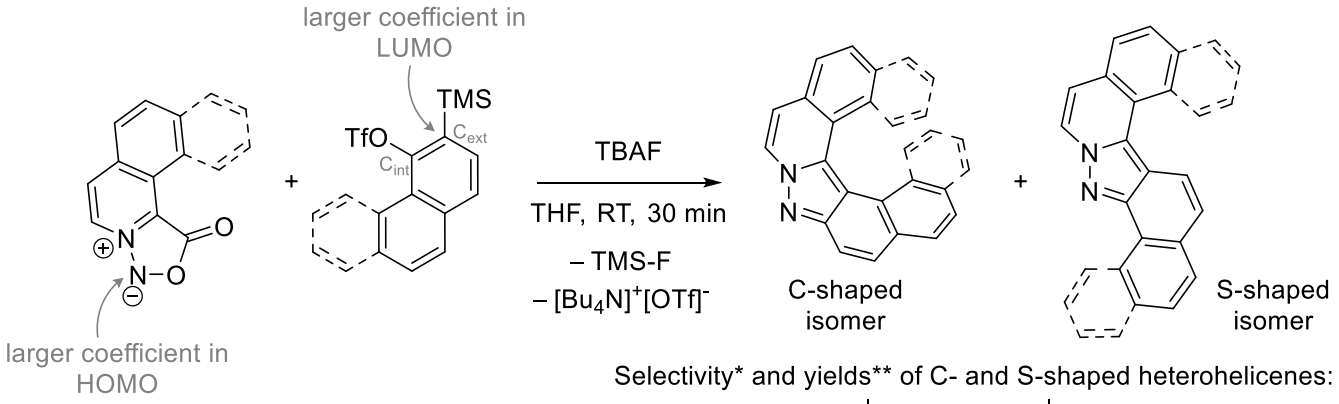

Selectivity* and yields** of C- and S-shaped heterohelicenes:

Naphthalyne	1 : 1 44% 30%	1.7 : 1 38% 28%
Phenanthryne	9 : 1 79% 6%	24 : 1 62% 4%
	Tricyclic sydnone	*Tetracyclic sydnone*

*Isomer ratios measured by ^{1}H NMR of crude mixture

**Isolated yields

Scheme 1.3.9. Cycloaddition of polyaromatic Sydnones with arynes to form pyrazole-containing helicenes.

Although aryne-Sydnone 1,3-dipolar cycloadditions are useful in fused heterocycle synthesis, they are not often employed in pharmaceutical design. As an exception, the Li group reported a novel method of aryne generation using the Grob fragmentation of benzocyclobutenols (Scheme 1.3.10).[70] The reaction proceeds *via* the initial generation of a triflate substituted aryne for [2+2] cycloaddition with a ketene silyl acetal. Subsequent attack of the OTBS group by a fluoride anion, followed by ring opening directed by both the leaving ability and electron withdrawing character of the OTf group, forms the corresponding 2,3-aryne intermediate for [3+2] cycloaddition with an *N*-aryl substituted Sydnone. This was applied to the preparation of Niraparib, a poly-ADP ribose polymerase (PARP) inhibitor useful in halting cancer cell repair.[71,72] The cycloaddition did not proceed with an appreciable regioselectivity, forming the desired cycloadduct in 42% yield. Conversion to the benzamide afforded a racemic mixture of Niraparib.

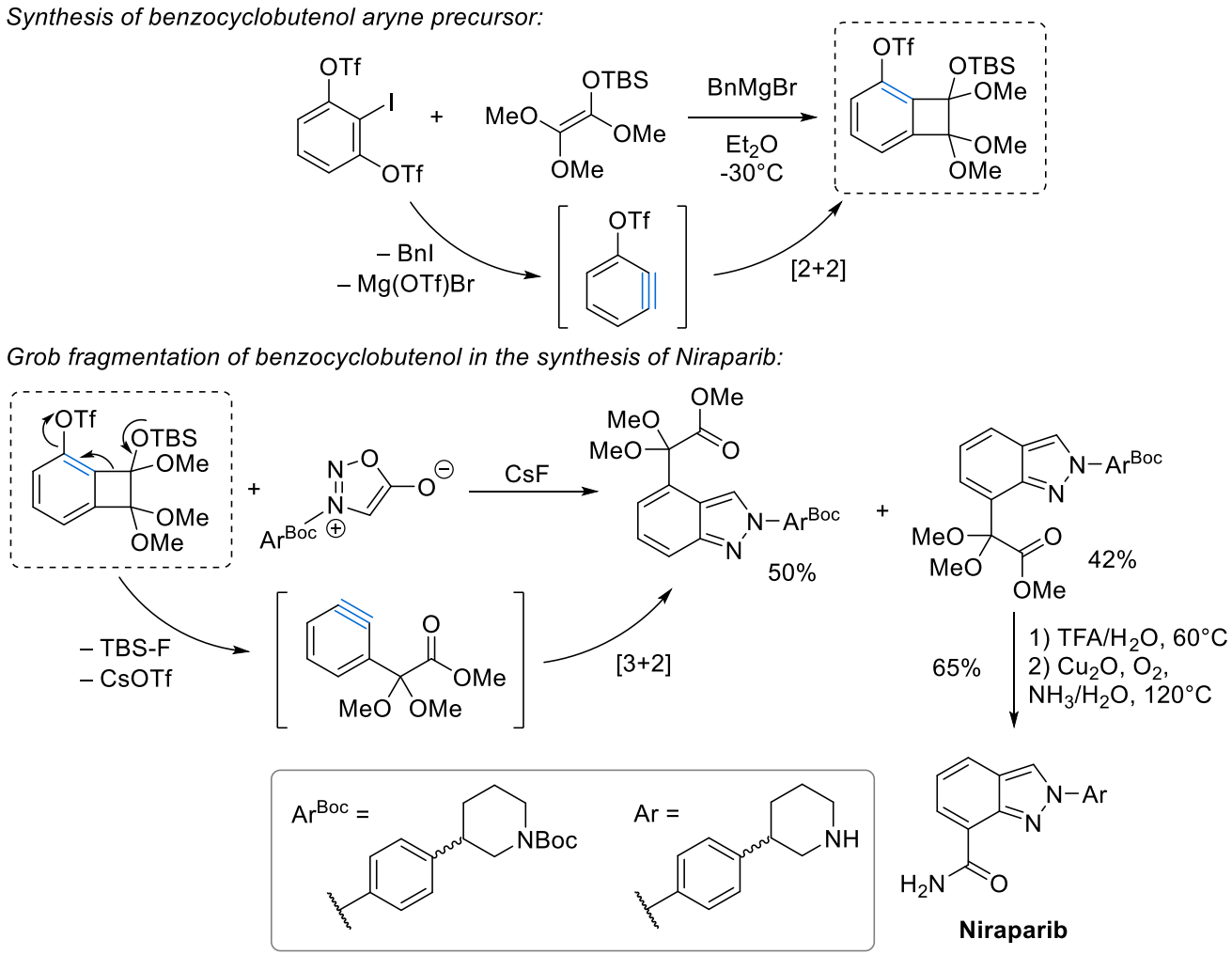

Scheme 1.3.10. Sydnone-benzyne cycloaddition to form Niraparib.

1.3.1.2 Reactions with 1,2,4-Triazolium-3-Olates

1,2,4-Triazolium-3-olates are another class of mesoionic 1,3-dipoles that were first synthesized by Busch in 1903.[73,74] Two general pathways have been developed to access these structures: one *via* the reaction of semicarbazides and formic acid that on heating, undergoes ring closure to form 1,2,4-triazolium-3-olates (Scheme 1.3.11a), and a second involves the reaction of iminyl chlorides and hydrazines to generate iminohydrazines, followed by reaction with phosgene and intramolecular cyclization (Scheme 1.3.11b).

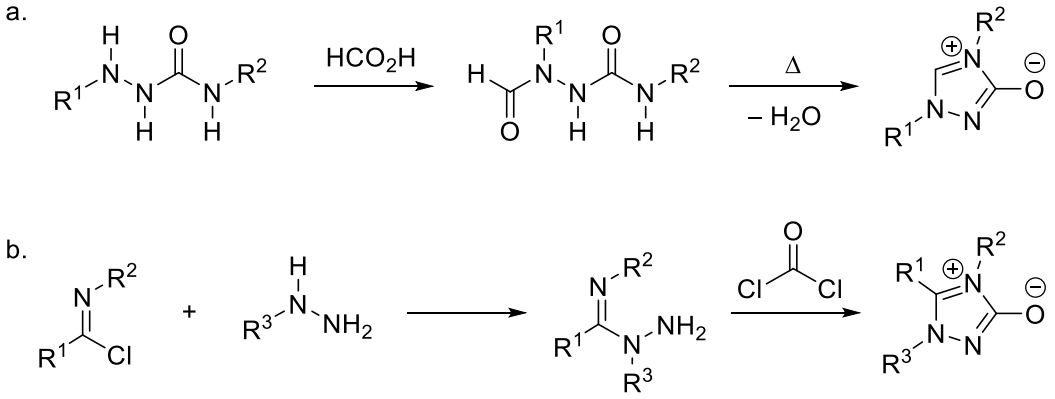

Scheme 1.3.11. The first synthetic methods to prepare substituted 1,2,4-triazolium-3-olates.

Kato later found that 1,2,4-triazolium-3-olates can also be prepared from the reaction of Sydnones, demonstrating an early example of the interchangeability of mesoionic ring systems.[75] The 1,3-dipolar addition reaction of 3-phenylsydnone with phenyl isocyanate releases carbon dioxide to form the corresponding 1,4-diphenyl substituted dipole (Scheme 1.3.12). Other cyclic 1,3-dipoles have also been used to access 1,2,4-triazolium-3-olates. For example, 1,2,4-triazolium-3-thiolates react with aryl isocyanate (Scheme 1.3.13).[76] Thiol derivatives of 1,2,4-triazolium-3-olates can also be synthesized by treating 5-thioxo-1,2,4-triazolin-3-ones with alkyl iodide and sodium methoxide.[77] Pyridine-based 1,2,4-triazolium-3-olates can be prepared in excellent yield *via* a base-catalyzed rearrangement of 1,3,4-oxadiazol-2-imines.[78]

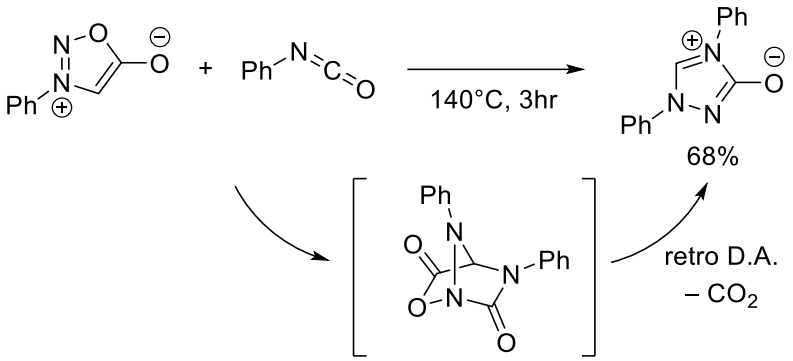

Scheme 1.3.12. The synthesis of 1,4-diphenyl-1,2,4-triazol-3-one *via* the 1,3-dipolar cycloaddition of *N*-phenylsydnone with phenyl isocyanate.

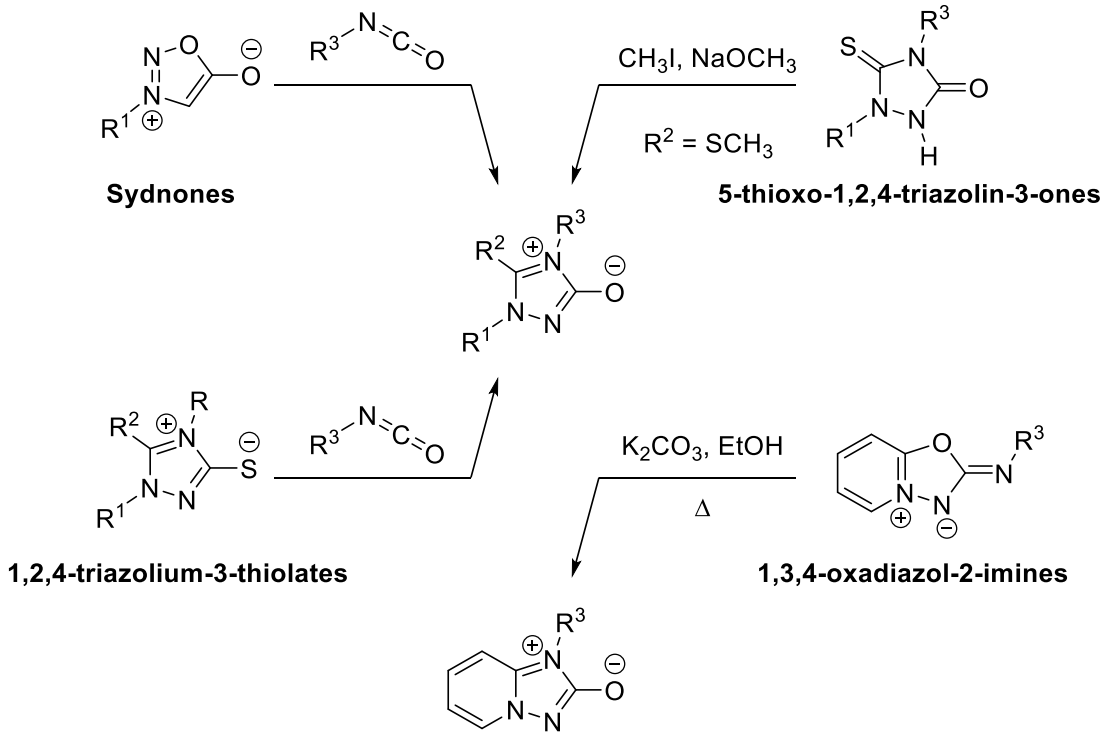

Scheme 1.3.13. Synthesis of 1,2,4-triazolium-3-olates from other mesoionic 1,3-dipoles.

Similar to Sydnones, the 1,3-dipolar cycloaddition of 1,2,4-triazolium-3-olates with benzynes also yield indazoles. This reaction was initially conducted by Kato, who found that 1,4-diphenyl-1,2,4-triazolium-3-olate yielded no reaction with benzyne generated from 1-amino-benzotriazole, but gave 2-phenylindazole in 34% yield using diphenyliodonium-2-carboxylate as the benzyne precursor (Scheme 1.3.14).[54,79] Similarly, Lwowski reported that the electron rich

dimethylamino-substituted 1,2,4-triazolium-3-olate reacts with benzyne generated from 1-amino-benzotriazole to form the corresponding indazole in 31% yield (Scheme 1.3.15).[80]

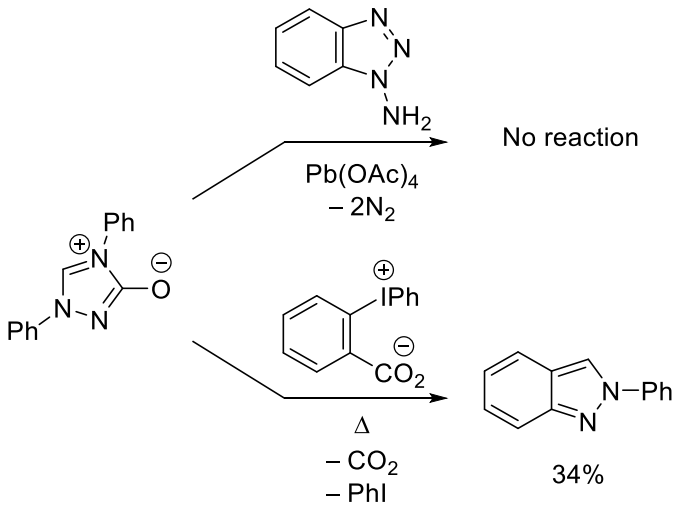

Scheme 1.3.14. 1,3-Dipolar cycloaddition of 1,4-diphenyl-1,2,4-triazolium-3-olate with different benzyne precursors.

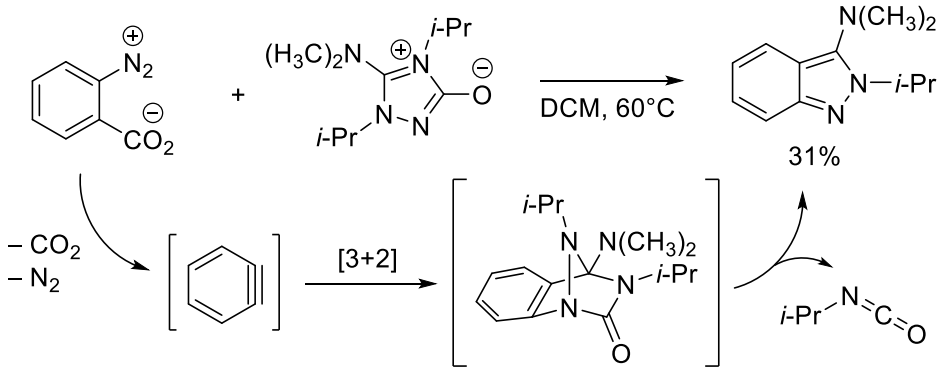

Scheme 1.3.15. 1,3-Dipolar cycloaddition of electron-rich amine-substituted 1,2,4-triazolium-3-olate with benzyne.

1.3.1.3 Reactions with 1,2,3,4-Tetrazolium-5-Thiolates

1,2,3,4-Tetrazolium-5-thiolates, also referred to as "dehydrodithizones", were first synthesized by Fischer and Besthorn in 1882 *via* the oxidation of diphenylthiocarbazone with manganese dioxide.[81] In later years oxidation continued to be a reliable method to access 2,3-diaryltetrazolium-5-olates. Irving employed this approach to form 2,3-diaryltetrazolium-5-olates

in good yields using potassium hexacyanoferrate(III) but low yields with other oxidants.[82,83] More recently, Jian described a mild oxidation of diarylthiocarbazones with hydrogen peroxide and air to give excellent yields of the corresponding mesoionic compounds.[84] Alternatively, Motoki treated diphenylthiocarbazone with dialkoxydisulfide to yield 2,3-diaryltetrazolium-5-thiolates in good to excellent yields.[85] The reaction proceeds through a nucleophilic substitution of the alkoxy group by the secondary amine of the thiocarbazone and subsequent elimination of the disulfide group forms a diazinyl intermediate that undergoes an intramolecular cyclization (Scheme 1.3.16).

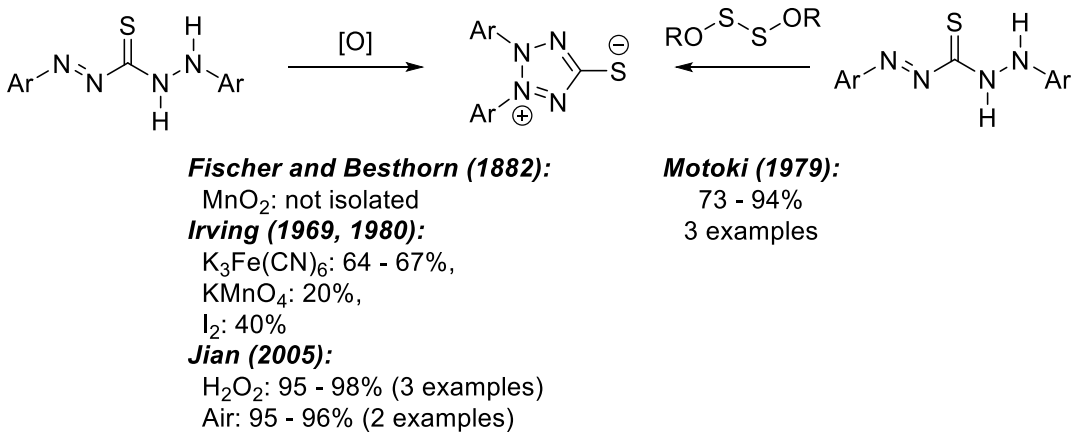

Scheme 1.3.16. Synthesis of 2,3-diaryltetrazolium-5-thiolates from diarylthiocarbazones.

1,2,3,4-Tetrazolium-5-thiolates differ from the other mesoionic 1,3-dipoles discussed in this chapter in that they do not contain a 1,3-dipole fragment in the cyclic core. There are referred to as Type B mesoionic rings, as opposed to Type A such as Sydnones and Münchnones. Classification of these two types of mesoionic compounds have been extensively described in several reviews.[86–88] These structural differences in Type B rings result in cycloadditions that differ from the classical 1,3-dipolar cycloaddition mechanism observed with Type A rings. As illustrated in Scheme 1.3.17, atoms *d* and *f* of the Type B mesoionic ring react with the dipolarophile, *D*-*E*, in which the exocyclic heteroatom *f* participates in the reaction. The bicyclic product can be stable or undergo subsequent ring opening at the *c*-*d* bond.

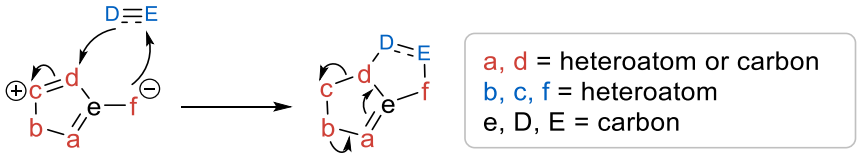

Scheme 1.3.17. 1,3-Dipolar cycloaddition of dipolarophiles with Type B mesoionic rings.

Lindley, Potts, and colleagues showed that cycloaddition of 1,2,3,4-tetrazolium-5-thiolates with benzyne generates an unstable antiaromatic tetrazoline ring that opens to a 1,5-dipolar azo-imide. Subsequent loss of phenylnitrene as the dimeric azobenzene gives 2-phenylazobenzothiazole isolated in 11% yield (Scheme 1.3.18).[89–91]

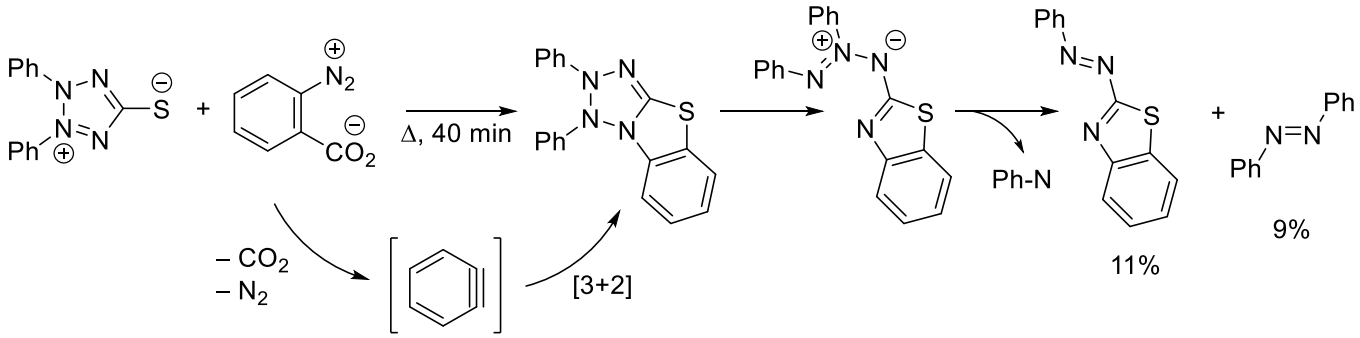

Scheme 1.3.18. 1,3-Dipolar cycloaddition of 1,2,3,4-tetrazolium-5-thiolates with benzyne to form 2-phenylazobenzothiazole.

1.3.1.4 Reactions with Münchnones (1,3-Oxazolium-5-Olates)

Münchnones (1,3-oxazolium-5-olates) were first synthesized in 1959 by Lawson and Miles through the cyclodehydration of 2-pyridine-*N*-acetic acid with acetic anhydride to form a pyridine-based Münchnone derivative.[92] The related cyclodehydration of simple *N*-acylamino acids has since become the most widely used and reliable method to prepare Münchnones. Other alternative methods to form Münchnones have been developed (Scheme 1.3.19). As examples, Hershenson and Tepe independently described the N-alkylation of azalactones with reactive alkylating agents (e.g. organic triflates and tetrafluoroborates[93] or silylated by silyl Lewis acids[94,95]) can generate substituted Münchnone derivatives. More recent methods for synthesizing these dipoles have been developed with carbon monoxide. Merlic employed acylamino chromium carbene complexes that undergo CO insertion to form ketene intermediates that cyclize to the corresponding Münchnone.[96] Additionally, our group has conducted extensive research on palladium-catalyzed multicomponent reactions with imines, acid chlorides, and carbon monoxide, leading to the formation of various heterocycles by trapping *in situ* generated Münchnones.[97–103] The majority of these Münchnones are unstable, and reactions involving them often involve their *in situ* formation and trapping.[104]

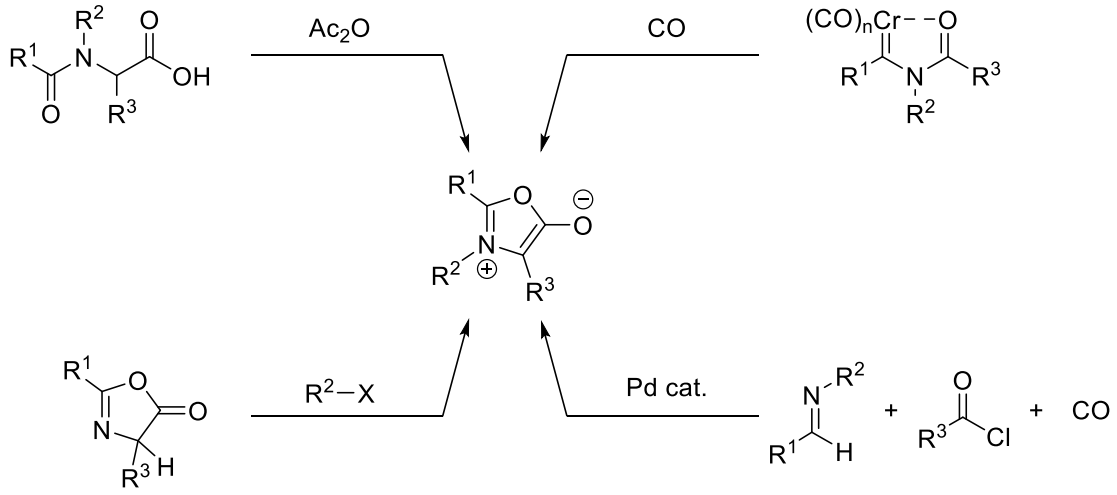

Scheme 1.3.19. Advances in synthetic methods to form Münchnones.

Huisgen *et al.* were the first to explore the cycloaddition reactivity of Münchnones to form heterocycles such as pyrrolines and pyrroles *via* 1,3-dipolar cycloaddition reactions with alkenes and alkynes, respectively.[105,106] Over time, Münchnones have served as key synthetic intermediates in the synthesis of natural products[5,107,108] and pharmaceutically relevant drugs including most notably atorvastatin (Lipitor).[109]

Kato reported the first benzyne cycloaddition between a Münchnone and benzyne. In this, 1-aminobenzotriazole served as the benzyne precursor that upon cycloaddition, forms a bicyclic intermediate that releases CO_2 upon a cycloreversion to give trace amounts (2%) of isoindole. Side products in the reaction include epiminoanthracene and biphenylene in 4% and 7% yields, respectively (Scheme 1.3.20).[79]

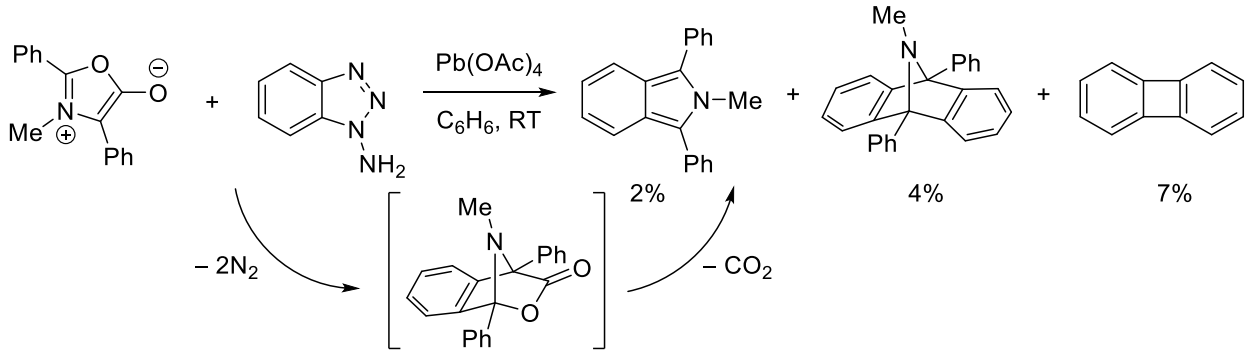

Scheme 1.3.20. First example of the synthesis of isoindoles and epiminoanthracenes through Münchnone [3+2] cycloaddition with 1-aminobenzotriazole.

These studies suggest that the oxidative conditions required to fragment the 1-aminobenzotriazole to form the benzyne intermediate are unsuitable for Münchnones, which are much less stable than Sydnones. In addition, the product of aryne cycloaddition is itself more reactive than Münchnones toward aryne cycloaddition and forms Diels-Alder products. To address these challenges, two groups independently described the [3+2] cycloaddition of Münchnones with *o*-trimethylsilylaryl triflates to form isoindoles and epiminoanthracenes. Larock and Shi used electron poor acyl-substituted Münchnones, which are crystalline and relatively stable, to form epiminoanthracenes in good to excellent yields (Scheme 1.3.21).[110] When the Münchnone was used as the limiting reagent and the aryne precursor was in excess along with a soluble fluoride source, an equal mixture of isoindole and epiminoanthracene, the cycloadduct formed from isoindole and benzyne, were obtained. Selectivity towards the isoindole could be achieved by varying the ratio of the Münchnone and aryne precursor. This was demonstrated by Gribble who employed the aryne precursors as the limiting reagent and CsF, a less soluble fluoride source to synthesize isoindoles in good to excellent yields (Scheme 1.3.22).[111]

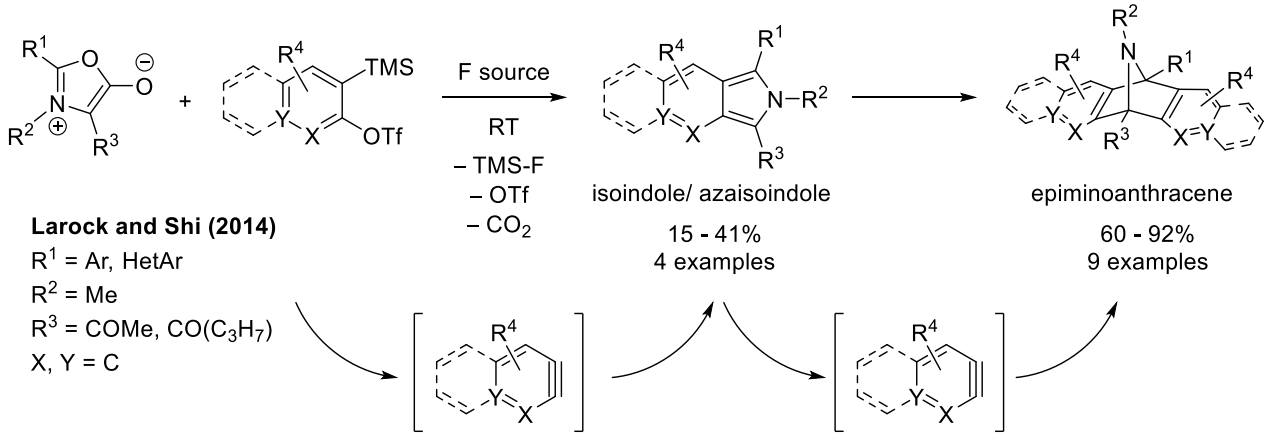

Scheme 1.3.21. Münchnone-benzyne [3+2] cycloaddition to form isoindoles and epiminoanthracenes.

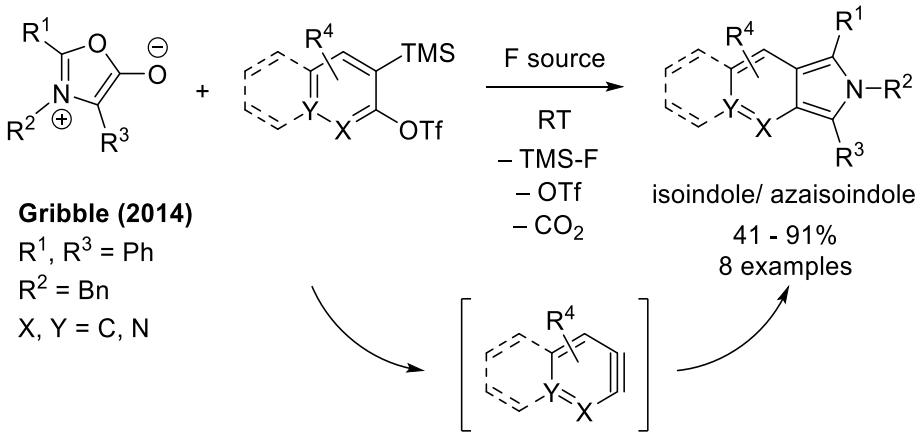

Scheme 1.3.22. Münchnone-benzyne [3+2] cycloaddition to selectively form isoindoles.

1.3.1.5 Reactions with Thioisomünchnones (1,3-Thiazolium-4-Olates)

Thioisomünchnones, 1,3-thiazolium-4-olates, are sulfur derivatives of isomünchnones that contain a thiocarbonyl ylide unit. Over the last few decades, the pioneering works of Potts and Robert were especially valuable for developing synthetic methods to generate these dipoles and studying their reactivity. Early methods to prepare thioisomünchnones involved the dehydration reaction of carboxymethylmercapto precursors with acetic anhydride and triethylamine (Scheme 1.3.23).[112,113] These mesoionic 1,3-dipoles can also be synthesized from the reaction of *gem*-dicyano epoxides with thioamides, resulting in the loss of hydrogen cyanide.[114] Polycyclic derivatives have been accessed through the condensation of cyclic thioureas or dithiocarbamates with α-bromoacyl chlorides.[115–117] More recently, the rhodium catalyzed decomposition of α-diazoamides has been used for the *in-situ* generation of thioisomünchnones.[118–121]

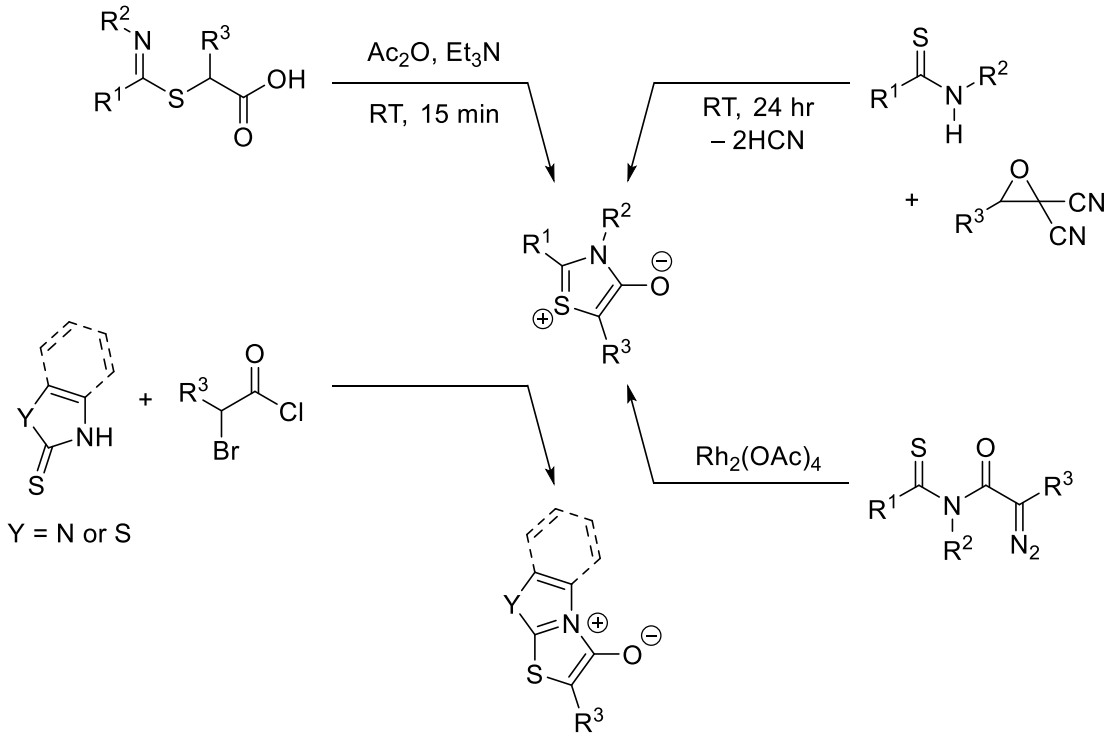

Scheme 1.3.23. Synthesis of thioisomünchnones and polycyclic derivatives.

Thioisomünchnones exhibit distinct reactivity in cycloadditions with alkenes and alkynes, compared to most other mesoionic 1,3-dipoles. Unlike cycloadducts derived from other mesoionic systems, which are often transient, many of those formed from thioisomünchnones are stable enough for isolation. In addition, depending on the substituents on the thioisomünchnone and reaction conditions, two possible pathways are possible to selectively yield pyridones or thiophenes.[122–129] Potts probed this selectivity in the reaction of di- and tri-phenyl substituted thioisomünchnones with dimethyl acetylenedicarboxylate (DMAD).[122] They found that when there was hydrogen at the C5-position of the 1,3-dipole, elimination of sulphur was favoured, resulting in the formation of the corresponding pyridone product in 70% yield. In contrast, when a phenyl group was present at C5, the cycloadduct undergoes fragmentation favouring the release of phenyl isocyanate to give the thiophene product in 90% yield (Scheme 1.3.24). The latter pathway aligns with typical mesoionic 1,3-dipolar cycloadditions.

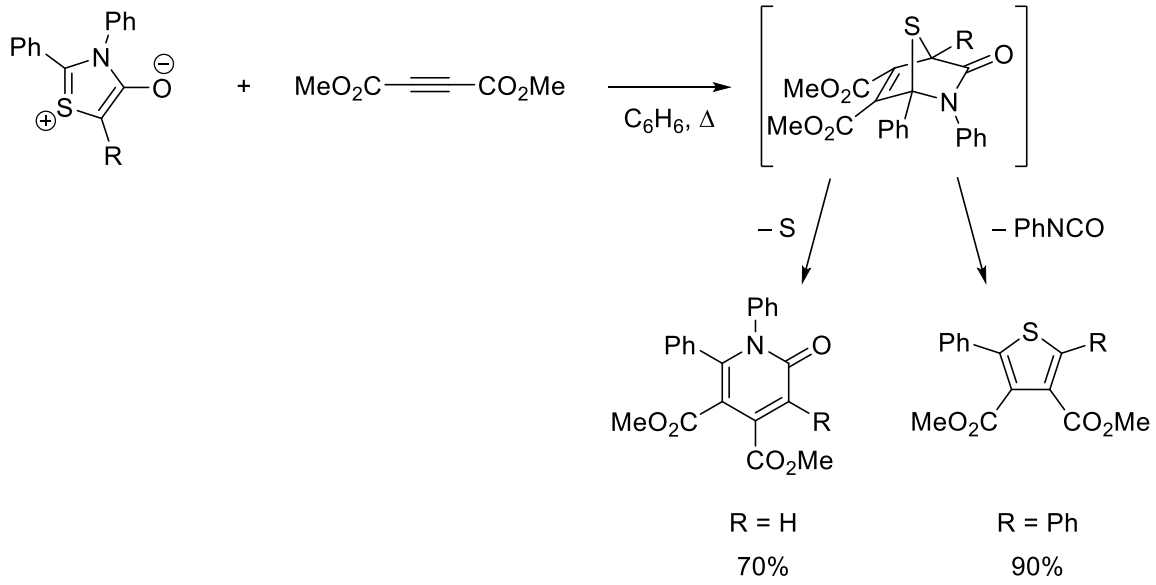

Scheme 1.3.24. Effect of C5-substituent on the regiospecificity of the 1,3-dipolar cycloaddition of thioisomünchnones with DMAD.

Palacios found that the selectivity to form the pyridone or thiophene product can also be influenced by the nature of the substituent at the endocyclic nitrogen of the thioisomünchnone and its ability to stabilize either a concerted, cheletropic transition state or, in the case of a stepwise mechanism, a dipolar intermediate (Scheme 1.3.25).[126]

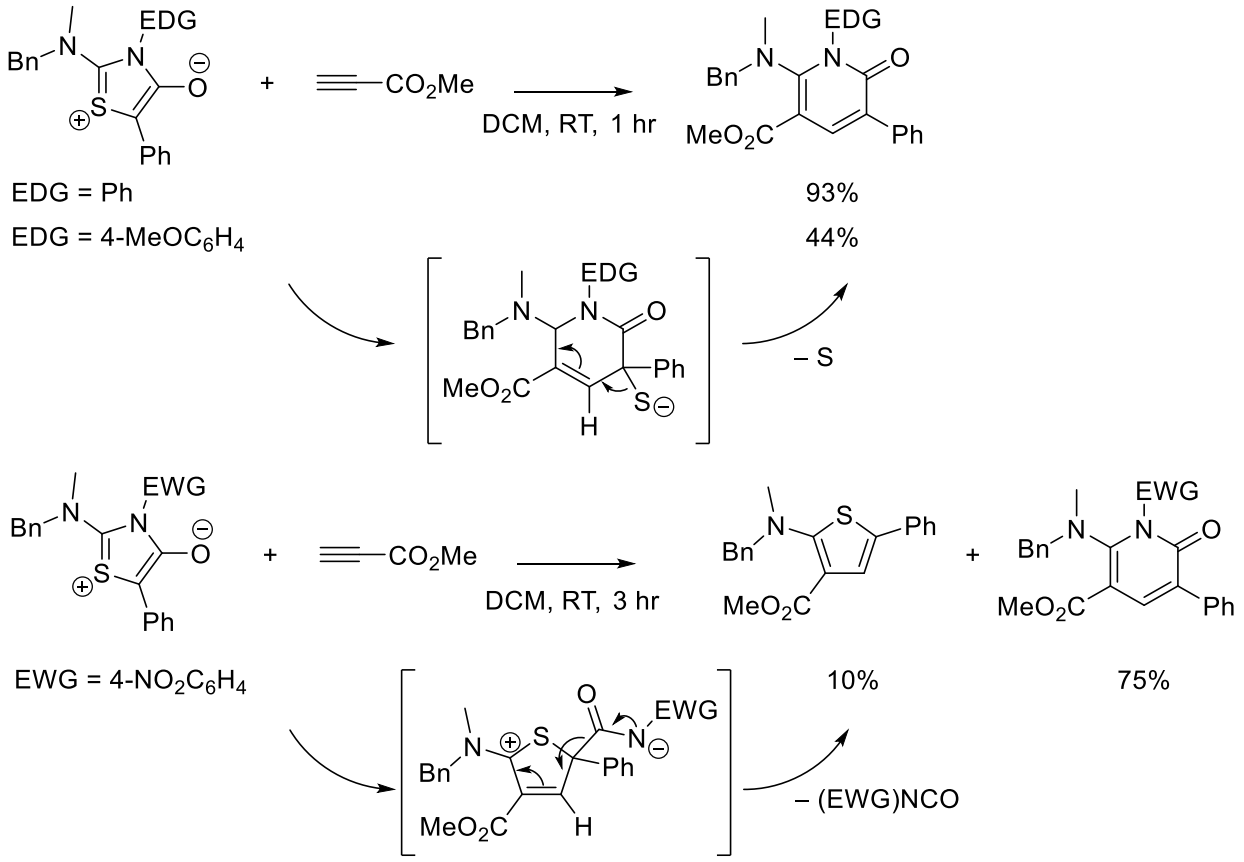

Scheme 1.3.25. Effect of N3-substituent on the regiospecificity of the 1,3-dipolar cycloaddition of thioisomünchnones with methyl propiolate.

Kato reported the cycloaddition of thioisomünchnones with benzyne.[54,79] Product selectivity was found to be influenced by the reaction conditions. Thus, refluxing the primary cycloadduct, which in this case was found to be isolable, formed from triphenyl-substituted thioisomünchnone, and benzyne resulted in the release of phenylisocyanate to form the corresponding benzo-fused thiophene in 67% yield. Alternatively, under UV photochemical irradiation of the same cycloadduct favoured the release of sulfur to form an isoquinolone in 60% yield (Scheme 1.3.26).

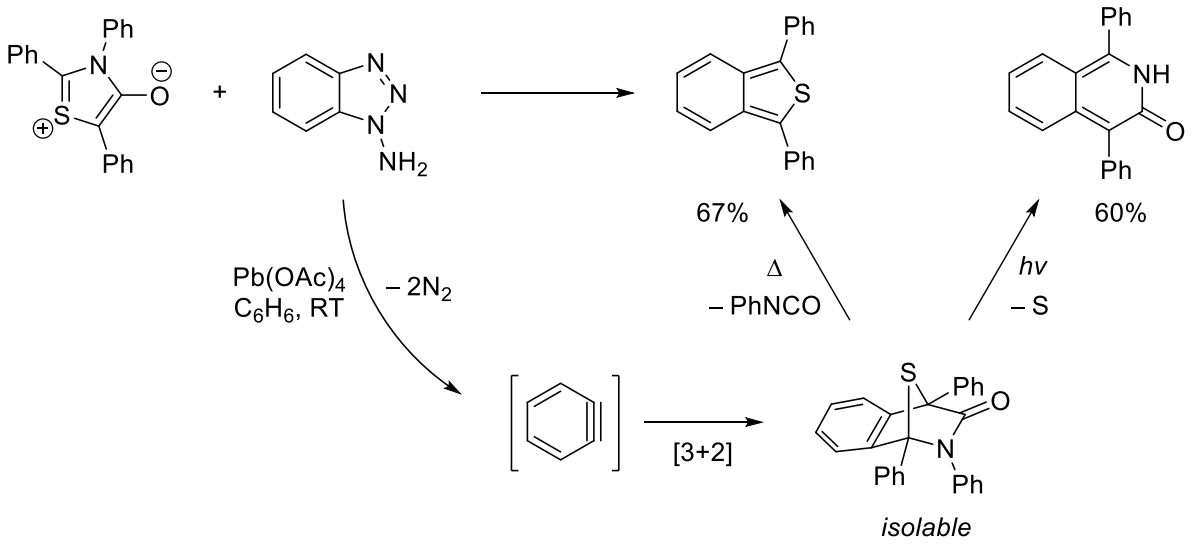

Scheme 1.3.26. 1,3-Dipolar cycloaddition of thioisomünchnone with benzyne under thermal and photochemical conditions.

1.3.1.6 Reactions with 1,3-Dithiolium-4-Olates

1,3-Dithiolium-4-olates, another class of mesoionic 1,3-dipoles, were synthesized by Gotthardt and Potts who independently reported that the cyclodehydration of substituted carboxylic acids using acetic anhydride and triethylamine under low temperatures can be used to form a range of alkyl and aryl disubstituted 1,3-dithiolium-4-olates (Scheme 1.3.27).[130–134] Alternatively, these dipoles can be made through the condensation of dithiobenzoic acids with α-haloacyl halides.[135]

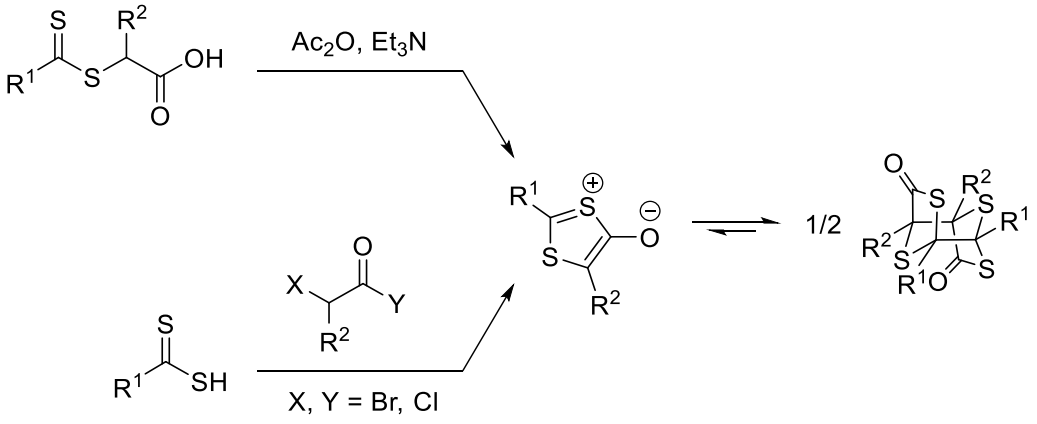

Scheme 1.3.27. Synthetic methods to form 1,3-dithiolium-4-olates.

A number of reports have shown that 1,3-dithiolium-4-olates undergo cycloaddition with alkynes to form thiophenes after elimination of carbonyl sulfide. Similarly, Kato reported the cycloaddition of these cyclic dipoles with benzyne. The reaction of 1-aminobenzotriazole as the benzyne precursor with diphenyl-1,3-dithiolium-4-olate gave 1,3-diphenylbenzo[*c*]thiophene in low yield (Scheme 1.3.28).[54,79]

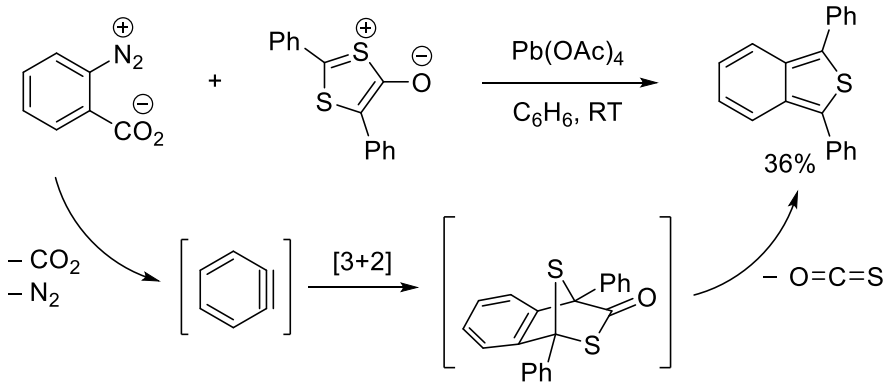

Scheme 1.3.28. Synthesis of diphenylbenzo[*c*]thiophene *via* benzyne 1,3-dipolar cycloaddition with a 1,3-dithiolium-4-olate.

More recently, fused thiophene derivatives with potential applications in materials science were prepared by Audisio and Taran using polyaromatic *o*-trimethylsilylaryl triflates and aromatic substituted 1,3-dithiolium-4-olates (Scheme 1.3.29).[136] They successfully prepared a wide range of benzo[*c*]thiophene derivatives in generally good yields and mild conditions, offering an efficient and direct approach to access polysubstituted thiophenes.

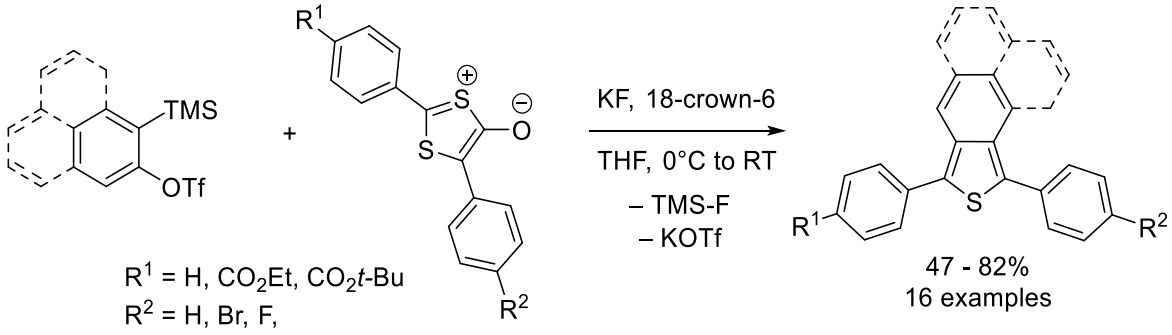

Scheme 1.3.29. Formation of polyaromatic benzo[*c*]thiophenes from 1,3-dipolar cycloaddition of *o*-trimethylsilylaryl triflates and 1,3-dithiolium-4-olates.

1.4 Overview of the Thesis

1,3-Dipolar cycloadditions have long served as an efficient strategy for the synthesis of 5-membered heterocycles. As highlighted above, these reactions typically involve the cycloaddition of a zwitterionic, 1,3-dipole with a multiple-bonded dipolarophile, resulting in the formation of a neutral bicyclic intermediate that undergoes cycloreversion to generate a five-membered ring. Unlike other methods for heterocycle synthesis, the versatility of 1,3-dipolar cycloadditions, enabled by the broad range of accessible 1,3-dipoles, allows synthetic chemists to prepare a range of heterocycles, many of which hold significant pharmaceutical relevance. Among the many heterocycle-containing drug molecules are those with fused heterocycles, which can be prepared *via* 1,3-dipolar cycloaddition with benzyne. This offers a convergent alternative to conventional methods involving intramolecular cyclization and annulations, which are often limited by the need to build up an appropriate precursor for cyclization. As discussed in Section 1.2, the reactive benzyne intermediate can be generated *in situ* under a variety of conditions. Notably, the Kobayashi method, which involves a mild, fluoride-induced elimination of *o*-trimethylsilylphenyl triflate, has contributed substantially to advancing research in modern aryne chemistry. This reactive intermediate can then undergo 1,3-dipolar cycloaddition with acyclic and cyclic 1,3-dipoles to yield a range of benzo-fused heterocyclic products.

Chapter 2 describes an application of this approach to the synthesis of pyrido[2,1-α]isoindoles through a palladium-catalyzed carbonylative coupling of imines, 2-bromopyridines, and *o*-trimethylsilylaryl triflates which is believed to proceed *via* the initial formation of 2-pyridyl acyl chloride that reacts with the imine to form a pyridine-based 1,3-dipole analogous to Münchnones. This intermediate then undergoes cycloaddition with the *in situ* generated benzyne leading to the formation of the corresponding pyrido[2,1-α]isoindole. Overall, this one pot, multicomponent reaction employs readily available or easily synthesized substrates, offering a modular and streamlined route to new variants of substituted pyrido[2,1-α]isoindoles.

1.5 References

(1) Breugst, M.; Reissig, H. U. The Huisgen Reaction: Milestones of the 1,3-Dipolar Cycloaddition. *Angew. Chem. Int. Ed.* **2020**, *59*, 12293–12307.

(2) Buchner, E. Einwirkung von Diazoessigäther auf die Aether ungesättigter Säuren. *Ber. Dtsch. Chem. Ges.* **1888**, *21*, 2637–2647.

(3) Huisgen, R. 1,3-Dipolar Cycloadditions. *Proc. Chem. Soc.* **1961**, 357–396.

(4) Huisgen, R. 1,3-Dipolar Cycloaddition Past and Future. *Angew. Chem. Int. Ed.* **1963**, *2*, 565–598.

(5) Gribble, G. W. Chapter 10 - Mesoionic Ring Systems. In *The Chemistry of Heterocyclic Compounds: Synthetic Applications of 1,3-Dipolar Cycloaddition Chemistry Toward Heterocycles and Natural Products*; 2002; Vol. 59, pp 681–753.

(6) Ollis, W. D.; Ramsden, C. A. Chapter 5 - Meso-Ionic Compounds. In *Advances in Heterocyclic Chemistry*; Elsevier, 2022; Vol. 137, pp 229–347.

(7) Huisgen, R. The Concerted Nature of 1,3-Dipolar Cycloadditions and the Question of Diradical Intermediates. *J. Org. Chem.* **1976**, *41*, 403–419.

(8) Heravi, M. M.; Zadsirjan, V. Prescribed Drugs Containing Nitrogen Heterocycles: An Overview. *RSC Adv.* **2020**, *10*, 44247–44311.

(9) Vitaku, E.; Smith, D. T.; Njardarson, J. T. Analysis of the Structural Diversity, Substitution Patterns, and Frequency of Nitrogen Heterocycles among U.S. FDA Approved Pharmaceuticals. *J. Med. Chem.* **2014**, *57*, 10257–10274.

(10) Marshall, C. M.; Federice, J. G.; Bell, C. N.; Cox, P. B.; Njardarson, J. T. An Update on the Nitrogen Heterocycle Compositions and Properties of U.S. FDA-Approved Pharmaceuticals (2013–2023). *J. Med. Chem.* **2024**, *67*, 11622–11655.

(11) *Name Reactions in Heterocyclic Chemistry*, 1st ed.; Li, J. J., Ed.; John Wiley & Sons, Ltd, 2004.

(12) *Name Reactions in Heterocyclic Chemistry II*, 1st ed.; Li, J. J., Ed.; John Wiley & Sons, Ltd, 2011.

(13) Ne Pellissier, H.; Santelli, M. The Use of Arynes in Organic Synthesis. *Tetrahedron* **2003**, *59*, 701–730.

(14) Tadross, P. M.; Stoltz, B. M. A Comprehensive History of Arynes in Natural Product Total Synthesis. *Chem. Rev.* **2012**, *112*, 3550–3577.

(15) *Modern Aryne Chemistry*; Biju, A., Ed.; Wiley-VCH: Weinheim, 2021.

(16) Bryce, M. R.; Vernon, M. Reactions of Benzyne with Heterocyclic Compounds. In *Advances in Heterocyclic Chemistry*; Katritzky, A. R., Boulton, A. J., Eds.; Academic Press, 1981; Vol. 28, pp 183–229.

(17) Dubrovskiy, A. V.; Markina, N. A.; Larock, R. C. Use of Benzynes for the Synthesis of Heterocycles. *Org. Biomol. Chem.* **2013**, *11*, 191–218.

(18) Sanz, R. Recent Applications of Aryne Chemistry to Organic Synthesis. A Review. *Org. Prep. Proced. Int.* **2008**, *40*, 215–291.

(19) Hamura, T. Chapter 3 - Pericyclic Reactions Including [2+2], [3+2], and [4+2] Cycloadditions. In *Comprehensive Aryne Synthetic Chemistry*; 2022; pp 267–330.

(20) Fittig, R. Ueber einige Derivate des Diphenyls. *Justus Liebigs Ann. Chem.* **1864**, *132*, 201–215.

(21) Stoermer, R.; Kahlert, B. Ueber Das 1- Und 2-Brom-cumaron. *Ber. Dtsch. Chem. Ges.* **1902**, *35*, 1633–1640.

(22) Roberts, J. D.; Simmons, H. E. Jr.; Carlsmith, L. A.; Vaughan, C. W. Rearrangement in the Reaction of Chlorobenzene-1-C14 with Potassium Amide. *J. Am. Chem. Soc.* **1953**, *75*, 3290–3291.

(23) Roberts, J. D.; Semenow, D. A.; Simmons, H. E. Jr.; Carlsmith, L. A. The Mechanism of Aminations of Halobenzenes. *J. Am. Chem. Soc.* **1956**, *78*, 601–611.

(24) Roberts, J. D.; Vaughan, C. W.; Carlsmith, L. A.; Semenow, D. A. Orientation in Aminations of Substituted Halobenzenes. *J. Am. Chem. Soc.* **1956**, *78*, 611–614.

(25) Wittig, G. Intermediare Bildung von Dehydrobenzol (Cyclohexa-dienin). *Angew. Chem.* **1955**.

(26) Heaney, H.; Mann, F. G.; Millar, I. T. The Reaction of O-Bromoiodobenzene with Magnesium and Lithium. *J. Chem. Soc.* **1957**, 3930–3938.

(27) Wittig, G.; Knauss, E. Dehydrobenzol und Cyclopentadien. *Chem. Ber.* **1958**, *91*, 895–907.

(28) Ebert, G. W.; Pfemig, D. R.; Suchan, S. D.; Jr, T. A. D. Remarkably Stable Ortho-Halophenylcopper Reagents. *Tetrahedron Lett.* **1993**, *34*, 2279–2282.

(29) Matsumoto, T.; Hosoya, T.; Katsuki, M.; Suzuki, K. New Efficient Protocol for Aryne Generation. Selective Synthesis of Differentially Protected 1,4,5-Naphthalenetriols. *Tetrahedron Lett.* **1991**, *32*, 6735–6736.

(30) Mesgar, M.; Nguyen-Le, J.; Daugulis, O. New Hindered Amide Base for Aryne Insertion into Si–P, Si–S, Si–N, and C–C Bonds. *J. Am. Chem. Soc.* **2018**, *140*, 13703–13710.

(31) Olofson, R. A.; Dougherty, C. M. Lithium 2,2,6,6-Tetramethylpiperidide and Related, Strong, Proton-Specific Bases. Evaluation in Synthesis. *J. Am. Chem. Soc.* **1973**, *95*, 582–584.

(32) Stiles, Martin.; Miller, R. G.; Burckhardt, Urs. Reactions of Benzyne Intermediates in Non-Basic Media. *J. Am. Chem. Soc.* **1963**, *85*, 1792–1797.

(33) Stiles, M.; Miller, R. G. Decomposition of Benzenediazonium-2-Carboxylate. *J. Am. Chem. Soc.* **1960**, *82*, 3802–3802.

(34) Wittig, G.; Hoffmann, R. W. Dehydrobenzol aus 1.2.3-Benzothiadiazol-1.1-dioxyd. *Chem. Ber.* **1962**, *95*, 2718–2728.

(35) Le Goff, Eugene. Aprotic Generation of Benzyne from Diphenyliodonium-2-Carboxylate. *J. Am. Chem. Soc.* **1962**, *84*, 3786–3786.

(36) Yoshimura, A.; Saito, A.; Zhdankin, V. V. Iodonium Salts as Benzyne Precursors. *Chem. Eur. J.* **2018**, *24*, 15156–15166.

(37) Campbell, C. D.; Rees, C. W. Oxidation of 1- and 2-Aminobenzotriazole. *Chem. Commun.* **1965**, 192.

(38) Campbell, C. D.; Rees, C. W. Reactive Intermediates. Part I. Synthesis and Oxidation of 1- and 2-Aminobenzotriazole. *J. Chem. Soc., C* **1969**, 742.

(39) Birkett, M. A.; Knight, D. W.; Little, P. B.; Mitchell, M. B. A New Approach to Dihydrobenzofurans and Dihydrobenzopyrans (Chromans) Based on the Intramolecular Trapping by Alcohols of Benzynes Generated from 7-Substituted-1-Aminobenzotriazoles. *Tetrahedron* **2000**, *56*, 1013–1023.

(40) Himeshima, Y.; Sonoda, T.; Kobayashi, H. Fluoride-Induced 1,2-Elimination of o-Trimethylsilylphenyl Triflate to Benzyne Under Mild Conditions. *Chem. Lett.* **1983**, *12*, 1211–1214.

(41) Shi, J.; Li, L.; Li, Y. O-Silylaryl Triflates: A Journey of Kobayashi Aryne Precursors. *Chem. Rev.* **2021**, *121*, 3892–4044.

(42) Yoshida, H. Chapter 1 - General Introduction to Comprehensive Aryne Synthetic Chemistry. In *Comprehensive Aryne Synthetic Chemistry*; Elsevier, 2022; pp 1–11.

(43) Sarmah, M.; Sharma, A.; Gogoi, P. Exploration of Kobayashi's Aryne Precursor: A Potent Reactive Platform for the Synthesis of Polycyclic Aromatic Hydrocarbons. *Org. Biomol. Chem.* **2021**, *19*, 722–737.

(44) Huisgen, R.; Knorr, R. Benz-in Als Dipolarophil. *Naturwissenschaften* **1961**, *48*, 716.

(45) Earl, J. C.; Mackney, A. W. The Action of Acetic Anhydride on N-Nitrosofihenylglycine and Some of Its Derivatives. *J. Chem. Soc.* **1935**, 899–900.

(46) Stewart, F. H. C. The Chemistry of the Sydnones. *Chem. Rev.* **1964**, *64*, 129–147.

(47) Newton, C. G.; Ramsden, C. A. Chapter Six - Meso-Ionic Heterocycles (1976–1980). In *Advances in Heterocyclic Chemistry*; Ramsden, C. A., Ed.; Heterocyclic Mesomeric Betaines and Mesoionic Compounds; Academic Press, 2022; Vol. 137, pp 351–424.

(48) Baker, W.; Ollis, W. D.; Poole, V. D. Cyclic Meso-Ionic Compounds. Part 1. The Structure of the Sydnone and Related Compounds. *J. Chem. Soc.* **1949**, *73*, 307–314.

(49) Shih, M.-H.; Ke, F.-Y. Syntheses and Evaluation of Antioxidant Activity of Sydnonyl Substituted Thiazolidinone and Thiazoline Derivatives. *Bioorg. Med. Chem.* **2004**, *12*, 4633–4643.

(50) Moustafa, M. A.; Gineinah, M. M.; Nasr, M. N.; Bayoumi, W. A. H. Novel Analogues of Sydnone: Synthesis, Characterization and Antibacterial Evaluation. *Archiv der Pharmazie* **2004**, *337*, 427–433.

(51) Galuppo, L. F.; dos Reis Lívero, F. A.; Martins, G. G.; Cardoso, C. C.; Beltrame, O. C.; Klassen, L. M. B.; Canuto, A. V. dos S.; Echevarria, A.; Telles, J. E. Q.; Klassen, G.; Acco, A. Sydnone 1: A Mesoionic Compound with Antitumoral and Haematological Effects In Vivo. *BCPT* **2016**, *119*, 41–50.

(52) Huisgen, R.; Grashey, R.; Gotthardt, H.; Schmidt, R. 1,3-Dipolar Additions of Sydnones to Alkynes. A New Route into the Pyrazole Series. *Angew. Chem., Int. Ed. Engl.* **1962**, *1*, 48–49.

(53) Gotthardt, H.; Huisgen, R.; Knorr, R. Reaktionen der Sydnone mit Benz-in und mit einigen Heteromehrfachbindungen. *Chem. Ber.* **1968**, *101*, 1056–1058.

(54) Nakazawa, S.; Kiyosawa, T.; Hirakawa, K.; Kato, H. Selectivity in the Thermal and Photochemical Fragmentation of the Cycloadduct from Benzyne and a Mesoionic Thiazol-4-One. *J. Chem. Soc., Chem. Commun.* **1974**, 621.

(55) Wu, C.; Fang, Y.; Larock, R. C.; Shi, F. Synthesis of 2H-Indazoles by the [3 + 2] Cycloaddition of Arynes and Sydnones. *Org. Lett.* **2010**, *12*, 2234–2237.

(56) Fang, Y.; Wu, C.; Larock, R. C.; Shi, F. Synthesis of 2H-Indazoles by the [3 + 2] Dipolar Cycloaddition of Sydnones with Arynes. *J. Org. Chem.* **2011**, *76*, 8840–8851.

(57) Orgel, L. E.; Cottrell, T. L.; Dick, W.; Sutton, L. E. The Calculation of the Electric Dipole Moments of Some Conjugated Heterocyclic Compounds. *Trans. Faraday Soc.* **1950**, *47*, 113.

(58) Houk, K. N.; Sims, Joyner.; Duke, R. E.; Strozier, R. W.; George, J. K. Frontier Molecular Orbitals of 1,3 Dipoles and Dipolarophiles. *J. Am. Chem. Soc.* **1973**, *95*, 7287–7301.

(59) Padwa, A.; Burgess, E. M.; Gingrich, H. L.; Roush, D. M. On the Problem of Regioselectivity in the 1,3-Dipolar Cycloaddition Reaction of Munchnones and Sydnones with Acetylenic Dipolarophiles. *J. Org. Chem.* **1982**, *47*, 786–791.

(60) Browne, D. L.; Harrity, J. P. A. Recent Developments in the Chemistry of Sydnones. *Tetrahedron* **2010**, *66*, 553–568.

(61) Soares, M. I. L.; Nunes, C. M.; Gomes, C. S. B.; Pinho e Melo, T. M. V. D. Thiazolo[3,4-b]Indazole-2,2-Dioxides as Masked Extended Dipoles: Pericyclic Reactions of Benzodiazafulvenium Methides. *J. Org. Chem.* **2013**, *78*, 628–637.

(62) Ikawa, T.; Masuda, S.; Takagi, A.; Akai, S. 1,3- and 1,4-Benzdiyne Equivalents for Regioselective Synthesis of Polycyclic Heterocycles. *Chem. Sci.* **2016**, *7*, 5206–5211.

(63) Ikawa, T.; Masuda, S.; Nakajima, H.; Akai, S. 2-(Trimethylsilyl)Phenyl Trimethylsilyl Ethers as Stable and Readily Accessible Benzyne Precursors. *J. Org. Chem.* **2017**, *82*, 4242–4253.

(64) Hatakeyama, T.; Hashimoto, S.; Oba, T.; Nakamura, M. Azaboradibenzo[6]Helicene: Carrier Inversion Induced by Helical Homochirality. *J. Am. Chem. Soc.* **2012**, *134*, 19600–19603.

(65) Yang, Y.; Da Costa, R. C.; Fuchter, M. J.; Campbell, A. J. Circularly Polarized Light Detection by a Chiral Organic Semiconductor Transistor. *Nat. Photonics* **2013**, *7*, 634–638.

(66) Collins, S. K.; Vachon, M. P. Unlocking the Potential of Thiaheterohelicenes: Chemical Synthesis as the Key. *Org. Biomol. Chem.* **2006**, *4*, 2518.

(67) Otani, T.; Tsuyuki, A.; Iwachi, T.; Someya, S.; Tateno, K.; Kawai, H.; Saito, T.; Kanyiva, K. S.; Shibata, T. Facile Two-Step Synthesis of 1,10-Phenanthroline-Derived Polyaza[7]Helicenes with High Fluorescence and CPL Efficiency. *Angew. Chem. Int. Ed.* **2017**, *56*, 3906–3910.

(68) Yen-Pon, E.; Champagne, P. A.; Plougastel, L.; Gabillet, S.; Thuéry, P.; Johnson, M.; Muller, G.; Pieters, G.; Taran, F.; Houk, K. N.; Audisio, D. Sydnone-Based Approach to Heterohelicenes through 1,3-Dipolar-Cycloadditions. *J. Am. Chem. Soc.* **2019**, *141*, 1435–1440.

(69) Yen-Pon, E.; Buttard, F.; Frédéric, L.; Thuéry, P.; Taran, F.; Pieters, G.; Champagne, P. A.; Audisio, D. Heterohelicenes through 1,3-Dipolar Cycloaddition of Sydnones with Arynes: Synthesis, Origins of Selectivity, and Application to pH-Triggered Chiroptical Switch with CPL Sign Reversal. *JACS Au* **2021**, *1*, 807–818.

(70) Shi, J.; Xu, H.; Qiu, D.; He, J.; Li, Y. Selective Aryne Formation via Grob Fragmentation from the [2+2] Cycloadducts of 3-Triflyloxyarynes. *J. Am. Chem. Soc.* **2017**, *139*, 623–626.

(71) Papeo, G.; Casale, E.; Montagnoli, A.; Cirla, A. PARP Inhibitors in Cancer Therapy: An Update. *Expert Opin. Ther. Patents* **2013**, *23*, 503–514.

(72) Yi, M.; Dong, B.; Qin, S.; Chu, Q.; Wu, K.; Luo, S. Advances and Perspectives of PARP Inhibitors. *Exp. Hematol. Oncol.* **2019**, *8*, 29.

(73) Busch, M. Über heterobicyklische Verbindungen der Thiobiazol- und Triazolreihe. *J. Prakt. Chem.* **1903**, *67*, 201–215.

(74) Ollis, W. D.; Baker, W. Meso-Ionic Compounds. *Q. Rev. Chem. Soc.* **1957**, *11*, 15–29.

(75) Kato, H.; Sato, S.; Ohta, M. The Cycloaddition of 3-Phenylsydnone with Phenyl Isocyanate. *Tetrahedron Lett.* **1967**, *8*, 4261–4262.

(76) Grashey, R.; Weidner, M.; Schroll, G. Mesoionische Azolium-Olate Aus Den Tholaten. *Chemischer Informationsdienst* **1976**, *100*, 497–498.

(77) Ziman, S. D. A New Mesoionic Species in the Synthesis of Some 5-Thioxo-1,2,4-Triazolin-3-Ones. *J. Heterocycl. Chem.* **1980**, *17*, 1319–1319.

(78) Molina, P.; Alajarin, M.; Arques, A.; Benzal, R.; Hernandez, H. Fused Mesoionic Heterocycles: Synthesis of 1,3,4-Triazolo[3,2-a] Pyridine Derivatives. *J. Chem. Soc., Perkin Trans. I* **1984**, 1891–1897.

(79) Kato, H.; Nakazawa, S.; Kiyosawa, T.; Hirakawa, K. Heterocycles by Cycloaddition. Part II. Cycloaddition-Extrusion Reactions of Five-Membered Mesoionic Compounds with Benzyne: Preparation of Benz[c]Azole and Benzo[c]Thiophen Derivatives. *J. Chem. Soc., Perkin Trans. I* **1976**, 672–675.

(80) Lwowski, W.; Kanemasa, S.; Murray, R. A.; Ramakrishnan, V. T.; Thiruvengadam, T. K.; Yoshida, K.; Subbaraj, A. The Photolysis of Carbamoyl Azides in the Presence of Carbodiimides. *J. Org. Chem.* **1986**, *51*, 1719–1723.

(81) Fischer, E.; Besthorn, E. Ueber Die Hydrazinverbindungen. *Justus Liebigs Annalen der Chemie* **1882**, *212*, 316–339.

(82) Ramakrishna, R. S.; Irving, H. M. N. H. The Non-Existence of Selenium Dithiozonate. *J. Chem. Soc. D* **1969**, 1356.

(83) Hutton, A. T.; Irving, H. M. N. H. 3-Carboxymethylthio-1,5-Diphenylformazan: A Potential Terdentate Ligand with Unusual Properties. *J. Chem. Soc., Perkin Trans. II* **1980**, 139.

(84) Jian, F.; Zhao, P.; Zhang, L.; Hou, Y. Synthesis of 2,3-Diaryltetrazole-5-Thiones and Theoretical Studies on Atomic Charge Distributions of 2,3-Diphenyltetrazole-5-Thione. *J. Org. Chem.* **2005**, *70*, 8322–8326.

(85) Kagami, H.; Motoki, S. Nucleophilic Substitution on Dialkoxy Bisulfides. II. Reactions with Hydrazine Derivatives. *Bull. Chem. Soc. Jpn.* **1979**, *52*, 3463–3464.

(86) Ollis, W. D.; Ramsden, C. A. Meso-Ionic Compounds*. In *Advances in Heterocyclic Chemistry*; Katritzky, A. R., Boulton, A. J., Eds.; Academic Press, 1976; Vol. 19, pp 1–122.

(87) Newton, C. G.; Ramsden, C. A. Meso-Ionic Heterocycles (1976–1980). *Tetrahedron* **1982**, *38*, 2965–3011.

(88) Dumitrascu, F.; Ramsden, C. A. Type B Mesoionic Compounds (1980–2020). In *Advances in Heterocyclic Chemistry*; Elsevier, 2022; Vol. 137, pp 191–225.

(89) Boyd, G. V.; Norris, T.; Lindley, P. F.; Mahmoud, M. M. Reactions of Dehydrodithizone with Dimethyl Acetylenedicarboxylate and with Benzyne. X-Ray Crystal Structure of Azobenzene N-(4,5-Bis-Methoxycarbonylthiazol-2-Yl)Imide, a Stable Dipole. *J. Chem. Soc., Perkin Trans. I* **1977**, 1612.

(90) Potts, K. T.; Elliott, A. J.; Titus, G. R.; Al-Hilal, D.; Lindley, P. F.; Boyd, G. V.; Norris, T. Reaction of Dehydrodithizone with Benzyne and Diphenylcyclopropenethione. Isolation of N-(1,2-Diphenyldiazonia)-1,3-Benzothiazole-2-Aminate and the Formation of 2-Phenylazo-4,6,7-Triphenyl-4H-1,3,4-Thiadiazepine-5-Thione. *J. Chem. Soc., Perkin Trans. I* **1981**, 2692–2694.

(91) Potts, K. T.; Elliott, A. J.; Titus, G. R.; Al-Hilal, D.; Lindley, P. F.; Boyd, G. V.; Norris, T. The Structure of Azobenzene N-(Benzothiazol-2-Yl)Imide [3-(2-Benzothiazolyl)-1,2-Diphenyltriazenium Hydroxide, Inner Salt]. *Acta Cryst.* **1982**, *B38*, 682–685.

(92) Lawson, A.; Miles, D. H. Some New Mesoionic Compounds. *J. Chem. Soc.* **1959**, 2865–2871.

(93) Hershenson, Fred. M.; Pavia, M. R. Synthesis of N-Substituted Pyrroles from Azlactones via 1,3-Oxazolium 5-Oxides. *Synthesis (Germany)* **1988**, 999–1001.

(94) Peddibhotla, S.; Jayakumar, S.; Tepe, J. J. Highly Diastereoselective Multicomponent Synthesis of Unsymmetrical Imidazolines. *Org. Lett.* **2002**, *4*, 3533–3535.

(95) Peddibhotla, S.; Tepe, J. J. Multicomponent Synthesisof Highly Substituted Imidazolines via a Silicon Mediated 1,3-DipolarCycloaddition. *Synthesis* **2003**, *9*, 1433–1440.

(96) Merlic, C. A.; Baur, A.; Aldrich, C. C. Acylamino Chromium Carbene Complexes: Direct Carbonyl Insertion, Formation of Münchnones, and Trapping with Dipolarophiles. *J. Am. Chem. Soc.* **2000**, *122*, 7398–7399.

(97) Dhawan, R.; Dghaym, R. D.; Arndtsen, B. A. The Development of a Catalytic Synthesis of Münchnones: A Simple Four-Component Coupling Approach to α-Amino Acid Derivatives. *J. Am. Chem. Soc.* **2003**, *125*, 1474–1475.

(98) Dhawan, R.; Dghaym, R. D.; St. Cyr, D. J.; Arndtsen, B. A. Direct, Palladium-Catalyzed, Multicomponent Synthesis of β-Lactams from Imines, Acid Chloride, and Carbon Monoxide. *Org. Lett.* **2006**, *8*, 3927–3930.

(99) Worrall, K.; Xu, B.; Bontemps, S.; Arndtsen, B. A. A Palladium-Catalyzed Multicomponent Synthesis of Imidazolinium Salts and Imidazolines from Imines, Acid Chlorides, and Carbon Monoxide. *J. Org. Chem.* **2011**, *76*, 170–180.

(100) Xu, B.; Worrall, K.; Arndtsen, B. A. Palladium-Catalyzed Multicomponent Synthesis of 2-Imidazolines from Imines and Acid Chlorides. *Molecules* **2012**, *17*, 13759–13768.

(101) Tjutrins, J.; Dhawan, R.; Lu, Y.; Arndtsen, B. A. Mechanism of the Palladium-Catalyzed Synthesis of Münchnones: The Role of Ligands in N-Acyl Iminium Salt Carbonylation. *Chem. Eur. J.* **2016**, *22*, 15945–15954.

(102) Torres, G. M.; De, M.; Macias, L. H.; Quesnel, J. S.; Williams, O. P.; Yempally, V.; Bengali, A. A.; Arndtsen, B. A. Palladium-Catalyzed, Multicomponent Approach to β-Lactams via Aryl Halide Carbonylation. *J. Org. Chem.* **2016**, *81*, 12106–12115.

(103) Tjutrins, J.; Arndtsen, B. A. A Palladium-Catalyzed Synthesis of (Hetero)Aryl-Substituted Imidazoles from Aryl Halides, Imines and Carbon Monoxide. *Chem. Sci.* **2017**, *8*, 1002–1007.

(104) Reissig, H.; Zimmer, R. Münchnones - New Facets after 50 Years. *Angew. Chem. Int. Ed.* **2014**, *53*, 9708–9710.

(105) Huisgen, R.; Gotthardt, H.; Bayer, H. O.; Schaefer, F. C. A New Type of Mesoionic Aromatic Compound and Its 1,3-Dipolar Cycloaddition Reactions with Acetylene Derivatives. *Angew. Chem., Int. Ed. Engl.* **1964**, *3*, 136–137.

(106) Huisgen, R.; Gotthardt, H.; Bayer, H. O. 1.3-Dipolare Cycloadditionen, LV. Δ^{1} -Pyrroline und 7-Aza-bicyclo[2.2.1]heptane aus Azlactonen und aktivierten Alkenen. *Chem. Ber.* **1970**, *103*, 2368–2387.

(107) Tokuyama, H. The Total Synthesis of Biosynthetically Related Monoterpene Indole Alkaloids. *J. Syn. Org. Chem., Jpn.* **2015**, *73*, 1120–1129.

(108) Sugimoto, K.; Miyakawa, Y.; Tokuyama, H. Total Synthesis of (−)-Rhazinilam Using 1,3-Dipolar Cycloaddition of Optically Active Münchnone Intermediate. *Tetrahedron* **2015**, *71*, 3619–3624.

(109) Lopchuk, J. M.; Gribble, G. W. Total Synthesis of Atorvastatin via a Late-Stage, Regioselective 1,3-Dipolar Münchnone Cycloaddition. *Tetrahedron Lett.* **2015**, *56*, 3208–3211.

(110) Fang, Y.; Larock, R. C.; Shi, F. Aryne Cycloaddition with Stable Münchnones: Synthesis of 9,10-Dihydro-9,10-Epiminoanthracenes and Isoindoles. *Asian. J. Org. Chem.* **2014**, *3*, 55–57.

(111) Lopchuk, J. M.; Gribble, G. W. The Reaction of Arynes with Münchnones: Synthesis of Isoindoles and Azaisoindoles. *Tetrahedron Lett.* **2014**, *55*, 2809–2812.

(112) Potts, K. T.; Singh, U. P.; Houghton, E. Mesoionic Compounds of the Thiazole Series: Anhydro-2,3-Diphenyl-4-Hydroxythiazolium Hydroxide. *J. Chem. Soc. D* **1969**, *19*, 1128–1129.

(113) Potts, K. T.; Choudhury, D. R. Mesoionic Compounds. 44. Synthesis and Cycloaddition Reactions of the Anhydro-1-Hydroxythiazolo[3,2-a]Quinolinium Hydroxide System. *J. Org. Chem.* **1978**, *43*, 2700–2702.

(114) Baudy, M.; Robert, A. A New Synthetic Route to Mesoionic Thiazoles. *J. Chem. Soc., Chem. Commun.* **1976**, 23–24.

(115) Potts, K. T.; Choudhury, D. R. Mesoionic Compounds. 43. Ring Annulation Utilizing the Isomeric Anhydro-2- and 3-Hydroxythiazolo[2,3-b]Benzothiazolium Hydroxide Mesoionic Systems. *J. Org. Chem.* **1978**, *43*, 2697–2700.

(116) Potts, K. T.; Kanemasa, S. Mesoionic Compounds. 49. Ring Annulation with Heterocyclic Ylides. Annulation of Pyridones to the Imidazole and 1,2,4-Triazole Systems. *J. Org. Chem.* **1979**, *44*, 3803–3808.

(117) Potts, K. T.; Kanemasa, S. Mesoionic Compounds. 50. Ring Annulation with Heterocyclic Ylides. Annulation of Pyridinones to the Thiazole and 1,3,4-Thiadiazole Systems. *J. Org. Chem.* **1979**, *44*, 3808–3811.

(118) Muthusamy, S.; Gangadurai, C. Domino Reactions of Bis-Diazo Compounds: Rhodium(II) Acetate Catalyzed Diastereoselective Synthesis of Epoxy- and Epithio-Bridged Heterocycle-Fused Quinolizinone Analogues. *Synthesis* **2016**, *48*, 2213–2225.

(119) Moody, C. J.; Slawin, A. M. Z.; Willows, D. Dirhodium(II) Tetraacetate Catalysed Reactions of Diazo Thioamides: Isolation and Cycloaddition of Anhydro-4-Hydroxy-1,3-Thiazolium Hydroxides (Thioisomünchnones), an Approach to Analogues of Dehydrogliotoxin. *Org. Biomol. Chem.* **2003**, *1*, 2716–2722.

(120) Padwa, A.; Kinder, F. R.; Nadler, W. R.; Zhi, L. Rhodium(II) Catalyzed Cyclization of Diazo Thiocarbonyl Compounds for Heterocyclic Synthesis. *Heterocycles* **1993**, *35*, 367–383.

(121) Padwa, A.; Kinder, F. R.; Zhi, L. Generation of Thiocarbonyl Ylides from the Rhodium(II) -Catalyzed Cyclization of Diazothiocarbonyl Compounds. *Synlett* **1991**, *4*, 287–288.

(122) Potts, K. T.; Houghton, E.; Singh, U. P. Cycloadditions of Anhydro-2,3-Diphenyl-4-Hydroxythiazolium Hydroxides: Reaction with Dimethyl Acetylenedicarboxylate. *J. Chem. Soc. D* **1969**, 1129–1130.

(123) Potts, K. T.; McKeough, D. Thieno[3,4-f]Benzo[c]Thiophene System, a Nonclassical 14.Pi.-Electron Heterocycle. *J. Am. Chem. Soc.* **1973**, *95*, 2750–2751.

(124) Robert, A.; Ferrey, M.; Le Maréchal, A. Quaternarisation de l'atome d'azote de systemes tautomeres de la serie des oxo-4 thiazoles. Cycloadditions dipolaires 1,3 des thiazoles mesoioniques formes in situ. *Tetrahedron* **1980**, *36*, 1571–1578.

(125) Baudy, M.; Robert, A.; Guimon, C. Reaction de Cycloaddition Dipolaire-1,3-Des Thiazolones et Des Selenazolones Mesoioniques Avec l'acetylene Dicarboxylate de

Methyle—II: Influence de La Nature Des Substituants Sur La Reactivite Observee et Sur La Nature Des Produits Obtenus. *Tetrahedron* **1982**, *38*, 2129–2137.

(126) Arevalo, M. J.; Avalos, M.; Babiano, R.; Cintas, P.; Hursthouse, M. B.; Jimenez, J. L.; Light, M. E.; Lopez, I.; Palacios, J. C. [3+2]-Cycloadditions of 2-Aminothioisomunchnones to Alkynes: Synthetic Scope and Mechanistic Insights. *Tetrahedron* **2000**, *56*, 1247–1255.

(127) Avalos, M.; Babiano, R.; Cabanillas, A.; Cintas, P.; Diánez, M. J.; Estrada, M. D.; Jiménez, J. L.; López-Castro, A.; Palacios, J. C.; Garrido, S. P. A Novel Highly Diastereoselective Synthesis of Chiral Dihydrothiophenes from Mesoionic Compounds. *J. Chem. Soc., Chem. Commun.* **1995**, 2213–2214.

(128) Avalos, M.; Babiano, R.; Cabanillas, A.; Cintas, P.; Higes, F. J.; Jiménez, J. L.; Palacios, J. C. Cycloaddition Chemistry of 1,3-Thiazolium-4-Olate Systems. Reaction with Nitroalkenes and Interpretation of Results Using PM3 Calculations. *J. Org. Chem.* **1996**, *61*, 3738–3748.

(129) García De La Concepción, J.; Ávalos, M.; Cintas, P.; Jiménez, J. L.; Light, M. E. Mechanistic Studies of 1,3-Dipolar Cycloadditions of Bicyclic Thioisomünchnones with Alkenes. A Computational Rationale Focused on Donor–Acceptor Interactions. *Org. Biomol. Chem.* **2018**, *16*, 3438–3452.

(130) Gotthardt, H.; Christl, B. Anhydro-5-Hydroxy-1.3-Dithiolium-Hydroxide, Eine Neue Klasse Mesoionischer Aromaten. *Tetrahedron Lett.* **1968**, *9*, 4743–4745.

(131) Gotthardt, H.; Weisshuhn, M. C.; Christl, B. Darstellung und physikalische Eigenschaften mesoionischer 1,3-Dithiolone. *Chemische Berichte* **1976**, *109*, 740–752.

(132) Potts, K. T.; Choudhury, D. R.; Elliott, A. J.; Singh, U. P. Mesoionic Compounds. 38. The Anhydro-2-Aryl-1,3-Dithiolium Hydroxide System. *J. Org. Chem.* **1976**, *41*, 1724–1728.

(133) Gotthardt, H.; Pflaumbaum, W. Synthese Und Physikalische Eigenschaften Neuer 2,2′-verbrückter Bis(1,3-dithiolylium-4-olate). *Chem. Ber.* **1987**, *120*, 61–66.

(134) Gotthardt, H.; Pflaumbaum, W. Synthese Und Physikalische Eigenschaften Erster 5, 5′-verbrückter Bis(1,3-dithiolylium-4-olate. *Chem. Ber.* **1987**, *120*, 411–420.

(135) Potts, K. T.; Chen, S. J.; Kane, J.; Marshall, J. L. Mesoionic Compounds. 39. Synthesis of Some Functionally Substituted Five-Membered Systems Using 1,2-Bielectrophiles as Cyclization Agents. *J. Org. Chem.* **1977**, *42*, 1633–1638.

(136) Kumar, R. A.; Pattanayak, M. R.; Yen-Pon, E.; Eliyan, J.; Porte, K.; Bernard, S.; Riomet, M.; Thuéry, P.; Audisio, D.; Taran, F. Strain-Promoted 1,3-Dithiolium-4-Olates–Alkyne Cycloaddition. *Angew. Chem. Int. Ed.* **2019**, *58*, 14544–14548.

Chapter 2 – Design of a Modular, Palladium-Catalyzed Carbonylative Synthesis of Pyrido[2,1-α]isoindoles *via* Benzyne 1,3-Dipolar Cycloaddition

2.1 Preface

As outlined in Chapter 1, 1,3-dipolar cycloadditions with arynes can efficiently synthesize a range of fused heterocycles. Among these are pyrido[2,1-α]isoindoles, a tricyclic 6:5:6 system, that is commonly formed *via* intramolecular cyclization or annulation reactions, both of which require the preparation of substituted precursors. The challenge of accessing substituted derivatives of pyrido[2,1-α]isoindoles can be addressed with multicomponent reactions using simple and easily modifiable building blocks. Our research group has previously reported a palladium-catalyzed carbonylative formation of pyridine-based 1,3-dipoles from the combination of imines and bromopyridines. Coupling this palladium-catalyzed carbonylative synthesis of pyridine-based 1,3-dipoles with *in situ* benzyne cycloaddition offers an efficient and modular route to form polysubstituted pyrido[2,1-α]isoindoles. The following chapter is a published manuscript (*Chem. Comm.*, 2025, DOI: 10.1039/D4CC06483F) detailing this research.

All experiments described in this chapter were performed by me.

2.2 Introduction

The development of modular and efficient approaches to assemble heterocyclic products has become an important thrust in synthetic chemistry. One common approach to this goal is *via* multicomponent coupling reactions.[1–3] Unlike more classical multistep synthetic procedures, multicomponent reactions provide an avenue to couple three or more starting materials in a single reaction. This can not only create a more streamlined synthesis, but, due to their modularity, can be readily diversified to change product structures, making them attractive as well for product design. Nevertheless, a challenge in the design of multicomponent coupling reactions is accessing the reactive building blocks needed to drive the consecutive formation of multiple bonds in a single reaction. These can themselves often require a multistep synthesis and thus detracts from the efficiency benefits of employing multicomponent reactions.

A useful approach to address this challenge is to exploit metal catalysis with energetic building blocks such as carbon monoxide. Carbon monoxide is a broadly available feedstock

chemical, which has helped make metal catalyzed carbonylation reactions among the most heavily employed transformations in chemical synthesis.[4] In addition, an underexploited feature of carbon monoxide is its energetics. The conversion of carbon monoxide to a carboxylic acid derivative is often highly exergonic. We and others have shown that this feature can be exploited to drive the catalytic build-up of a range of reactive products,[5–12] such as the modular assembly of 1,3-dipoles as a route into multicomponent heterocycle synthesis.[13–16] An example of this chemistry is the formation of pyridine-based 1,3-dipole **1**, which, following cycloaddition with electron deficient alkynes offers a multicomponent synthesis of indolizines (Figure 2.2.1a).[17]

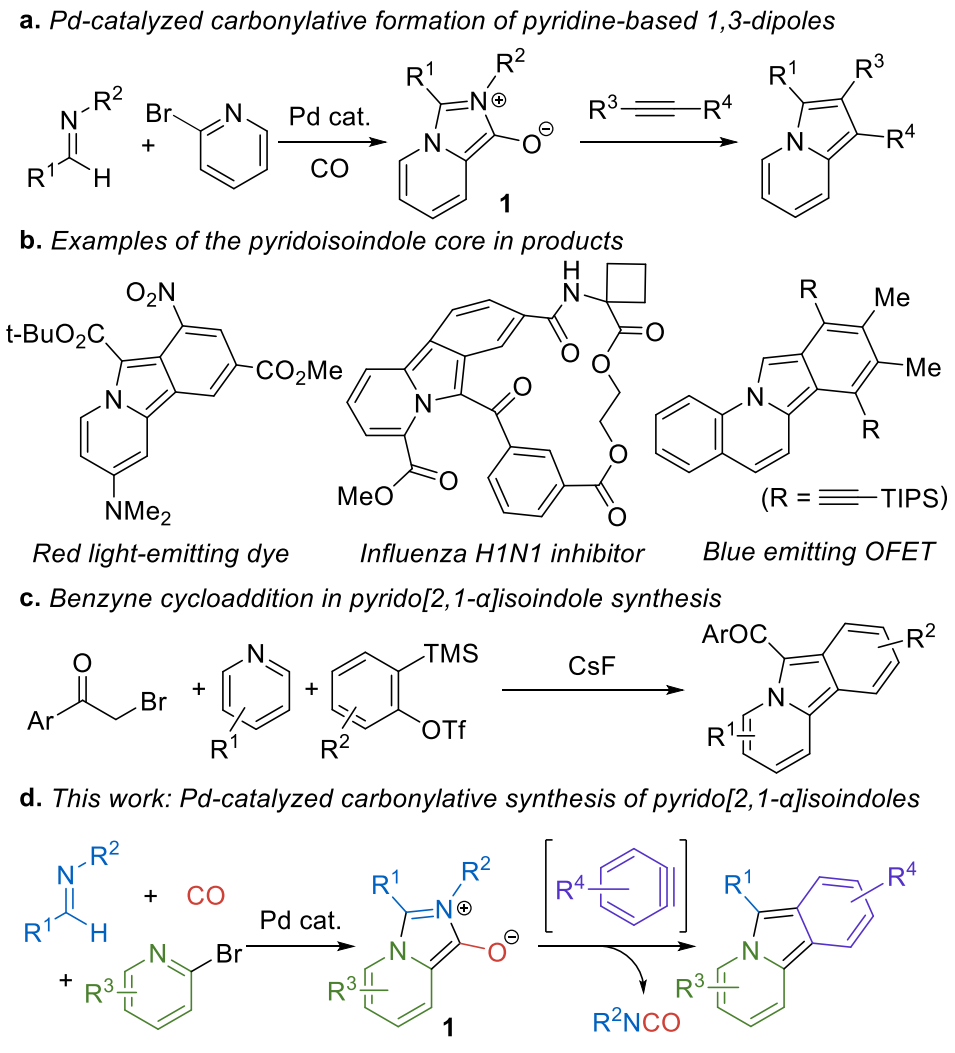

Figure 2.2.1. Carbonylative formation of 1,3-dipoles and benzyne cycloaddition routes to pyrido[2,1-α]isoindole synthesis.

In considering the reactivity of **1**, we questioned if this 1,3-dipolar cycloaddition manifold might be directed toward other products. For example, benzynes have attracted significant research attention due to the reactivity of their strained triple bond, including their use in nucleophilic additions, pericyclic chemistry, and related transformations.[18,19] This synthetic utility is facilitated in part by the low lying LUMO energy of the triple bond in benzynes, which imparts similar reactivity to electron deficient alkynes.[20,21] The latter suggests that benzyne cycloaddition might be employed in this sequence with **1** to access, in this case, fused ring pyrido[2,1-α]isoindoles. Although less extensively studied as indolizines, pyrido[2,1-α]isoindoles have found use in pharmaceutically relevant products, and their delocalized 14π-electron aromatic system has led to their application in electronic materials and dyes (Figure 2.2.1b).[22–24] Additionally, reduced forms of pyrido[2,1-α]isoindoles are found in various alkaloids and therapeutic agents.[25–28] Pyrido[2,1-α]isoindoles are most commonly prepared *via* cyclization reactions. While effective, these typically require the multistep build-up of the appropriately substituted precursor.[29–32] Benzyne cycloaddition to pyridinium ylides can also access these structures (Figure 2.2.1c), although these are limited to forming products with strong electron withdrawing *C*-acyl units to access the dipole itself.[33,34] As an alternative, we describe here how pyrido[2,1-α]isoindoles can be generated in a modular fashion *via* palladium-catalyzed carbonylation reactions. This involves the cycloaddition of benzyne derivatives to *in situ* generated **1** and provides a method to assemble these structures in one pot, with minimal waste, and where each of the imine, bromopyridine, and benzyne units can be systematically modified to access a range of new variants of these structures (Figure 2.2.1d).

2.3 Results and Discussion

There are a number of methods available to generate arynes.[35,36] One of the most versatile is the fluoride induced 1,2-elimination from *o*-trimethylsilylphenyl triflates developed by Kobayashi.[37,38] Considering the mild conditions of this reaction and the stability of *o*-trimethylsilylphenyl triflates, our initial studies explored if this approach could allow benzyne generation to be compatible with the formation of 1,3-dipole **1**. The palladium-catalyzed carbonylative coupling of the imine *p*-tolyl(H)C=NBn, 2-bromopyridine, and *o*-trimethylsilylphenyl triflate in the presence of CsF as an activating agent in acetonitrile does lead to the formation of 6-(*p*-tolyl)pyrido[2,1-α]isoindole **2a**, but does so in very low yield (9%, Table

2.3.1, entry 1). Examination of the reaction mixture by ^{1}H NMR analysis shows significant amounts of unreacted imine and 2-bromopyridine. Increasing the amount of benzyne precursor completely inhibits the reaction (entry 2). Similar results were observed with other palladium catalysts (entries 3-7, see Table 2.5.1 for full development).

Table 2.3.1. Development of a palladium-catalyzed synthesis of pyrido[2,1-α]isoindoles.

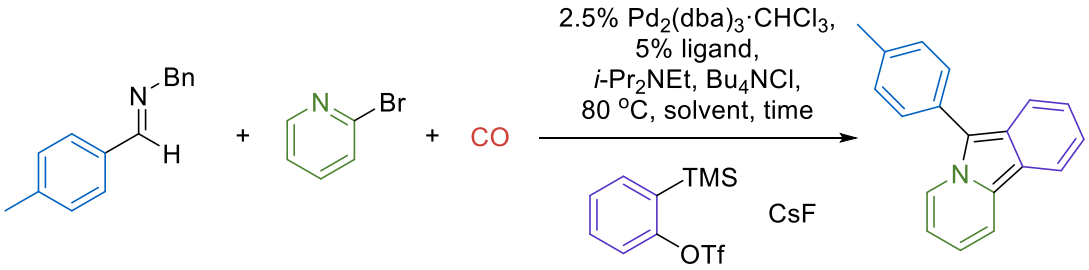

Procedures

A: Reaction of all reagents, 24 hr

B: Benzyne precursor / CsF in CH_3CN added after catalysis, RT, 24 hr.

Entry	Procedure	Ligand	Solvent	%2a[d]
1	A	Xantphos	CH_3CN	9%
2[a]	A	Xantphos	CH_3CN	0%
3[b,f]	A	DPEphos	C_6H_6	5%
4[b,f]	A	dppe	C_6H_6	0%
5[b,f]	A	P(*t*-Bu)$_3$	C_6H_6	6%
6[b,f]	A	P(Ph)$_3$	C_6H_6	0%
7[b,f]	A	JohnPhos	C_6H_6	2%
8[c]	B	Xantphos	C_6H_6	53%
9[b]	B	Xantphos	C_6H_6	65% (60%)[e]
10[b,f]	A	Xantphos	C_6H_6	57%

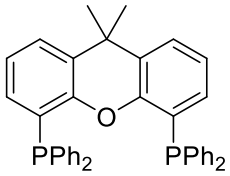

Xantphos

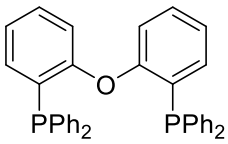

DPEphos

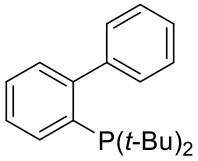

JohnPhos

Procedure A: *p*-tolyl(H)C=NBn (34 mg, 0.16 mmol); 2-bromopyridine (38 mg, 0.24 mmol); *o*-trimethylsilylphenyltriflate (48 mg, 0.16 mmol); CsF (109 mg, 0.72 mmol); *i*-Pr_2NEt (25 mg, 0.19 mmol); $Pd_2(dba)_3{\cdot}CHCl_3$ (4.1 mg, 0.004 mmol); ligand (0.008 mmol bidentate, 0.016 mmol monodentate); Bu_4NCl (67 mg, 0.24 mmol); 3.2 mL solvent, 5 atm CO; 80 °C. **Procedure B:** All reagents except benzyne precursor/CsF in C_6H_6, 80°C, 4 hr, then *o*-trimethylsilylphenyl triflate (33 mg, 0.11 mmol); CsF (75 mg, 0.50 mmol). 3 mL CH_3CN, RT, 24 hr. ([a] 0.35 mmol, [b] 0.11 mmol, or [c] 0.16 mmol o-trimethylsilylphenyl triflate). [d] ^{1}H NMR yield. [e] Isolated yield. [f] 48 hr.

Our previous results have shown that 1,3-dipole **1a** is generated in high yield with these substrates,[17] suggesting the presence of benzyne inhibiting catalysis. As such, a straightforward solution is to add *o*-trimethylsilylphenyl triflate and CsF to the catalytically generated 1,3-dipole, which results in cycloaddition to afford **2a** in 53% yield (entry 8). We observe the formation of side products in this reaction that may arise from the cycloaddition of benzyne to the product **2a**.[39] This can be minimized by employing benzyne as the limiting reagent and leads to the formation of **2a** in slightly enhanced yield of 65% (entry 9).[40] Under these conditions in benzene solvent, benzyne generation can be carried out during the palladium catalyzed reaction in somewhat lower yield (57%, entry 10).

A useful feature of this transformation is its modularity, where systematic changes to the imine, bromopyridine, and benzyne reagents can be employed to readily access a range of new variants of pyrido[2,1-α]isoindoles. For example, as shown in Table 2.3.2, a number of substituted *C*-aryl imines can be incorporated into the reaction. The reaction conditions for the build-up of the 1,3-dipole are influenced by the imine, with more nucleophilic imines accelerating the reaction (**2a-d**), while those with electron-withdrawing substituents (**2f**, **2h**) requiring more pressing conditions or longer reaction times (see SI for details). Regardless of the reaction rate, imines with both electron donating and electron withdrawing *C*-aryl substituents form the corresponding pyrido[2,1-α] isoindole in good overall yield (**2a-e, 2h**). Heterocycles such as pyridine (**2f**) and thiophene (**2g**) can also be incorporated into the product from the appropriate imine. The use of polyaromatic substituted imines lead to the corresponding pyrido[2,1-α]isoindoles (**2i-j**), as does the more sterically hindered *o*-tolyl imine (**2e**). *C*-aliphatic imines were also viable substrates and form cycloaddition products in reasonable yields. In the case of **2k-l**, the formation of the 1,3-dipole must be performed in the more polar solvent, which presumably enhances the ability of this imine to trap an *in situ* generated acid chloride (*vide infra*).

Table 2.3.2. Modulation of imines, bromopyridines, and arynes in pyrido[2,1-α]isoindole synthesis.

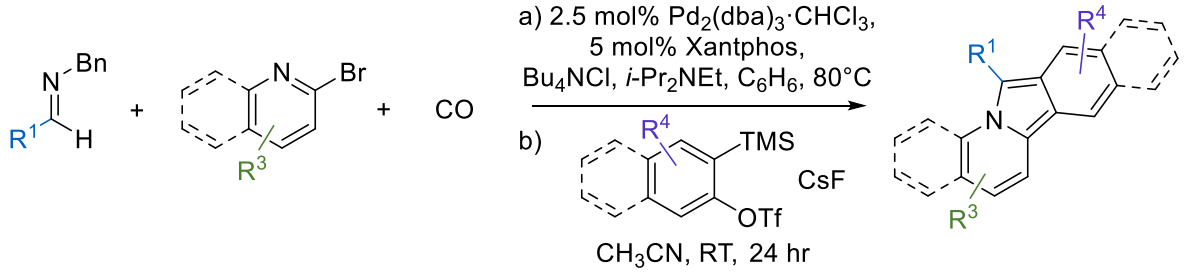

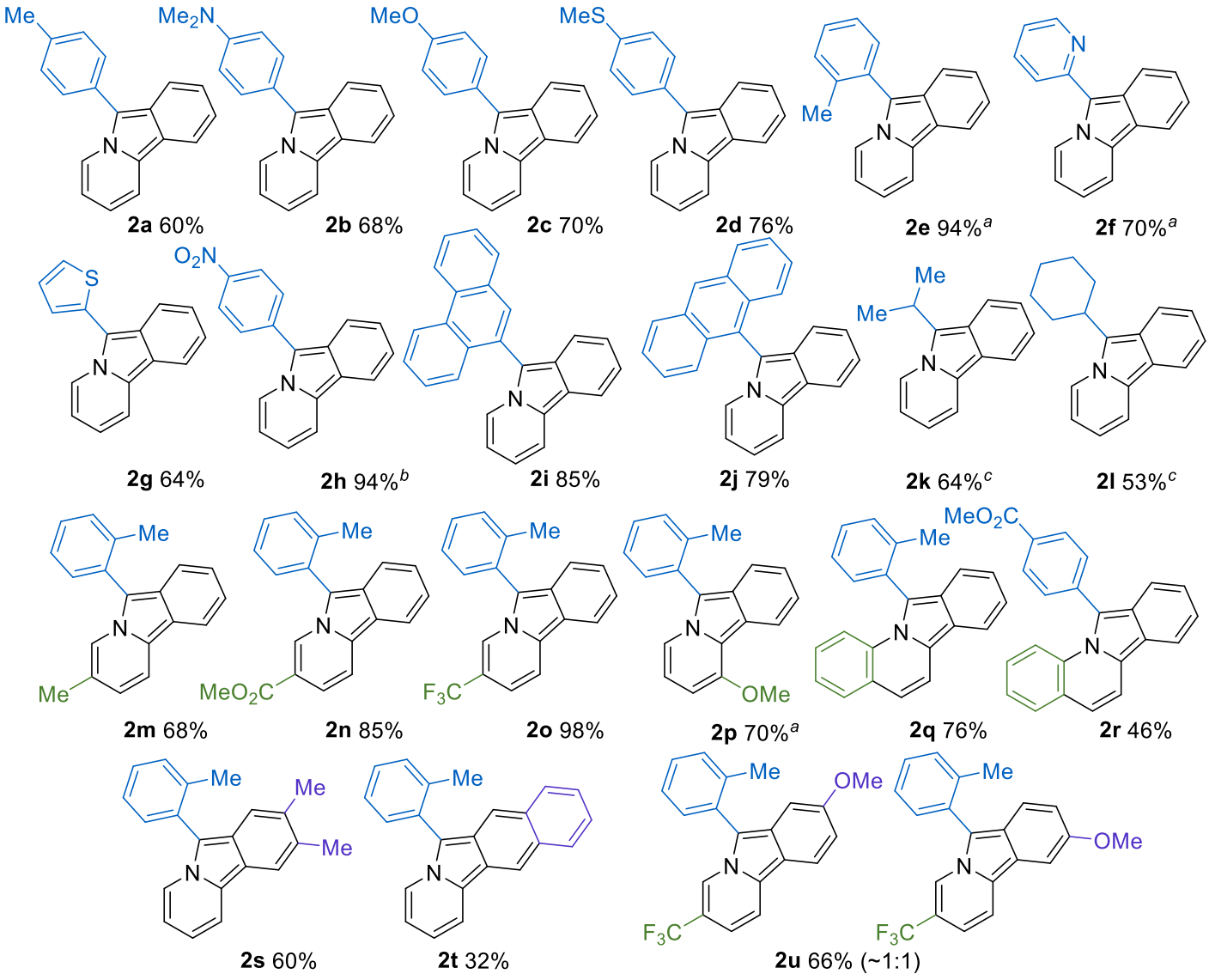

a) Imine (0.16 mmol); 2-Bromopyridine (0.24 mmol); $Pd_2(dba)_3{\cdot}CHCl_3$ (4.1 mg, 0.004 mmol); Xantphos (4.6 mg, 0.008 mmol); Bu_4NCl (67 mg, 0.24 mmol); *i*-Pr_2NEt (25 mg, 0.19 mmol); CO (5 atm); C_6H_6 (3.2 mL), 80°C, 4 hr, see SI for reaction time variations. b) *o*-Trimethylsilylaryltriflate (0.11 mmol); CsF (75 mg, 0.50 mmol); CH_3CN (3.2 mL). Step a) [a] 24 hr. [b] 120°C, Bu_4NCl (0.48 mmol), 5% $Pd_2(dba)_3{\cdot}CHCl_3$, 10% Xantphos. [c] In CH_3CN.

The 2-bromopyridine unit can also be modulated. As examples, electron donating and withdrawing groups on the pyridine component are well tolerated (**2m-o**), as are substituents closer to the pyrrole unit (e.g. **2p**). The 2-bromopyridine unit can be replaced with 2-bromoquinoline to form more extended conjugated products (**2q-r**). Finally, the benzyne precursor can also be tuned. In the case of 4,5-dimethyl substituted trimethylsilyl aryl triflate, the product **2s** is formed in good overall yield, as is the fused ring product **2t**. However, unsymmetrical arynes form a mixture of cycloaddition products (**2u**). The latter contrasts with results using substituted alkynes,[17] and presumably arises from the high aryne reactivity and the moderate electronic influence of the remote 4-methoxy substituent on selectivity.[41]

Pyrido[2,1-α]isoindoles are often sensitive to oxidation.[42] Nevertheless, we have found that the products here are indefinitely stable when stored under an inert atmosphere. Under these conditions, crystals of **2c** can be obtained from diethyl ether/acetonitrile, and its structure confirmed by X-ray crystallography. As shown in Figure 2.3.1, **2c** has a relatively planar π-conjugated core (dihedral angle: C5–C6–C7–C12: 0.3°). The C–C bonds in the pyridine ring are shortened relative to those in the pyrrole (e.g. C2–C3: 1.354(4) Å vs. C8–C13: 1.395(3) Å), suggesting a higher degree of aromaticity in the pyridine. The aromatic substituent on C13 is twisted out of the plane of the pyrido[2,1-α]isoindole presumably due to steric clashes between the *ortho*-arene hydrogens and the heterocyclic core (N1–C13–C14–C19: 49.8°). The crystal does not exhibit a π-stacking system between pyrido[2,1-α]isoindoles; however, there are C–H π-interactions between C12–H and a second pyrido[2,1-α]isoindole (see SI for details).

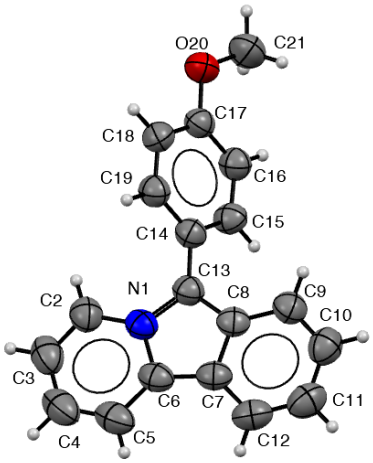

Figure. 2.3.1. Crystal structure of **2c**. *Select bond lengths* [Å]: N1–C13 1.385(3), N1– C2 1.396(3), N1–C6 1.415(3), C6–C7 1.403(3), C7–C8 1.418(3), C8–C13 1.395(3), C2–C3 1.354(4). *Bond angles* (°): C13–N1–C6 110.08(18), N1–C13–C8 106.47(19), C13–C8–C7 109.65(18), C6–C7–C8 106.87(19). *Dihedral angles* (°): C5–C6–C7–C12 0.3, C2–N1–C13–C8 176.4, N1–C13–C8–C9 177.6.

Our preliminary postulate for the mechanism of this multicomponent reaction is shown in Figure 2.3.2. The oxidative addition of aryl bromides to Pd(0) is well-established and would form here a Pd(II)-(2-pyridyl) complex **3** that can undergo CO insertion to form the Pd-acyl complex **4**. In the presence of chloride, anionic exchange can occur to form the chloride complex **5**. As we have previously noted,[6] chloride significantly enhances the rate of 1,3-dipole **1** formation by allowing the reductive elimination of an electrophilic acid chloride, which offers a lower barrier pathway to incorporate the weakly nucleophilic imine than direct reaction with complex **4** for subsequent cyclization to 1,3-dipole **1**. The rigid, large bite-angle Xantphos ligand presumably also facilitates this step by creating a sterically encumbered palladium to drive the disfavored reductive elimination of acid chloride.[17] In analogy to reports of benzyne addition to mesoionic 1,3-dipoles such as Münchnones,[43,44] the *in situ* generation of aryne after 1,3-dipole formation leads to its rapid cycloaddition followed by cycloreversion to release isocyanate to form pyrido[2,1-α]isoindole **2**. The isocyanate can be clearly seen by *in situ* ^{1}H NMR analysis of the reaction mixture (see Figure 2.5.1). The inhibitory influence of benzyne generation during catalysis could be tied to the presence of fluoride, which may slow the generation of the 1,3-dipole **1**, or the formation of benzyne before the 1,3-dipole is present, leading to its decomposition.

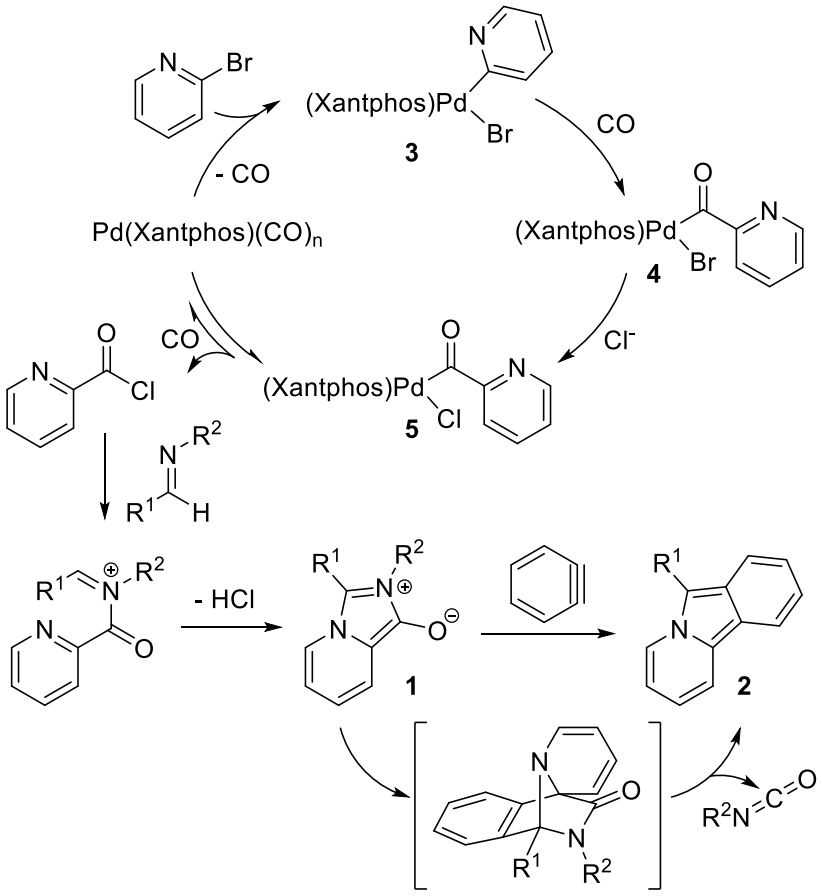

Figure 2.3.2. Proposed reaction mechanism of pyrido[2,1-α]isoindole formation.

2.4 Conclusions

In conclusion, we have described a multicomponent route to form substituted pyrido[2,1-α]isoindoles. This couples the palladium-catalyzed carbonylative formation of pyridine-based 1,3-dipoles with their ability to undergo cycloaddition with *in situ* generated arynes. The systematic variation of any of the three substrates can allow a range of new variants of these structures to be generated in one pot, and from either commercially available or easily generated building blocks.

We would like to thank the Natural Science and Engineering Research Council of Canada (NSERC), McGill University and the FRQNT supported by the Centre for Green Chemistry and Catalysis for funding this research.

2.5 Supporting Information

2.5.1 General Considerations

All reactions were carried out under a nitrogen atmosphere in a glovebox. Reactions used CO of 99.5% purity from Linde. Unless otherwise noted, all starting materials were purchased from commercial sources. Liquid reagents were degassed by freeze-pump-thaw method or by bubbling N_2 for 15 minutes before bringing them into a glovebox. Bu_4NCl was dissolved in dry dichloromethane in a glovebox, decanted, and dried *in vacuo*. CsF was placed in a vacuum oven at 100°C overnight to remove moisture before bringing it into a glovebox. Benzene, acetonitrile, diethyl ether, pentanes, dichloromethane, and toluene solvents were dried using a solvent purification system and stored over activated molecular sieves (4Å) inside the glovebox. Deuterated chloroform and acetonitrile were stirred over calcium hydride overnight, vacuum transferred into an oven-dried Schlenk flask, degassed, and stored over activated molecular sieves (4Å) in a glovebox. Imines and $Pd_2(dba)_3{\cdot}CHCl_3$ were prepared according to literature procedures.[45,46] To avoid decomposition, all starting materials and reagents were stored in a glovebox and $Pd_2(dba)_3{\cdot}CHCl_3$ in a -35°C freezer in the glovebox. Prepacked silica columns were purchased from commercial sources. Final compounds were purified using 10% diethyl ether or tetrahydrofuran in pentanes with 1% triethylamine depending on thin layer chromatography (TLC) results of the crude reaction mixture.

Nuclear magnetic resonance (NMR) characterizations were performed on a 500 MHz or 800 MHz spectrometers for ^1H NMR, and 126 MHz, or 201 MHz for ^{13}C NMR. ^1H and ^{13}C NMR chemical shifts were referenced to residual solvent. High resolution mass spectra (HRMS) of pure compounds were obtained using either electrospray ionization (ESI) or atmospheric-pressure chemical ionization (APCI) and quadrupole, time-of-flight (TOF), or orbitrap detection.

2.5.2 Supplementary Tables and Figures

Table 2.5.1. Palladium catalyst development for a one-step synthesis of pyrido[2,1-α]isoindoles.

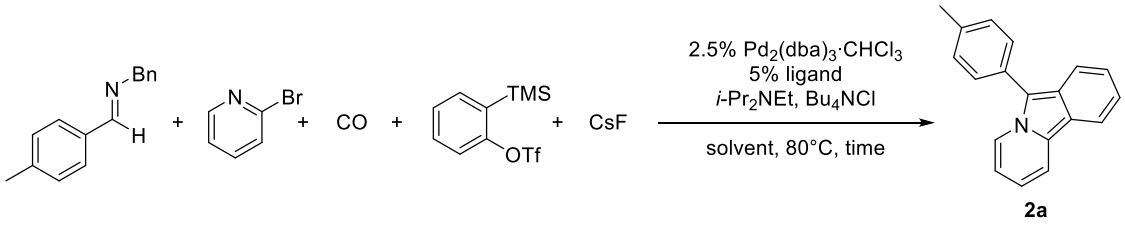

2a

Entry	Ligand	Solvent	Time	%2a[e]
1[a]	Xantphos	CH_3CN	24 hr	0%
2[b]	Xantphos	CH_3CN	24 hr	9%
3	Xantphos	CH_3CN	24 hr	27%
4	Xantphos	DCM	24 hr	6%
5	Xantphos	C_6H_6	24 hr	29%
6	Xantphos	Toluene	24 hr	21%
7	Xantphos	CH_3CN	4 hr	2%
8	Xantphos	CH_3CN	48 hr	29%
9	Xantphos	C_6H_6	4 hr	3%
10	Xantphos	C_6H_6	48 hr	57%
11	DPEphos	C_6H_6	48 hr	5%
12	dppe	C_6H_6	48 hr	0%
13	P(*t*-Bu)$_3$	C_6H_6	48 hr	6%
14	P(Ph)$_3$	C_6H_6	48 hr	0%
15	JohnPhos	C_6H_6	48 hr	2%
16[c]	Xantphos	C_6H_6	48 hr	52%
17[d]	Xantphos	C_6H_6	48 hr	45%

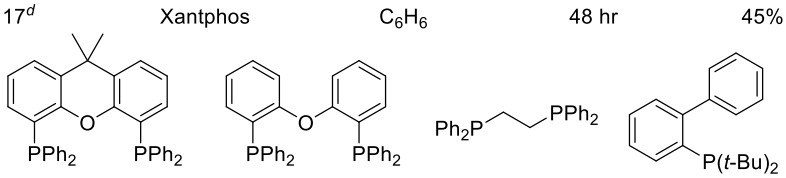

Xantphos DPEphos dppe JohnPhos

p-tolyl(H)C=NBn (34 mg, 0.16 mmol); 2-bromopyridine (38 mg, 0.24 mmol); *i*-Pr_2NEt (25 mg, 0.19 mmol); Bu_4NCl (67 mg, 0.24 mmol); $Pd_2(dba)_3{\cdot}CHCl_3$ (4.1 mg, 0.004 mmol); ligand (5 mol% bidentate, 0.008 mmol or 10 mol% monodentate, 0.016 mmol); *o*-trimethylsilylphenyl triflate (33 mg, 0.11 mmol); CsF (75 mg, 0.50 mmol); benzyl benzoate (34.0 mg, 0.16 mmol) as internal standard; solvent (3.2 mL). [a] *o*-trimethylsilylphenyl triflate (104 mg, 0.35 mmol); CsF (239 mg, 1.58 mmol). [b] *o*-trimethylsilylphenyl triflate (48 mg, 0.16 mmol); CsF (109 mg, 0.72 mmol). [c] 100°C. [d] 120°C. [e] The %**2a** yield determined relative to the internal standard by ^{1}H NMR analysis.

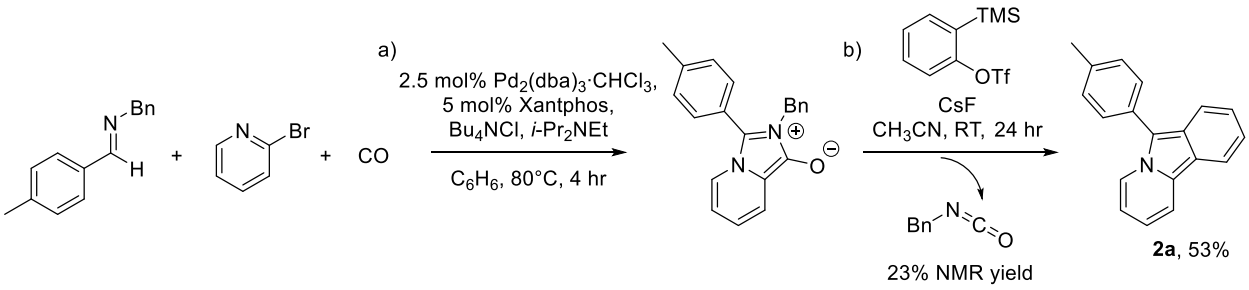

Figure 2.5.1. *In situ* ^{1}H NMR analysis of reaction (Table 2.3.1, entry 8).

2.5.3 General Experimental Procedures

2.5.3.1 Reaction Development for a One-Step Synthesis of Pyrido[2,1-α]isoindoles (Table 2.3.1, entries 1-7 and 10 and Table 2.5.1)

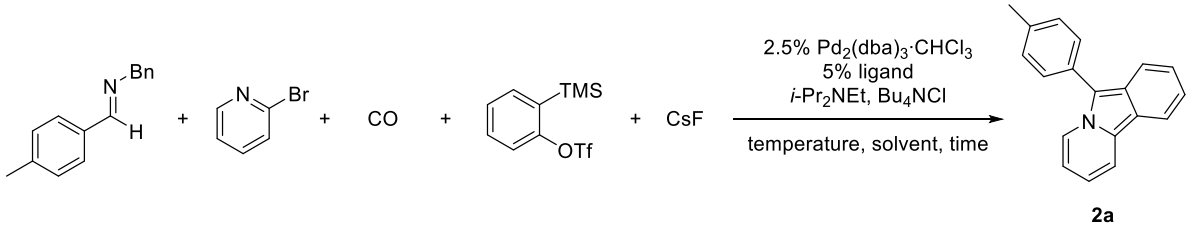

Scheme 2.5.1. One-step synthesis of pyrido[2,1-α]isoindole **2a** with *in situ* formed benzyne.

In a glovebox, p-tolyl(H)C=NBn (34 mg, 0.16 mmol), 2-bromopyridine (38 mg, 0.24 mmol), *i*-Pr$_2$NEt (25 mg, 0.19 mmol), o-trimethylsilylphenyl triflate (33 mg, 0.11 mmol or 48 mg, 0.16 mmol or 104 mg, 0.35 mmol), and benzyl benzoate (34 mg, 0.16 mmol) as internal standard were transferred to a 25 mL Teflon cap sealable, thick walled Schlenk flask equipped with a stir bar using 2 mL of solvent. To this solution, Bu$_4$NCl (67 mg, 0.24 mmol), Pd$_2$(dba)$_3$·CHCl$_3$ (4.1 mg, 0.004 mmol), ligand (5 mol% bidentate, 0.008 mmol or 10 mol% monodentate, 0.016 mmol), and CsF (75 mg, 0.50 mmol or 109 mg, 0.72 mmol or 239 mg, 1.58 mmol) were dry transferred and any residual solids were rinsed with 1.2 mL of solvent. The solution was stirred for 5 minutes before a small aliquot was dissolved in CDCl$_3$ for an initial ^{1}H NMR analysis. The reaction flask was closed and brought outside of the glovebox where the solution was frozen in liquid N$_2$, evacuated, thawed, and 5 atm of CO was added (as measured by a pressure gauge on the CO tank, 60 psi on top of atmospheric pressure). The flask was then placed in an oil bath.

Once the reaction was complete, the flask was removed from the oil bath and the CO was removed on a Schlenk line where the solution was frozen in liquid N_2, evacuated, and thawed. The flask was then brought back into the glovebox and a small aliquot was dissolved in $CDCl_3$ for ^1H NMR analysis. The ^1H NMR spectra taken before and after the reaction was used to calculate *in situ* yield of **2a** using integrations of signals relative to the internal standard. Afterwards, the isocyanate byproduct in the reaction solution was quenched by the addition of benzylamine (26 mg, 0.24 mmol) prior to bringing the reaction flask out of the glovebox.

2.5.3.2 Reaction Development for a One-Pot Synthesis of Pyrido[2,1-α]isoindoles (Table 2.3.1, entries 8-9).

In a glovebox, *p*-tolyl(H)C=NBn (34 mg, 0.16 mmol), 2-bromopyridine (38 mg, 0.24 mmol), *i*-Pr_2NEt (25 mg, 0.19 mmol), and benzyl benzoate (34.0 mg, 0.16 mmol) as internal standard were transferred to a 25 mL Teflon cap sealable, thick walled Schlenk flask equipped with a stir bar using 2 mL of solvent. To this solution, Bu_4NCl (67 mg, 0.24 mmol), $Pd_2(dba)_3{\cdot}CHCl_3$ (4.1 mg, 0.004 mmol), and Xantphos (4.6 mg, 0.008 mmol) were dry transferred and any residual solids were rinsed with 1.2 mL of benzene. The solution was stirred for 5 minutes before a small aliquot was dissolved in $CDCl_3$ for an initial ^1H NMR analysis. The reaction flask was sealed and brought outside of the glovebox where the solution was frozen in liquid N_2, evacuated, thawed, and 5 atm of CO was added (as measured by a pressure gauge on the CO tank, 60 psi on top of atmospheric pressure). The flask was then placed in an oil bath at 80°C for 4 hours.

Once the reaction was complete, the flask was removed from the oil bath and the CO was removed on a Schlenk line where the solution was frozen in liquid N_2, evacuated, and thawed. The flask was then brought back into the glovebox where 3 mL of acetonitrile was added to the solution to facilitate the removal of the reaction solvent *in vacuo*. Once this crude mixture was dry, *o*-trimethylsilylphenyl triflate (48 mg, 0.16 mmol) was added in 2 mL of acetonitrile. CsF (109 mg, 0.72 mmol) was then dry transferred followed by the rinsing of residual solids with 1.2 mL of acetonitrile. The solution was stirred for 5 minutes before a small aliquot was dissolved in $CDCl_3$ for ^1H NMR analysis. The flask was then sealed and was left in the glovebox to stir at the maximum speed for 24 hours. Once the reaction was complete, a small aliquot was dissolved in $CDCl_3$ for ^1H NMR analysis. The ^1H NMR spectra taken before and after the reaction was used to calculate

the *in situ* yield of **2a** (53% with Xantphos as ligand in benzene solvent) and BnNCO (23% with these same conditions) using integrations of signals relative to the internal standard. Afterwards, the isocyanate byproduct was quenched by the addition of benzylamine (26 mg, 0.24 mmol) prior to bringing the reaction flask out of the glovebox.

2.5.3.3 Typical Procedure for the Synthesis of Pyrido[2,1-α]isoindoles (Tables 2.3.2).

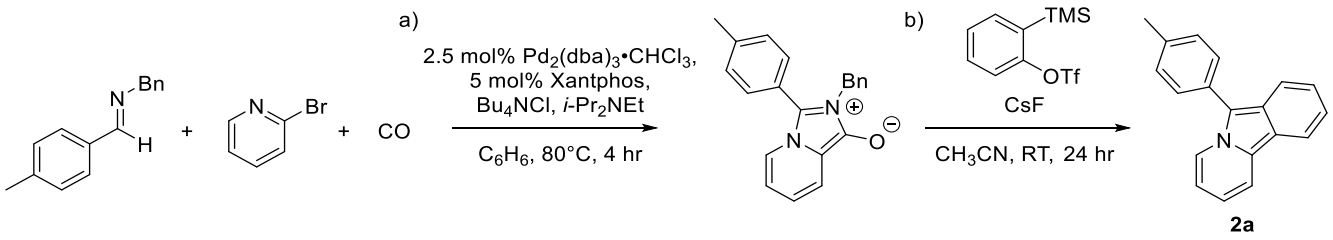

Scheme 2.5.2. Two-step synthesis of pyrido[2,1-α]isoindole **2a**.

In a glovebox, *p*-tolyl(H)C=NBn (34 mg, 0.16 mmol), 2-bromopyridine (38 mg, 0.24 mmol), and *i*-Pr_2NEt (25 mg, 0.19 mmol) were transferred to a 25 mL Teflon cap sealable, thick walled Schlenk flask equipped with a stir bar using 2 mL of benzene. To this solution, Bu_4NCl (67 mg, 0.24 mmol), $Pd_2(dba)_3{\cdot}CHCl_3$ (4.1 mg, 0.004 mmol), and Xantphos (4.6 mg, 0.008 mmol) were dry transferred and any residual solids were rinsed with 1.2 mL of benzene. The flask was sealed and brought outside of the glovebox where the solution was frozen in liquid N_2, evacuated, thawed, and 5 atm of CO was added (as measured by a pressure gauge on the CO tank, 60 psi on top of atmospheric pressure). The flask was then placed in an 80°C oil bath for 4 hours.

Once the reaction was complete, the flask was removed from the oil bath and the CO was removed on a Schlenk line where the solution was frozen in liquid N_2, evacuated, and thawed. The flask was then brought back into the glovebox where 3 mL of acetonitrile was added to the solution to facilitate the removal of all the solvent *in vacuo*. Once this crude mixture was dry, *o*-trimethylsilylphenyl triflate (33 mg, 0.11 mmol) was added in 2 mL of acetonitrile. CsF (75 mg, 0.50 mmol) was then dry transferred to the reaction mixture followed by the rinsing of residual solids with 1.2 mL of acetonitrile. The flask was left in the glovebox to stir at the maximum speed for 24 hours. Once the reaction was complete, the isocyanate byproduct was quenched by the addition of benzylamine (26 mg, 0.24 mmol), and the solvent was removed *in vacuo*. The product was purified by column chromatography (neutralized silica gel, 10% diethyl ether in pentanes with

1% triethylamine) inside the glovebox (see details on procedure below) to afford the corresponding pyrido[2,1-α]isoindole **2a** as a yellow oil (16 mg, 0.064 mmol, 60%).

The reaction time for step a) to form the 1,3-dipole differed from the typical procedure described above for several compounds; see characterization section for variation.

2.5.3.4 Typical Isolation of Pyrido[2,1-α]isoindoles Under an Inert Atmosphere

Neutralized silica for product loading: Neutralized silica was prepared outside of the glovebox by stirring silica in hexanes with 2% triethylamine for 30 minutes followed by the removal of solvent under vacuum. The neutralized silica was then placed in a vacuum oven at 100°C overnight to remove moisture. Once the neutralized silica was dried, it was brought into the glovebox.

Silica column preparation: With an automated flash chromatography system, a prepacked silica column was flushed with 3 CVs (column volumes) of hexanes with 2% triethylamine. The column was sealed tightly on both ends with a cap secured with parafilm prior to promptly bringing it into the glovebox. In the glovebox, using a 12 mL syringe, 2 CVs of pentanes was used to flush out the hexanes into a waste bottle.

Procedure: In the glovebox, the crude product mixture was pre-adsorbed onto neutralized silica (prepare as above) as follows. The crude product mixture was dissolved in 5 mL of dichloromethane in a 25 mL vial. To this solution, ~500 mg of neutralized silica (see below) and a stir bar were added. The solvent was removed *in vacuo* while stirring until the solvent was completely removed. The pre-adsorbed silica was transferred to an empty 12 g cartridge equipped with a frit and connected to the top of the prepacked silica column (prepare as above). To this layer of silica, a 2 cm layer of sand was added on top, and the cartridge was capped. The eluent of 10% diethyl ether in pentanes with 1% triethylamine was prepared in the glovebox using a 100 mL graduated cylinder and a 1000 µL micropipette to add the triethylamine. The eluent was mixed and stored in a capped bottle. A 12 mL syringe with Luer-Lok was used to push the eluent from the top of the cartridge and into the column until yellow fractions (3 mL each) were collected into 25 mL vials. Each fraction was concentrated under vacuum in the glovebox, characterized by ^{1}H NMR analysis, and pure fractions were combined and concentrated under vacuum. The prepacked column was capped and taken out of the glovebox where it was flushed with 3 CVs of isopropanol.

The glovebox was then purged for 30 minutes to remove solvent vapours. Pyrido[2,1-α]isoindoles are known to oxidize to their corresponding 2-pyridyl phenyl ketone under ambient conditions, therefore all isolated products were stored in a glovebox.[47-49] Due to this lability, trace solvents remaining in the samples were not removed.

2.5.4 Characterization Data of Pyrido[2,1-α]isoindoles (Table 2.3.2)

6-(p-tolyl)pyrido[2,1-α]isoindole (**2a**)

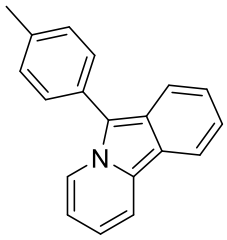

Isolated by column chromatography (10% diethyl ether in pentanes with 1% triethylamine) as a yellow oil, 16 mg, 60%. **^{1}H NMR** (500 MHz, $CDCl_3$): δ 8.57 (dt, *J* = 7.0, 1.2 Hz, 1H), 8.15 (dt, *J* = 8.3, 1.1 Hz, 1H), 8.13-8.08 (m, 1H), 7.82 (dt, *J* = 8.6, 1.0 Hz, 1H), 7.62 (d, *J* = 8.1 Hz, 2H), 7.39 (d, *J* = 7.8 Hz, 2H), 7.34 (ddd, *J* = 8.5, 6.6, 1.1 Hz, 1H), 7.19 (ddd, *J* = 7.8, 6.6, 1.0 Hz, 1H), 6.90 (td, *J* = 6.7, 1.8 Hz, 1H), 6.85 (ddd, *J* = 7.8, 6.6, 1.3 Hz, 1H), 2.47 (s, 3H). **^{13}C NMR** (126 MHz, $CDCl_3$): δ 136.99, 130.13, 129.07, 128.89, 125.95, 125.87, 124.95, 120.24, 119.42, 119.38, 118.69, 117.54, 117.15, 115.40, 114.43, 113.82, 21.54. **HRMS** ($APCI^+$) for $C_{19}H_{16}N$; calculated 258.1277, found 258.1276 (error m/z = 0.3 ppm).

N,N-dimethyl-4-(pyrido[2,1-α]isoindol-6-yl)aniline (**2b**)

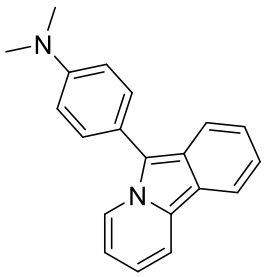

Isolated by column chromatography (10% diethyl ether in pentanes with 1% triethylamine) as a yellow solid, 21 mg, 68%. **^{1}H NMR** (500 MHz, $CDCl_3$): δ 8.51 (d, *J* = 7.1 Hz, 1H), 8.14 (dt, *J* = 8.4, 1.1 Hz, 1H), 8.08 (d, *J* = 8.6 Hz, 1H), 7.80 (d, *J* = 8.6 Hz, 1H), 7.58 (d, *J* = 8.3 Hz, 2H), 7.31 (ddd, *J* = 8.5, 6.6, 1.0 Hz, 1H), 7.17 (t, *J* = 7.4 Hz, 1H), 6.93 (d, *J* = 8.8 Hz, 2H), 6.87 (t, *J* = 6.6 Hz, 1H), 6.80 (t, *J* = 7.6 Hz, 1H), 3.06 (s, 6H). **^{13}C NMR** (126 MHz, CD_3CN): δ 149.75, 130.34, 125.72, 125.21, 124.47, 120.22, 119.48, 119.35, 119.15, 118.61, 117.82, 116.95, 115.12, 115.03, 113.12, 113.02, 88.31, 40.69. **HRMS** (ESI^+) for $C_{20}H_{19}N_2$; calculated 287.1543, found 287.1535 (error m/z = 2.7 ppm).

6-(4-methoxyphenyl)pyrido[2,1-α]isoindole (**2c**)

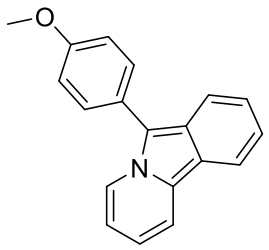

Isolated by column chromatography (10% diethyl ether in pentanes with 1% triethylamine) as a yellow solid, 21 mg, 70%. Step a) reaction time: 2.5 hr. **^{1}H NMR** (500 MHz, CD_3CN): δ 8.55 (dt, *J* = 7.0, 1.1 Hz, 1H), 8.19 (dt, *J* = 8.4, 1.0 Hz, 1H), 8.18 (dt, *J* = 8.6, 1.3 Hz, 1H), 7.72 (dt, *J* = 8.6, 1.0 Hz, 1H), 7.66 (d, *J* = 8.9 Hz, 2H), 7.32 (ddd, *J* = 8.5, 6.5, 1.0 Hz, 1H), 7.19-7.14 (m, 3H), 6.99 (td, *J* = 6.8 Hz, 1H), 6.92 (ddd, *J* = 8.7, 6.6, 1.0 Hz, 1H), 3.89 (s, 3H). **^{13}C NMR** (126 MHz, CD_3CN): δ 159.91, 131.43, 126.54, 126.29, 125.75, 124.62, 121.18, 120.43, 120.08, 119.42, 118.09, 117.97, 117.83, 116.51, 115.78, 114.92, 56.08. **HRMS** (ESI^+) for $C_{19}H_{16}NO$; calculated 274.1226, found 274.1217 (error m/z = 3.5 ppm). Crystallographically characterized.

6-(4-(methylthio)phenyl)pyrido[2,1-α]isoindole (**2d**)

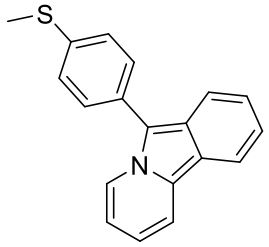

Isolated by column chromatography (10% diethyl ether in pentanes with 1% triethylamine) as a yellow oil, 24 mg, 76%. Step a) reaction time: 20 hr. **^{1}H NMR** (500 MHz, $CDCl_3$): δ 8.57 (dd, *J* = 6.8, 1.5 Hz, 1H), 8.15 (dt, *J* = 8.4, 1.1 Hz, 1H), 8.11 (dt, *J* = 8.3, 1.3 Hz, 1H), 7.82 (d, *J* = 8.6 Hz, 1H), 7.65 (d, *J* = 8.3 Hz, 2H), 7.46 (d, *J* = 8.4 Hz, 2H), 7.36 (ddd, *J* = 8.5, 6.6, 1.0 Hz, 1H), 7.22 – 7.18 (m, 1H), 6.94 – 6.85 (m, 2H), 2.58 (s, 3H). **^{13}C NMR** (126 MHz, $CDCl_3$): δ 137.17, 129.41, 128.60, 127.52, 126.15, 126.04, 125.18, 120.18, 119.51, 119.48, 118.73, 117.33, 117.25, 115.57, 114.16, 113.85, 16.06. **HRMS** (ESI^+) for $C_{19}H_{15}NS$; calculated 289.0920, found 289.0906 (error m/z = 4.6 ppm).

6-(o-tolyl)pyrido[2,1-α]isoindole (**2e**)

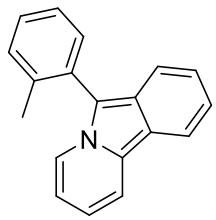

Isolated by column chromatography (50% diethyl ether in pentanes with 1% triethylamine) as a yellow oil, 27 mg, 94%. Step a) reaction time: 24 hr. **^{1}H NMR** (500 MHz, CD_3CN): δ 8.22 (dt, *J* = 8.4, 1.1 Hz, 1H), 8.21 (dt, *J* = 8.6, 1.3 Hz, 1H), 7.85 (dt, *J* = 7.0, 1.0 Hz, 1H), 7.51-7.36 (m, 5H), 7.30 (ddd, *J* = 8.5, 6.6, 1.0 Hz, 1H), 7.16 (ddd, *J* = 8.4, 6.5, 1.0 Hz, 1H), 6.97 (td, *J* = 6.8, 1.6 Hz, 1H), 6.92 (ddd,

J = 8.6, 6.6, 1.1 Hz, 1H), 2.01 (s, 3H). **^{13}C NMR** (126 MHz, CD_3CN): δ 139.85, 132.73, 131.86, 131.25, 129.65, 127.40, 126.92, 126.24, 125.63, 121.62, 120.53, 119.90, 119.36, 118.04, 117.54, 116.47, 114.70, 114.61, 19.73. **HRMS** (ESI^+) for $C_{19}H_{16}N$; calculated (258.12660), found 258.12773 (error m/z = -4.4 ppm).

6-(pyridin-2-yl)pyrido[2,1-α]isoindole (**2f**)

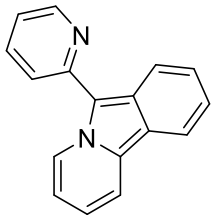

Isolated by column chromatography (10% diethyl ether in pentanes with 1% triethylamine) as a yellow oil, 19 mg, 70%. Step a) reaction time: 24 hr. **^{1}H NMR** (500 MHz, $CDCl_3$): δ 10.03 – 9.98 (m, 1H), 8.74 (ddd, *J* = 4.9, 1.9, 1.0 Hz, 1H), 8.19 (dt, *J* = 8.3, 1.0 Hz, 1H), 8.17 – 8.12 (m, 1H), 8.10 (dd, *J* = 8.6, 1.0 Hz, 1H), 7.88 (dt, *J* = 8.2, 1.2 Hz, 1H), 7.81 (td, *J* = 7.7, 1.9 Hz, 1H), 7.47 (ddd, *J* = 8.5, 6.7, 1.1 Hz, 1H), 7.24 (ddd, *J* = 8.2, 6.6, 0.9 Hz, 1H), 7.11 (ddd, *J* = 7.4, 4.9, 1.2 Hz, 1H), 7.09 – 7.04 (m, 2H). **^{13}C NMR** (126 MHz, $CDCl_3$): δ 152.48, 149.13, 136.63, 128.62, 127.19, 126.41, 124.15, 122.54, 119.91, 119.64, 119.40, 118.23, 117.91, 117.38, 117.23, 116.09, 112.62. **HRMS** (ESI^+) for $C_{17}H_{13}N_2$; calculated 245.1073, found 245.1067 (error m/z = 2.7 ppm).

6-(thiophen-2-yl)pyrido[2,1-α]isoindole (**2g**)

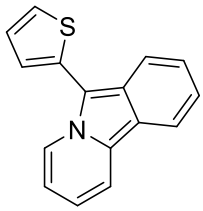

Isolated by column chromatography (10% diethyl ether in pentanes with 1% triethylamine) as a yellow oil, 18 mg, 64%. Step a) reaction time: 3 hr. **^{1}H NMR** (500 MHz, $CDCl_3$): δ 8.74 (dt, *J* = 7.0 1.1 Hz, 1H), 8.15 (dt, *J* = 8.4, 1.0 Hz, 1H), 8.11 (dt, *J* = 8.6, 1.2 Hz, 1H), 7.97 (dt, *J* = 8.7, 0.9 Hz, 1H), 7.47 (dd, *J* = 5.2, 1.2 Hz, 1H), 7.44-7.38 (m, 2H), 7.28 (dd, *J* = 5.2, 3.6 Hz, 1H), 7.22 (ddd, *J* = 8.3, 6.6, 0.9 Hz, 1H), 7.00 (td, *J* = 6.9, 1.5 Hz, 1H), 6.93 (ddd, *J* = 8.6, 6.6, 1.1 Hz, 1H). **^{13}C NMR** (126 MHz, $CDCl_3$): δ 133.08, 127.85, 127.16, 126.81, 125.94, 125.59, 125.02, 121.19, 119.69, 119.41, 118.51, 117.73, 117.33, 115.90, 114.84, 107.73. **HRMS** (ESI^+) for $C_{16}H_{11}NS$; calculated 249.06041, found 249.06067 (error m/z = -1.0 ppm).

6-(4-nitrophenyl)pyrido[2,1-α]isoindole (**2h**)

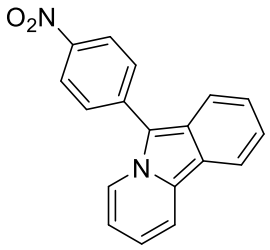

Isolated by column chromatography (30% diethyl ether in pentanes with 1% triethylamine) as a purple oil, 30 mg, 94%. Step a) reaction time: 5.5 hr at 120°C with 0.48 mmol Bu_4NCl, 5 mol% $Pd_2(dba)_3 \cdot CHCl_3$, and 10 mol% Xantphos. **^{1}H NMR** (500 MHz, $CDCl_3$): δ 8.79 – 8.73 (m, 1H), 8.40 (d, *J* = 8.8 Hz, 2H), 8.16 (ddt, *J* = 8.0, 7.0, 1.1 Hz, 2H), 7.93 – 7.87 (m, 3H), 7.46 (ddd, *J* = 8.3, 6.7, 1.1 Hz, 1H), 7.29 – 7.25 (m, 1H), 7.08 – 7.01 (m, 2H). **^{13}C NMR** (126 MHz, $CDCl_3$): δ 144.93, 138.57, 128.61, 127.56, 127.15, 126.69, 124.93, 120.47, 120.42, 119.71, 118.86, 118.22, 116.95, 116.63, 116.52, 112.47. **HRMS** ($APCI^+$) for $C_{18}H_{13}N_2O_2$; calculated 289.0972, found 289.0975 (error m/z = -1.2 ppm).

6-(phenanthren-9-yl)pyrido[2,1-α]isoindole (**2i**)

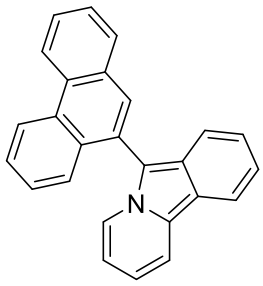

Isolated by column chromatography (10% diethyl ether in pentanes with 1% triethylamine) as a yellow solid, 32 mg, 85%. **^{1}H NMR** (500 MHz, $CDCl_3$): δ 8.86 (d, *J* = 8.3 Hz, 1H), 8.82 (d, *J* = 8.3, Hz, 1H), 8.27 (dt, *J* = 8.4, 1.1 Hz, 1H), 8.22 (dt, *J* = 8.7, 1.3 Hz, 1H), 8.04 (s, 1H), 7.94 (dd, *J* = 7.9, 1.4 Hz, 1H), 7.90 (d, *J* = 7.0 Hz, 1H), 7.75 (ddd, *J* = 8.4, 7.0, 1.4 Hz, 1H), 7.71 (ddd, *J* = 8.4, 6.8, 1.5 Hz, 1H), 7.67 (td, *J* = 8.1, 6.8, 1.1 Hz, 1H), 7.62 (d, *J* = 8.5 Hz, 1H), 7.46 (ddd, *J* = 8.0, 6.8, 1.2 Hz, 1H), 7.43-7.38 (m, 1H), 7.35 (ddd, *J* = 8.3, 6.6, 1.1 Hz, 1H), 7.27-7.22 (m, 1H), 6.92 (td, *J* = 7.6, 1.0 Hz, 1H), 6.84 (td, *J* = 6.8, 1.5 Hz, 1H). **^{13}C NMR** (126 MHz, $CDCl_3$): δ 132.11, 131.28, 131.04, 130.74, 129.00, 127.67, 127.46, 127.35, 127.20, 127.12, 127.05, 126.88, 126.17, 124.93, 123.46, 122.86, 121.47, 119.55, 119.30, 118.57, 117.83, 117.14, 115.29, 113.87, 112.45. **HRMS** ($APCI^+$) for $C_{26}H_{18}N$; calculated 344.1434, found 344.1426 (error m/z = 2.3 ppm).

6-(anthracen-9-yl)pyrido[2,1-α]isoindole (**2j**)

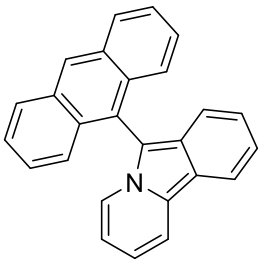

Isolated by column chromatography (10% diethyl ether in pentanes with 1% triethylamine) as an orange solid, 30 mg, 79%. **^{1}H NMR** (500 MHz, $CDCl_3$): δ 8.67 (s, 1H), 8.32 (dt, *J* = 7.8, 1.3 Hz, 1H), 8.27 (dt, *J* = 8.8, 1.3 Hz, 1H), 8.15 (d, *J* = 8.2 Hz, 2H), 7.51-7.47 (m, 3H), 7.37-7.34 (m, 3H), 7.31-7.24 (m, 4H), 6.93 (ddd, *J* = 8.7, 6.6, 1.0 Hz, 1H), 6.78 (td, *J* = 6.8, 1.4 Hz, 1H). **^{13}C NMR** (126 MHz, $CDCl_3$): δ 132.11, 132.05, 129.11, 128.64, 128.49, 128.35, 126.56, 126.45, 125.62, 125.06, 124.96, 121.36, 119.68, 119.29, 118.55, 118.04, 117.10, 115.35, 113.89, 110.09. **HRMS** (ESI^+) for $C_{26}H_{18}N$; calculated 344.1434, found 344.1421 (error m/z = 3.8 ppm).

6-isopropylpyrido[2,1-α]isoindole (**2k**)

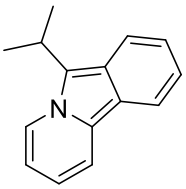

Isolated by column chromatography (10% diethyl ether in pentanes with 1% triethylamine) as a yellow oil, 15 mg, 64%. Step a) reaction time: 27 hr in CH_3CN. **^{1}H NMR** (500 MHz, $CDCl_3$): δ 8.14-8.09 (m, 2H), 8.08 (dt, *J* = 8.6, 1.3 Hz, 1H), 7.91 (dt, *J* = 8.7, 1.0 Hz, 1H), 7.29 (ddd, *J* = 8.7, 6.5, 1.1 Hz, 1H), 7.12 (ddd, *J* = 8.4, 6.5, 0.9 Hz, 1H), 6.97 (td, *J* = 6.9, 1.5 Hz, 1H), 6.77 (ddd, *J* = 8.6, 6.6, 1.0 Hz, 1H), 3.75 (hept, *J* = 7.1 Hz, 1H), 1.61 (d, *J* = 7.1 Hz, 6H). **^{13}C NMR** (126 MHz, $CDCl_3$): δ 124.73, 123.98, 123.68, 120.00, 119.58, 118.54, 118.33, 118.29, 118.09, 116.81, 115.19, 111.36, 26.56, 20.86. **HRMS** ($APCI^+$) for $C_{15}H_{16}N$; calculated 210.1277, found 210.1279 (error m/z = -0.8 ppm).

6-cyclohexylpyrido[2,1-α]isoindole (**2l**)

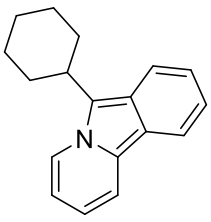

Isolated by column chromatography (10% diethyl ether in pentanes with 1% triethylamine) as a yellow oil, 14 mg, 53%. Step a) reaction time: 50 min in CH_3CN. **^{1}H NMR** (500 MHz, CD_3CN): δ 8.31 (dq, *J* = 7.0, 0.9 Hz, 1H), 8.12 (ddt, *J* = 8.7, 7.6, 1.1 Hz, 2H), 7.94 (dt, *J* = 8.7, 1.0 Hz, 1H), 7.24 (ddd, *J* = 8.7, 6.5, 1.2 Hz, 1H), 7.07 (ddd, *J* = 8.4, 6.5, 0.9 Hz, 1H), 7.01 (td, *J* = 6.8, 1.5 Hz, 1H), 6.80 (ddd, *J* = 8.7, 6.6, 1.0 Hz, 1H), 3.41 (tt, *J* = 12.0, 3.8 Hz, 1H), 2.15-1.97 (m, 5H), 1.88-1.81 (m, 1H), 1.64-1.42 (m, 4H). **^{13}C NMR** (126 MHz, CD_3CN): δ 129.32, 125.16, 124.89, 124.38, 121.49, 120.41,

119.17, 119.15, 119.07, 117.63, 116.02, 112.63, 37.59, 31.79, 27.86, 27.00. **HRMS** (APCI$^+$) for $C_{18}H_{20}N$; calculated 250.1590, found 250.1590 (error m/z = 0.1 ppm).

3-methyl-6-(o-tolyl)pyrido[2,1-α]isoindole (**2m**)

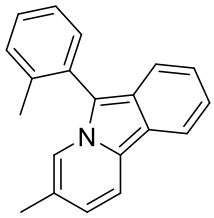

Isolated by column chromatography (10% diethyl ether in pentanes with 1% triethylamine) as a yellow oil, 20 mg, 68%. **^{1}H NMR** (500 MHz, CD_3CN): δ 8.17 (dt, *J* = 8.4, 1.0 Hz, 1H), 8.10 (dd, *J* = 8.8, 1.0 Hz, 1H), 7.66 (sext, *J* = 1.2 Hz, 1H), 7.51-7.36 (m, 5H), 7.26 (ddd, *J* = 8.5, 6.5, 1.0 Hz, 1H), 7.12 (ddd, *J* = 8.4, 6.6, 1.0 Hz, 1H), 6.79 (dd, *J* = 8.8, 1.4 Hz, 1H), 2.30 (s, 3H), 2.01 (s, 3H). **^{13}C NMR** (126 MHz, CD_3CN): δ 139.88, 132.75, 131.86, 131.41, 129.58, 127.37, 126.97, 126.57, 125.27, 125.00, 120.32, 119.73, 119.32, 118.78, 117.96, 117.71, 117.58, 114.25, 19.76, 18.92. **HRMS** (APCI$^+$) for $C_{20}H_{18}N$; calculated 272.1434, found 272.1431 (error m/z = 1.1 ppm).

Methyl 6-(o-tolyl)pyrido[2,1-α]isoindole-3-carboxylate (**2n**)

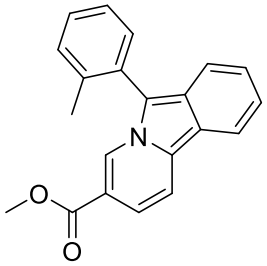

Isolated by column chromatography (10% diethyl ether in pentanes with 1% triethylamine) as an orange solid, 30 mg, 85%. Step a) reaction time: 20 hr. **^{1}H NMR** (500 MHz, $CDCl_3$): δ 8.62 (t, *J* = 1.2 Hz, 1H), 8.18 (dt, *J* = 8.5, 0.9 Hz, 1H), 8.16 (dd, *J* = 9.1, 0.9 Hz, 1H), 7.54 (*J* = 8.6, 1.0 Hz, 1H), 7.50-7.38 (m, 5H), 7.35 (ddd, *J* = 8.6, 6.5, 1.0 Hz, 1H), 7.23 (ddd, *J* = 8.4, 6.5, 1.0 Hz, 1H), 3.91 (s, 3H), 2.07 (s, 3H). **^{13}C NMR** (126 MHz, $CDCl_3$): δ 166.54, 139.13, 132.13, 131.20, 129.79, 129.07, 127.52, 126.64, 125.90, 125.58, 124.98, 120.34, 119.78, 118.81, 118.16, 117.97, 116.91, 115.94, 112.58, 52.43, 19.87. **HRMS** (APCI$^+$) for $C_{21}H_{18}NO_2$; calculated 316.1332, found 316.1342 (error m/z = -3.0 ppm).

6-(o-tolyl)-3-(trifluoromethyl)pyrido[2,1-α]isoindole (**2o**)

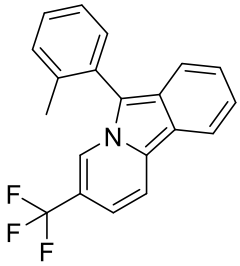

Isolated by column chromatography (100% pentanes with 1% triethylamine) as a yellow solid, 35 mg, 98%. Step a) reaction time: 3 hr. **^{1}H NMR** (500 MHz, CD_3CN): δ 8.35 (dt, *J* = 9.1, 0.9 Hz, 1H), 8.27 (dt, *J*= 8.5, 1.1 Hz, 1H), 8.17 (sext, *J* = 1.3 Hz, 1H), 7.54-7.49 (m, 1H), 7.49-7.45 (m, 3H), 7.44-7.40 (m, 1H), 7.37 (ddd, *J* = 8.6, 6.5, 1.0 Hz, 1H), 7.26 (ddd, *J* = 8.5, 6.6, 1.0 Hz, 1H), 7.05 (dd, *J* = 9.0, 1.6 Hz, 1H), 2.01 (s, 3H). **^{13}C NMR** (126 MHz, CD_3CN): δ 139.89, 132.62, 132.06, 130.26, 130.09, 128.00, 127.58, 126.58, 126.38, 126.13, 124.23, 121.53, 120.76, 120.30, 119.70, 119.44, 118.60, 118.09, 117.28, 19.68. **HRMS** ($APCI^+$) for $C_{20}H_{15}F_3N$; calculated 326.1151, found 326.1167 (error m/z = -5.0 ppm).

1-methoxy-6-(o-tolyl)pyrido[2,1-α]isoindole (**2p**)

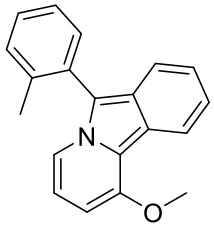

Isolated by column chromatography (10% diethyl ether in pentanes with 1% triethylamine) as a yellow oil, 22 mg, 70%. Step a) reaction time: 24 hr. **^{1}H NMR** (500 MHz, CD_3CN): δ 8.41 (dt, *J* = 8.5, 1.1 Hz, 1H), 7.50 (dd, *J* = 6.9, 0.7 Hz, 1H), 7.48-7.34 (m, 5H), 7.25 (ddd, *J* = 8.5, 6.6, 1.1 Hz, 1H), 7.14 (ddd, *J* = 8.4, 6.6, 1.0 Hz, 1H), 6.87 (dd, *J* = 7.6, 6.9 Hz, 1H), 6.39 (dd, *J* = 7.6, 0.6 Hz, 1H), 4.11 (s, 3H), 1.99 (s, 3H). **^{13}C NMR** (126 MHz, CD_3CN): δ 155.68, 139.94, 132.81, 131.80, 131.39, 129.71, 127.34, 126.36, 124.85, 122.97, 120.31, 118.20, 117.85, 117.45, 116.23, 115.62, 115.39, 94.23, 56.40, 19.75. **HRMS** ($APCI^+$) for $C_{20}H_{18}NO$; calculated 288.1383, found 288.1380 (error m/z = 1.0 ppm).

11-(o-tolyl)isoindolo[2,1-α]quinoline (**2q**)

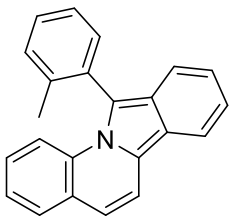

Isolated by column chromatography (10% diethyl ether in pentanes with 1% triethylamine) as a neon yellow solid, 26 mg, 76%. Step a) reaction time: 3hr. **^{1}H NMR** (500 MHz, $CDCl_3$): δ 8.19-8.13 (m, 1H), 8.06 (d, *J* = 9.1 Hz, 1H), 7.82 (dd, *J* = 7.9, 1.6 Hz, 1H), 7.69 (d, *J* = 8.6 Hz, 1H), 7.58-7.50 (m, 2H), 7.49-7.38 (m, 4H), 7.30-7.24 (m, 2H), 7.24-7.17 (m, 2H), 1.96 (s, 3H). **^{13}C NMR** (126 MHz,

$CDCl_3$): δ 139.50, 134.28, 133.71, 131.93, 130.68, 128.94, 128.54, 128.48, 127.24, 126.56, 126.54, 126.49, 124.79, 123.92, 123.70, 120.95, 118.84, 118.66, 118.10, 117.73, 117.33, 115.52, 20.07. **HRMS** ($APCI^+$) for $C_{23}H_{18}N$; calculated 308.1434, found 308.1437 (error m/z = -1.1 ppm).

methyl 4-(isoindolo[2,1-α]quinolin-11-yl)benzoate (**2r**)

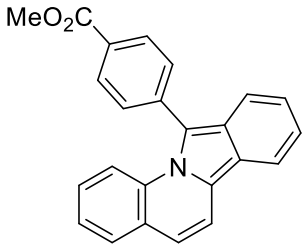

Isolated by column chromatography (10% diethyl ether in pentanes with 1% triethylamine) as a yellow solid, 17 mg, 46%. Step a) reaction time: 6.5 hr. **^{1}H NMR** (500 MHz, $CDCl_3$): δ 8.21 (d, *J* = 8.4 Hz, 2H), 8.10 (d, *J* = 8.4 Hz, 1H), 8.01 (d, *J* = 9.0 Hz, 1H), 7.82 (dd, *J* = 7.9, 1.6 Hz, 1H), 7.76 (d, *J* = 8.7 Hz, 1H), 7.70-7.65 (m, 3H), 7.41 (ddd, *J* = 8.1, 7.1, 1.1 Hz, 1H), 7.32-7.27 (m, 2H), 7.26-7.21 (m, 2H), 4.00 (s, 3H). **^{13}C NMR** (126 MHz, $CDCl_3$): δ 167.13, 139.11, 132.79, 130.27, 129.66, 128.89, 128.75, 127.58, 127.48, 126.47, 125.64, 125.21, 125.10, 121.47, 119.96, 119.18, 118.89, 118.12, 118.02, 117.32, 117.07, 52.37. **HRMS** (ESI^+) for $C_{24}H_{18}NO_2$; calculated 352.1332, found 352.1339 (error m/z = -1.9 ppm).

8,9-dimethyl-6-(o-tolyl)pyrido[2,1-α]isoindole (**2s**)

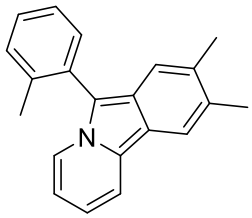

Isolated by column chromatography (5% diethyl ether in pentanes with 1% triethylamine) as a yellow oil, 19 mg, 60%. Step a) reaction time: 5 hr. **^{1}H NMR** (500 MHz, $CDCl_3$): δ 8.06 (dt, *J* = 8.4, 1.3 Hz, 1H), 7.95 (s, 1H), 7.78 (dt, *J* = 6.9, 1.1 Hz, 1H), 7.51-7.35 (m, 4H), 7.33 (s, 1H), 6.84 (td, *J* = 6.8, 1.6 Hz, 1H), 6.80 (ddd, *J* = 8.5, 6.6, 1.2 Hz, 1H), 2.49 (s, 3H), 2.42 (s, 3H), 2.09 (s, 3H). **^{13}C NMR** (126 MHz, $CDCl_3$): δ 139.12, 134.65, 132.12, 130.99, 130.90, 128.88, 128.44, 126.40, 125.77, 124.92, 120.46, 118.60, 118.29, 116.77, 115.96, 114.66, 113.25, 112.59, 21.13, 20.80, 19.79. **HRMS** ($APCI^+$) for $C_{21}H_{20}N$; calculated 286.1590, found 286.1585 (error m/z = 2.0 ppm).

6-(o-tolyl)benzo[f]pyrido[2,1-α]isoindole (**2t**)

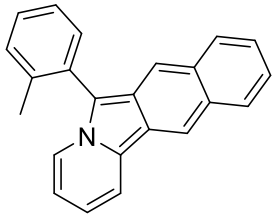

Isolated by column chromatography (10% diethyl ether in pentanes with 1% triethylamine) as a red solid, 10 mg, 32%. Step a) reaction time: 5 hr. **^{1}H NMR** (500 MHz, $CDCl_3$): δ 8.82 (s, 1H), 8.40 (dt, *J* = 8.5, 1.2 Hz, 1H), 8.04 (s, 1H), 8.02 (dt, *J* = 8.5, 0.9 Hz, 1H), 7.96 (dt, *J* = 7.0, 1.0 Hz, 1H), 7.86 (dt, *J* = 8.5, 1.1 Hz, 1H), 7.61 – 7.57 (m, 1H), 7.52 – 7.48 (m, 1H), 7.48 – 7.40 (m, 2H), 7.30 (ddd, *J* = 8.4, 6.4, 1.4 Hz, 1H), 7.25 (ddd, *J* = 7.8, 6.3, 1.3 Hz, 1H), 7.10 (td, *J* = 6.8, 1.4 Hz, 1H), 6.94 (ddd, *J* = 8.0, 6.7, 1.0 Hz, 1H), 2.11 (s, 3H). **^{13}C NMR** (126 MHz, $CDCl_3$): δ 139.26, 132.18, 132.05, 131.16, 130.88, 129.02, 128.68, 128.14, 127.83, 126.72, 126.65, 125.63, 124.40, 122.32, 119.57, 119.07, 119.01, 117.76, 117.55, 113.29, 112.21, 112.01, 19.88. **HRMS** (ESI^+) for $C_{23}H_{18}N$; calculated 308.1434, found 308.1448 (error m/z = -4.7 ppm).

8-methoxy-6-(o-tolyl)-3-(trifluoromethyl)pyrido[2,1-α]isoindole **and** 9-methoxy-6-(o-tolyl)-3-(trifluoromethyl)pyrido[2,1-α]isoindole (**2u**)

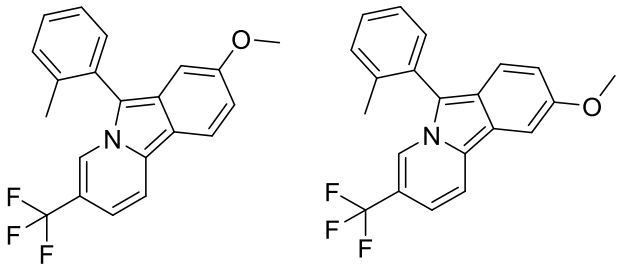

Isomer 1: Isolated by column chromatography (10% diethyl ether in pentanes with 1% triethylamine) as a yellow solid, 13 mg, 34%. Step a) reaction time: 3 hr. **^{1}H NMR** (500 MHz, $CDCl_3$): δ 8.11-8.08 (m, 2H), 8.06 (dd, *J* = 9.0, 0.7 Hz, 1H), 7.52-7.45 (m, 3H), 7.45-7.39 (m, 1H), 7.00-6.96 (m, 1H), 6.94 (dd, *J* = 9.0, 2.2 Hz, 1H), 6.72 (d, *J* = 2.2 Hz, 1H), 3.83 (s, 3H), 2.08 (s, 3H). **^{13}C NMR** (126 MHz, $CDCl_3$): δ 158.51, 139.09, 131.90, 131.34, 129.73, 129.21, 128.28, 126.85, 125.73, 121.06, 118.43, 118.17, 118.08, 115.72, 115.29, 113.04, 109.20, 109.18, 94.81, 55.45, 19.74. **HRMS** ($APCI^+$) for $C_{21}H_{17}ONF_3$; calculated 356.12470, found 356.12568 (error m/z = -2.7 ppm).

Isomer 2: Isolated by column chromatography (10% diethyl ether in pentanes with 1% triethylamine) as a yellow solid, 12 mg, 32%. Step a) reaction time: 3 hr. **^{1}H NMR** (500 MHz, $CDCl_3$): δ 8.10 (d, *J* = 9.1 Hz, 1H), 8.05 (q, *J* = 1.4 Hz, 1H), 7.50-7.36 (m, 6H), 7.09 (dd, *J* = 9.2, 2.3 Hz, 1H), 6.85 (dd, *J* = 9.1, 1.6 Hz, 1H), 3.97 (s, 3H), 2.06 (s, 3H). **^{13}C NMR** (201 MHz, $CDCl_3$): δ 154.96, 138.92, 131.91, 131.25, 129.44, 129.28, 129.13, 126.71, 124.22, 123.66, 120.14, 119.91,

119.38, 119.35, 119.18, 117.19, 116.71, 107.37, 96.87, 55.65, 19.74. **HRMS** ($APCI^+$) for $C_{21}H_{17}ONF_3$; calculated 356.12472, found 356.12568 (error m/z = -2.7 ppm).

2.5.5 Crystallographic Data

*Crystallization of **2c**:*

In a 25 mL vial, 21 mg of **2c** were dissolved in a minimum amount of acetonitrile (1 mL) to which diethyl ether (5 mL) was carefully overlayed. The solution was left under vacuum in the glovebox. The vacuum adapter was opened to allow the solvent to be removed as slowly as possible (45 minutes). The crystals were then left under vacuum overnight for the removal of trace solvent to give thin yellow crystal flakes. The X-ray crystal structure is available at the Cambridge Crystallographic Data Centre (CCDC) under the deposition number 2386038.

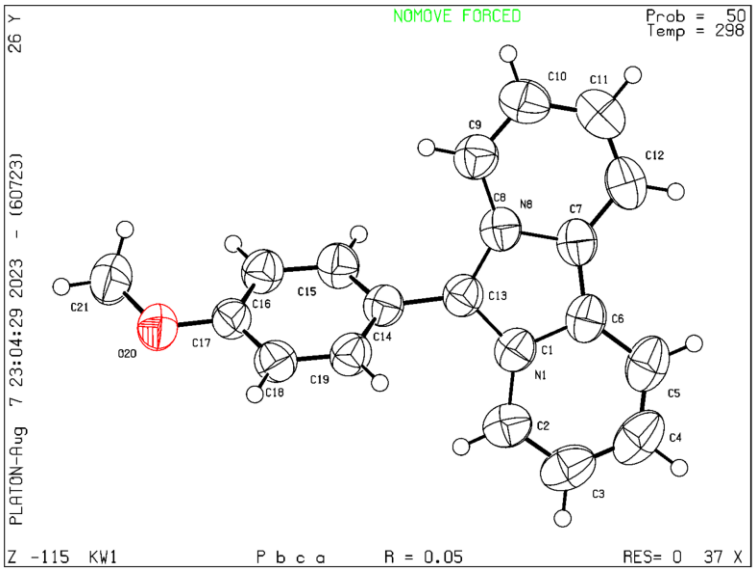

Figure 2.5.2. ORTEP diagram of **2c** with the numbering scheme adopted. Ellipsoid drawn at 50% probability level.

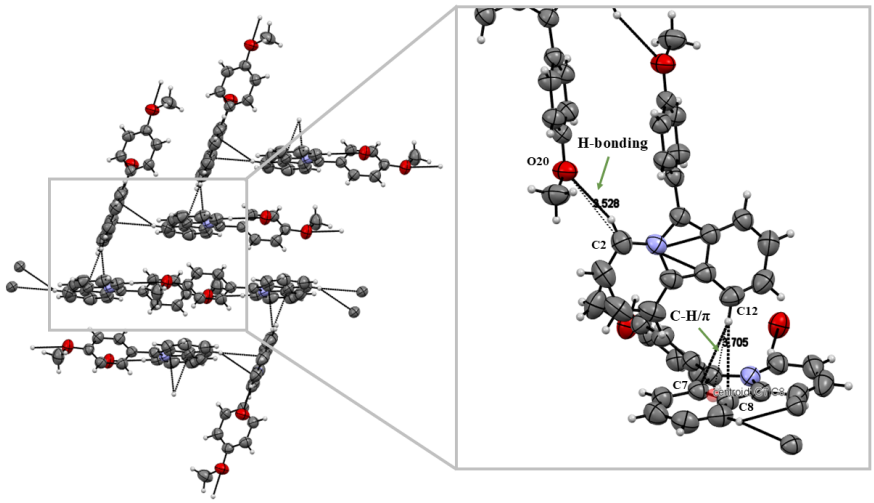

Figure 2.5.3. Intermolecular interactions within the crystal lattice of **2c**: C-H/π (3.705 Å) between C12-H and the pyrido[2,1-α]isoindole core; H-bonding (3.528 Å) between the *p*-OCH_3 group and C2-H.

Table 2.5.2. Crystal data and structure refinement for **2c**.

Identification code	KW1
Empirical formula	$C_{19}H_{15}NO$
Formula weight	273.32
Temperature/K	298(2)
Crystal system	orthorhombic
Space group	Pbca
a/Å	16.4292(4)
b/Å	7.6601(2)
c/Å	22.9023(6)
α/°	90
β/°	90
γ/°	90
Volume/$Å^3$	2882.24(13)
Z	8
$\rho_{calc}g/cm^3$	1.260
μ/mm^{-1}	0.609
F(000)	1152.0
Crystal size/mm^3	0.177 × 0.102 × 0.022
Radiation	CuKα (λ = 1.54178)
2Θ range for data collection/°	7.72 to 144.912
Index ranges	$-19 \leq h \leq 20$, $-9 \leq k \leq 9$, $-28 \leq l \leq 28$

Reflections collected	41004
Independent reflections	2849 [R_{int} = 0.0982, R_{sigma} = 0.0374]
Data/restraints/parameters	2849/0/192
Goodness-of-fit on F^2	1.102
Final R indexes [I>=2σ (I)]	R_1 = 0.0509, wR_2 = 0.1290
Final R indexes [all data]	R_1 = 0.0836, wR_2 = 0.1730
Largest diff. peak/hole / e $Å^{-3}$	0.12/-0.16

Table 2.5.3. Fractional Atomic Coordinates ($\times 10^4$) and Equivalent Isotropic Displacement Parameters ($Å^2 \times 10^3$) for **2c**. U_{eq} is defined as 1/3 of the trace of the orthogonalised U_{IJ} tensor.

Atom	***x***	***y***	***z***	**U(eq)**
N1	4648.8(11)	-180(3)	3716.2(8)	60.2(6)
C8	5844.9(11)	-292(3)	3260.5(8)	59.3(6)
C1	4648.8(11)	-180(3)	3716.2(8)	60.2(6)
N8	5844.9(11)	-292(3)	3260.5(8)	59.3(6)
C3	3295.8(15)	-777(4)	4014.5(12)	83.3(8)
C2	3964.6(13)	252(4)	4047.3(10)	70.9(6)
C4	3270.6(17)	-2262(4)	3653.8(12)	90.9(9)
C5	3923.8(17)	-2683(4)	3318.7(12)	81.9(8)
C6	4623.3(14)	-1644(3)	3339.6(9)	64.1(6)
C7	5374.3(13)	-1708(3)	3048.8(9)	62.5(6)
C9	6648.4(13)	-100(3)	3064.1(10)	68.4(6)
C10	6950.4(16)	-1226(4)	2664.0(11)	78.4(7)
C11	6472.6(18)	-2594(4)	2436.0(12)	82.8(8)
C12	5702.0(17)	-2834(3)	2626.7(10)	74.7(7)
C13	5394.3(12)	651(3)	3669.5(9)	58.8(5)
C14	5654.7(12)	2222(3)	3982.6(9)	57.4(5)
C15	5986.2(13)	3623(3)	3682.8(9)	64.2(6)
C16	6274.5(13)	5092(3)	3970.8(10)	63.8(6)
C17	6224.0(12)	5180(3)	4570.0(9)	58.4(5)
C18	5870.3(13)	3822(3)	4880.2(9)	63.7(6)
C19	5593.1(13)	2365(3)	4588.6(9)	62.8(6)
O20	6509.9(10)	6551(2)	4897.1(7)	75.5(5)
C21	6949.9(18)	7871(4)	4600.2(13)	91.1(8)

Table 2.5.4. Anisotropic Displacement Parameters ($Å^2 \times 10^3$) for **2c**. The Anisotropic displacement factor exponent takes the form: $-2\pi^2[h^2a^{*2}U_{11}+2hka^*b^*U_{12}+\ldots]$.

Atom	U_{11}	U_{22}	U_{33}	U_{23}	U_{13}	U_{12}
N1	58.3(11)	64.3(12)	58.1(11)	4.0(9)	-8.3(8)	-2.9(9)
C8	59.5(11)	62.1(12)	56.3(11)	1.1(9)	-9.7(8)	1.6(9)
C1	58.3(11)	64.3(12)	58.1(11)	4.0(9)	-8.3(8)	-2.9(9)
N8	59.5(11)	62.1(12)	56.3(11)	1.1(9)	-9.7(8)	1.6(9)
C3	62.8(14)	113(2)	74.2(16)	19.5(16)	-3.5(11)	-7.3(14)
C2	62.3(13)	85.2(17)	65.2(13)	7.6(12)	-3.1(10)	1.6(12)
C4	77.9(16)	113(2)	82.1(17)	23.0(17)	-17.9(14)	-31.6(16)
C5	85.9(17)	82.7(18)	77.2(16)	9.7(13)	-21.9(13)	-22.5(14)
C6	68.6(13)	62.7(13)	60.9(12)	4.8(10)	-14.9(10)	-6.4(10)
C7	68.1(13)	61.7(12)	57.6(11)	-0.7(10)	-14.5(9)	0.3(10)
C9	61.6(12)	74.6(15)	68.9(14)	-0.1(11)	-6.4(10)	-0.2(11)
C10	72.8(14)	89.2(18)	73.1(15)	0.4(13)	2.6(12)	13.5(13)
C11	94.5(18)	81.9(18)	72.0(15)	-10.8(13)	-2.3(13)	17.3(15)
C12	93.0(17)	65.8(14)	65.3(14)	-8.4(11)	-15.4(12)	2.0(13)
C13	57.6(11)	62.0(12)	57.0(11)	-0.2(10)	-5.3(9)	-2.7(9)
C14	55.5(11)	58.2(12)	58.4(11)	0.9(9)	-4.5(9)	-0.4(9)
C15	74.5(13)	64.3(13)	54.0(11)	2.3(10)	-4.2(10)	-4.2(11)
C16	67.9(13)	61.2(13)	62.2(13)	4.5(10)	-1.0(10)	-4.8(10)
C17	52.0(10)	59.6(12)	63.8(12)	-6.2(10)	-2.8(9)	-0.8(9)
C18	64.3(12)	72.7(14)	54.2(11)	-3.3(10)	-0.4(9)	-3.1(11)
C19	65.1(12)	64.4(13)	58.9(12)	4.4(10)	-0.4(9)	-8.6(10)
O20	79.6(10)	74.3(11)	72.5(10)	-12.6(8)	2.6(8)	-17.4(8)
C21	100.8(19)	78.5(17)	94.0(19)	-11.0(15)	10.4(15)	-28.8(15)

Table 2.5.5. Bond Lengths for **2c**.

Atom	Atom	Length/Å	Atom	Atom	Length/Å
N1	C2	1.396(3)	C5	C6	1.399(3)
N1	C6	1.415(3)	C6	C7	1.403(3)
N1	C13	1.385(3)	C7	C12	1.403(3)
C8	C7	1.418(3)	C9	C10	1.353(3)
C8	C9	1.402(3)	C10	C11	1.410(4)
C8	C13	1.395(3)	C11	C12	1.352(4)
C1	C2	1.396(3)	C13	C14	1.464(3)
C1	C6	1.415(3)	C14	C15	1.386(3)
C1	C13	1.385(3)	C14	C19	1.396(3)
N8	C7	1.418(3)	C15	C16	1.388(3)
N8	C9	1.402(3)	C16	C17	1.376(3)

Table 2.5.5. Bond Lengths for **2c**.

Atom	Atom	Length/Å	Atom	Atom	Length/Å
N8	C13	1.395(3)	C17	C18	1.387(3)
C3	C2	1.354(4)	C17	O20	1.373(2)
C3	C4	1.407(4)	C18	C19	1.378(3)
C4	C5	1.358(4)	O20	C21	1.417(3)

Table 2.5.6. Bond Angles for **2c**.

Atom	Atom	Atom	Angle/°	Atom	Atom	Atom	Angle/°
C2	N1	C6	119.68(19)	C12	C7	N8	119.8(2)
C13	N1	C2	130.2(2)	C12	C7	C6	133.3(2)
C13	N1	C6	110.08(18)	C10	C9	C8	119.7(2)
C9	C8	C7	118.9(2)	C10	C9	N8	119.7(2)
C13	C8	C7	109.65(18)	C9	C10	C11	121.4(2)
C13	C8	C9	131.3(2)	C12	C11	C10	120.2(2)
C2	C1	C6	119.68(19)	C11	C12	C7	119.9(2)
C13	C1	C2	130.2(2)	N1	C13	C8	106.47(19)
C13	C1	C6	110.08(18)	N1	C13	C14	126.75(19)
C9	N8	C7	118.9(2)	C8	C13	C14	126.78(19)
C13	N8	C7	109.65(18)	C1	C13	N8	106.47(19)
C13	N8	C9	131.3(2)	C1	C13	C14	126.75(19)
C2	C3	C4	121.8(3)	N8	C13	C14	126.78(19)
C3	C2	N1	119.0(3)	C15	C14	C13	120.56(18)
C3	C2	C1	119.0(3)	C15	C14	C19	117.4(2)
C5	C4	C3	120.0(2)	C19	C14	C13	122.03(19)
C4	C5	C6	119.7(3)	C14	C15	C16	121.8(2)
C5	C6	N1	119.7(2)	C17	C16	C15	119.5(2)
C5	C6	C1	119.7(2)	C16	C17	C18	120.0(2)
C5	C6	C7	133.3(2)	O20	C17	C16	124.1(2)
C7	C6	N1	106.94(18)	O20	C17	C18	115.94(19)
C7	C6	C1	106.94(18)	C19	C18	C17	119.8(2)
C6	C7	C8	106.87(19)	C18	C19	C14	121.5(2)
C6	C7	N8	106.87(19)	C17	O20	C21	117.30(19)
C12	C7	C8	119.8(2)				

Table 2.5.7. Hydrogen Atom Coordinates (Å×10^4) and Isotropic Displacement Parameters (Å^2×10^3) for **2c**.

Atom	***x***	***y***	***z***	**U(eq)**
H3	2840.67	-493.09	4236.51	100
H2	3968.05	1231.87	4287	85
H4	2806.39	-2955.98	3644.77	109
H5	3905.99	-3656.42	3076.54	98
H9	6972.2	798.03	3208.31	82
H10	7484.42	-1094.42	2536.69	94
H11	6688.18	-3333.88	2153.56	99
H12	5389.5	-3743.57	2478.21	90
H15	6016.29	3577.17	3277.55	77
H16	6500.32	6010.63	3760.5	77
H18	5820.4	3894.68	5283.98	76
H19	5359.79	1457.81	4800.15	75
H21A	7169.4	8679.85	4878.91	137
H21B	6592.31	8477.29	4338.01	137
H21C	7386.17	7349.63	4382.51	137

Table 2.5.8. Atomic Occupancy for **2c**.

Atom	***Occupancy***	**Atom**	***Occupancy***	**Atom**	***Occupancy***
N1	0.629(18)	C8	0.629(18)	C1	0.371(18)
N8	0.371(18)				

2.5.6 References

(1) D'Souza, D. M.; Müller, T. J. J. Multi-Component Syntheses of Heterocycles by Transition-Metal Catalysis. *Chem. Soc. Rev.* **2007**, *36*, 1095–1108.

(2) Orru, R. V. A.; Ruijter, E. *Synthesis of Heterocycles via Multicomponent Reactions. I*; Topics in heterocyclic chemistry; Springer-Verlag: Berlin, 2010.

(3) Rotstein, B. H.; Zaretsky, S.; Rai, V.; Yudin, A. K. Small Heterocycles in Multicomponent Reactions. *Chem. Rev.* **2014**, *114*, 8323–8359.

(4) *Applied Homogeneous Catalysis with Organometallic Compounds: A Comprehensive Handbook in Four Volumes*; Cornils, B., Herrmann, W. A., Beller, M., Paciello, R., Eds.; John Wiley & Sons, 2017; Vol. 4.

(5) Quesnel, J. S.; Arndtsen, B. A. A Palladium-Catalyzed Carbonylation Approach to Acid Chloride Synthesis. *J. Am. Chem. Soc.* **2013**, *135*, 16841–16844.

(6) Kinney, G.; Tjutrins, J.; Torres, G. M.; Liu, N. J.; Kulkarni, O.; Arndtsen, B. A. A General Approach to Intermolecular Carbonylation of Arene C–H Bonds to Ketones through Catalytic Aroyl Triflate Formation. *Nat. Chem.* **2018**, *10*, 193–199.

(7) Kinney, R. G.; Arndtsen, B. A. Decarboxylation with Carbon Monoxide: The Direct Conversion of Carboxylic Acids into Potent Acid Triflate Electrophiles. *Angew. Chem. Int. Ed.* **2019**, *58*, 5085–5089.

(8) Levesque, T. M.; Kinney, R. G.; Arndtsen, B. A. A Palladium-Catalyzed C–H Functionalization Route to Ketones *via* the Oxidative Coupling of Arenes with Carbon Monoxide. *Chem. Sci.* **2020**, *11*, 3104–3109.

(9) Liu, Y.; Kaiser, A. M.; Arndtsen, B. A. Palladium Catalyzed Carbonylative Generation of Potent, Pyridine-Based Acylating Electrophiles for the Functionalization of Arenes to Ketones. *Chem. Sci.* **2020**, *11*, 8610–8616.

(10) Munday, R. H.; Martinelli, J. R.; Buchwald, S. L. Palladium-Catalyzed Carbonylation of Aryl Tosylates and Mesylates. *J. Am. Chem. Soc.* **2008**, *130*, 2754–2755.

(11) Brennführer, A.; Neumann, H.; Beller, M. Palladium-Catalyzed Carbonylation Reactions of Aryl Halides and Related Compounds. *Angew. Chem. Int. Ed.* **2009**, *48*, 4114–4133.

(12) Burhardt, M. N.; Taaning, R. H.; Skrydstrup, T. Pd-Catalyzed Thiocarbonylation with Stoichiometric Carbon Monoxide: Scope and Applications. *Org. Lett.* **2013**, *15*, 948–951.

(13) Arndtsen, B. A. Metal-Catalyzed One-Step Synthesis: Towards Direct Alternatives to Multistep Heterocycle and Amino Acid Derivative Formation. *Chem. Eur. J.* **2009**, *15*, 302–313.

(14) Bontemps, S.; Quesnel, J. S.; Worrall, K.; Arndtsen, B. A. Palladium-Catalyzed Aryl Iodide Carbonylation as a Route to Imidazoline Synthesis: Design of a Five-Component Coupling Reaction. *Angew. Chem.* **2011**, *123*, 9110–9113.

(15) Leitch, D. C.; Kayser, L. V.; Han, Z.-Y.; Siamaki, A. R.; Keyzer, E. N.; Gefen, A.; Arndtsen, B. A. A Palladium-Catalysed Multicomponent Coupling Approach to Conjugated Poly(1,3-Dipoles) and Polyheterocycles. *Nat. Commun.* **2015**, *6*, 7411.

(16) Tjutrins, J.; Arndtsen, B. A. A Palladium-Catalyzed Synthesis of (Hetero)Aryl-Substituted Imidazoles from Aryl Halides, Imines and Carbon Monoxide. *Chem. Sci.* **2017**, *8*, 1002–1007.

(17) Roy, S. A.; Zgheib, J.; Zhou, C.; Arndtsen, B. A. Palladium Catalyzed Synthesis of Indolizines via the Carbonylative Coupling of Bromopyridines, Imines and Alkynes. *Chem. Sci.* **2021**, *12*, 2251–2256.

(18) *Modern Aryne Chemistry*; Biju, A., Ed.; Wiley-VCH: Weinheim, 2021.

(19) Ne Pellissier, H.; Santelli, M. The Use of Arynes in Organic Synthesis. *Tetrahedron* **2003**, *59*, 701–730.

(20) Rondan, N. G.; Domelsmith, L. N.; Houk, K. N.; Bownelb, A. T.; Levin, R. H. The Relative Rates of Electron-Rich and Electron-Deficient Alkene Cycloadditions to Benzyne Enhanced Electrophilicity as a Consequence of Alkyne Bending Distortions. *Tetrahedron Lett.* **1979**, 3237–5240.

(21) Maier, W. F.; Lau, G. C.; McEwen, A. B. Effect of Bending on the Reactivity of Alkynes: A Semiempirical Study. *J. Am. Chem. Soc.* **1985**, *107*, 4724–4731.

(22) Badaro, J. S. A.; Koszarna, B.; Bousquet, M. H. E.; Ouellette, E. T.; Jacquemin, D.; Gryko, D. T. The Kröhnke Synthesis of Benzo[a]Indolizines Revisited: Towards Small, Red Light Emitters. *Org. Chem. Front.* **2022**, *9*, 1861–1874.

(23) Mitsumori, T.; Bendikov, M.; Dautel, O.; Wudl, F.; Shioya, T.; Sato, H.; Sato, Y. Synthesis and Properties of Highly Fluorescent Indolizino[3,4,5-Ab] Isoindoles. *J. Am. Chem. Soc.* **2004**, *126*, 16793–16803.

(24) Pareek, A.; Mehboob, M. Y.; Cieplak, M.; Majdecki, M.; Szabat, H.; Noworyta, K.; Połczyński, P.; Morawiak, M.; Sharma, P. S.; Foroutan-Nejad, C.; Gaweł, P. Indoloindolizines: The Complete Story of a Polycyclic Aromatic Scaffold from Theoretical Design to Organic Field-Effect Transistor Applications. *J. Am. Chem. Soc.* **2025**, DOI: 10.1021/jacs.4c16189.

(25) Song, B.; Guo, X.; Yang, L.; Yu, H.; Zong, X.; Liu, X.; Wang, H.; Xu, Z.; Lin, Z.; Yang, W. Rhodium(III)-Catalyzed C-H/O2 Dual Activation and Macrocyclization: Synthesis and Evaluation of Pyrido[2,1-a]Isoindole Grafted Macrocyclic Inhibitors for Influenza H1N1. *Angew. Chem. Int. Ed.* **2023**, *62*, e202218886.

(26) Speck, K.; Magauer, T. The Chemistry of Isoindole Natural Products. *Beilstein J. Org. Chem.* **2013**, *9*, 2048–2078.

(27) Hamlin, A. M.; Kisunzu, J. K.; Sarpong, R. Synthetic Strategies toward Hetidine and Hetisine-Type Diterpenoid Alkaloids. *Org. Biomol. Chem.* **2014**, *12*, 1846–1860.

(28) Pelletier, S. W. Research in the Chemistry of Diterpenoid Alkaloids. *Pure Appl. Chem.* **1997**, *69*, 119–124.

(29) Pokholenko, A. A.; Vojtenko, Z. V.; Kovtunenko, V. A. Pyrido- and Pyrimidoisoindoles: Methods of Synthesis and Properties. *Russ. Chem. Rev.* **2004**, *73*, 833–849.

(30) Zhao, B.; Yu, M.; Liu, H.; Chen, Y.; Yuan, Y.; Xie, X. Rhodium-Catalyzed Direct Oxidative C-H Acylation of 2-Arylpyridines with Terminal Alkynes: A Synthesis of Pyrido[2,1-a]Isoindoles. *Adv. Synth. Catal.* **2014**, *356*, 3295–3301.

(31) Li, W.; Zhang, S.; Feng, X.; Yu, X.; Yamamoto, Y.; Bao, M. A Strategy for Amide C−N Bond Activation with Ruthenium Catalyst: Selective Aromatic Acylation. *Org. Lett.* **2021**, *23*, 2521–2526.

(32) Shi, D.; Zeng, T.; Lei, X.; Wu, X.; Li, M.; Zhang, Y. Unexpected Pyridinyl Group Mediated Metal-Free Wacker-Type Oxidation En Route to Pyrido[2,1-a]Isoindol-5-Ium Salts. *Synthesis* **2022**, *54*, 5434–5444.

(33) Xie, C.; Zhang, Y.; Xu, P. Novel Synthesis of Pyrido[2,1-a]Isoindoles via a Three-Component Assembly Involving Benzynes. *Synlett* **2008**, *20*, 3115–3120.

(34) Huang, X.; Zhang, T. Multicomponent Reactions of Pyridines, α-Bromo Carbonyl Compounds and Silylaryl Triflates as Aryne Precursors: A Facile One-Pot Synthesis of Pyrido[2,1-a]Isoindoles. *Tetrahedron Lett.* **2009**, *50*, 208–211.

(35) Idiris, F. I. M.; Jones, C. R. Recent Advances in Fluoride-Free Aryne Generation from Arene Precursors. *Org. Biomol. Chem.* **2017**, *15*, 9044–9056.

(36) *Comprehensive Aryne Synthetic Chemistry*; Yoshida, H., Ed.; Elsevier Science, 2022.

(37) Himeshima, Y.; Sonoda, T.; Kobayashi, H. Fluoride-Induced 1,2-Elimination of o-Trimethylsilylphenyl Triflate to Benzyne Under Mild Conditions. *Chem. Lett.* **1983**, *12*, 1211–1214.

(38) Shi, J.; Li, L.; Li, Y. O-Silylaryl Triflates: A Journey of Kobayashi Aryne Precursors. *Chem. Rev.* **2021**, *121*, 3892–4044.

(39) Hennige, H.; Kreher, R.; Uhrig, J. 3-Alkoxy-1H-Isoindole. *Synthesis* **1982**, *10*, 842–844.

(40) All benzyne is consumed under these conditions, and small amounts of products from its addition to **2a** are formed, suggesting this is the highest efficiency accessible in the reaction.

(41) Ikawa, T.; Masuda, S.; Takagi, A.; Akai, S. 1,3- and 1,4-Benzdiyne Equivalents for Regioselective Synthesis of Polycyclic Heterocycles. *Chem. Sci.* **2016**, *7*, 5206–5211.

(42) Asako, S.; Kobashi, T.; Takai, K. Use of Cyclopropane as C1 Synthetic Unit by Directed Retro-Cyclopropanation with Ethylene Release. *J. Am. Chem. Soc.* **2018**, *140*, 15425–15429.

(43) Dubrovskiy, A. V.; Markina, N. A.; Larock, R. C. Use of Benzynes for the Synthesis of Heterocycles. *Org. Biomol. Chem.* **2013**, *11*, 191–218.

(44) Lopchuk, J. M.; Gribble, G. W. Total Synthesis of Atorvastatin via a Late-Stage, Regioselective 1,3-Dipolar Münchnone Cycloaddition. *Tetrahedron Lett.* **2015**, *56*, 3208–3211.

(45) Layer, R. W. The Chemistry of Imines. *Chem. Rev.* **1963**, 63, 489–510.

(46) Zalesskiy, S. S.; Ananikov, V. P. $Pd_2(dba)_3$ as a Precursor of Soluble Metal Complexes and Nanoparticles: Determination of Palladium Active Species for Catalysis and Synthesis. *Organometallics* **2012**, 31, 2302–2309.

(47) Fozard, A.; Bradsher, C. K. Synthesis of the Pyrido[2,1-α]Isoindole System by an Intramolecular Photochemical Cyclization. *J. Org. Chem.* **1967**, *32*, 2966–2969.

(48) Asako, S.; Kobashi, T.; Takai, K. Use of Cyclopropane as C1 Synthetic Unit by Directed Retro-Cyclopropanation with Ethylene Release. *J. Am. Chem. Soc.* **2018**, 140, 15425–15429.

(49) Badaro, J. S. A.; Koszarna, B.; Bousquet, M. H. E.; Ouellette, E. T.; Jacquemin, D.; Gryko, D. T. The Kröhnke Synthesis of Benzo[a]Indolizines Revisited: Towards Small, Red Light Emitters. *Org. Chem. Front.* **2022**, 9, 1861–1874.

Chapter 3 – Conclusions

A large portion of pharmaceutical drugs contain a fused heterocycle. These heterocyclic systems are typically synthesized *via* intramolecular cyclization and annulation reactions, which require the synthesis of prefunctionalized precursors that limits product accessibility. A potential solution to this issue is to employ 1,3-dipolar cycloaddition with benzyne. As discussed in Chapter 1, methods to generate benzyne have evolved towards more mild conditions that have enabled chemists to explore and expand the application of benzyne in a wide range of reactions including 1,3-dipolar cycloadditions with both acyclic and cyclic 1,3-dipoles, providing a more efficient, alternative route to form a variety of fused heterocycles.

Chapter 2 demonstrates this approach in the synthesis of pyrido[2,1-α]isoindoles *via* a palladium-catalyzed carbonylative coupling of imines, 2-bromopyridines, and *o*-trimethylsilylaryl triflates. The use of carbon monoxide as an energetic building block alongside catalysis allows us to form carboxylic acid derivatives in an exergonic process. The mechanistic insight of this system suggests the initial *in situ* formation of 2-pyridyl acyl chloride electrophiles that react with the imines to form mesoionic pyridine-based 1,3-dipoles. These intermediates then undergo cycloaddition with *in situ* generated arynes under mild conditions to form pyrido[2,1-α]isoindoles. Overall, this strategy offers a one-pot and modular approach to build polysubstituted pyrido[2,1-α]isoindoles using simple and modifiable building blocks.

Appendix I. NMR Spectra of Pyrido[2,1-α]isoindoles in Chapter 2

6-(p-tolyl)pyrido[2,1-α]isoindole (**2a**)

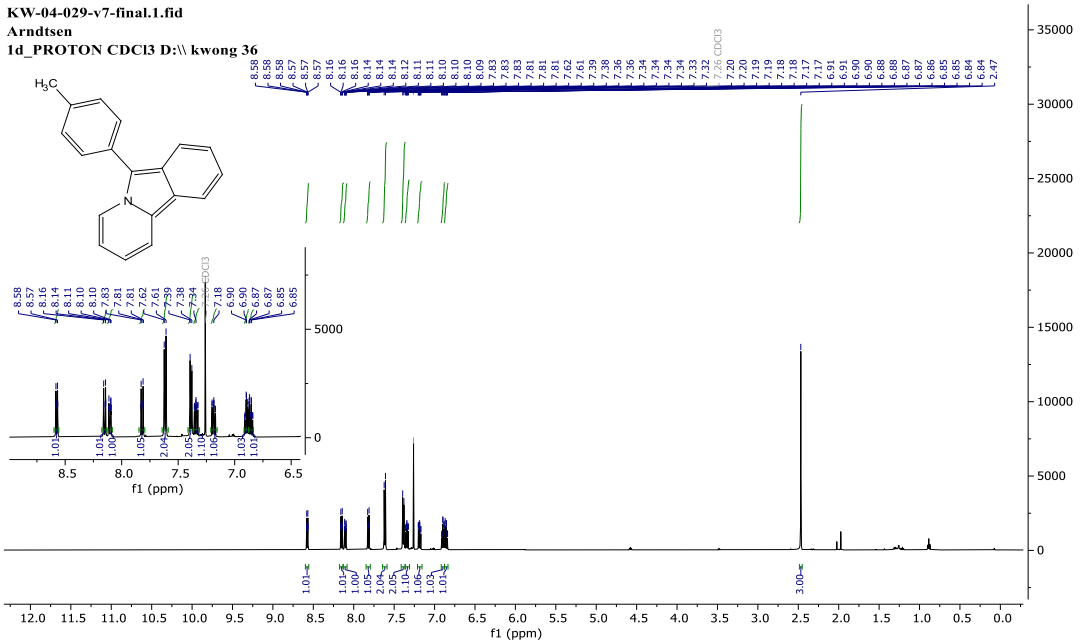

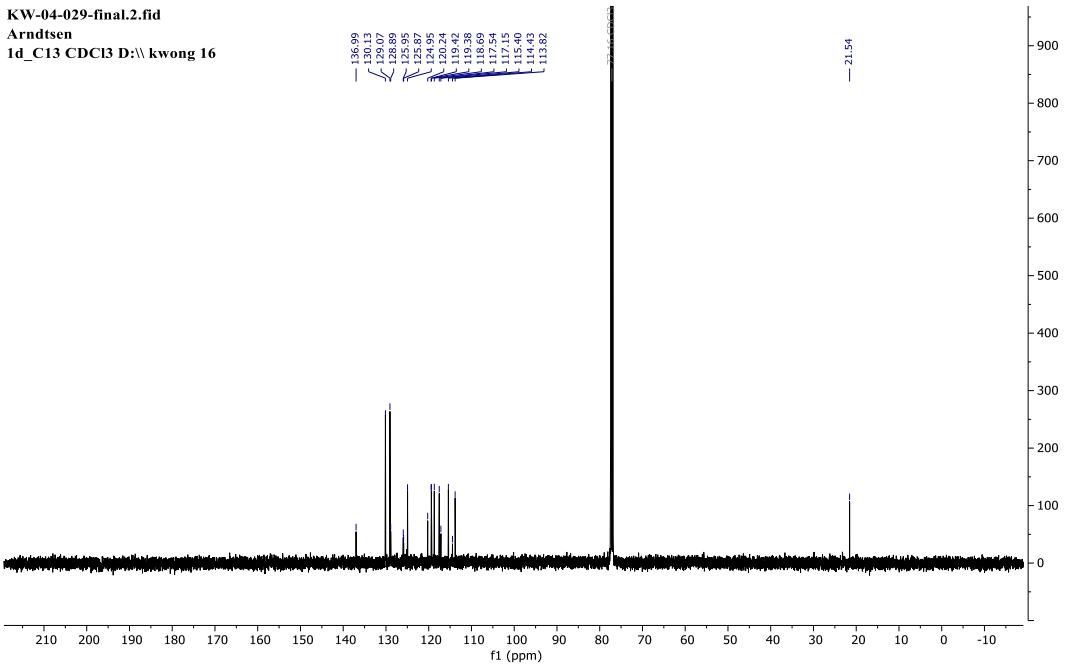

N,N-dimethyl-4-(pyrido[2,1-α]isoindol-6-yl)aniline (**2b**)

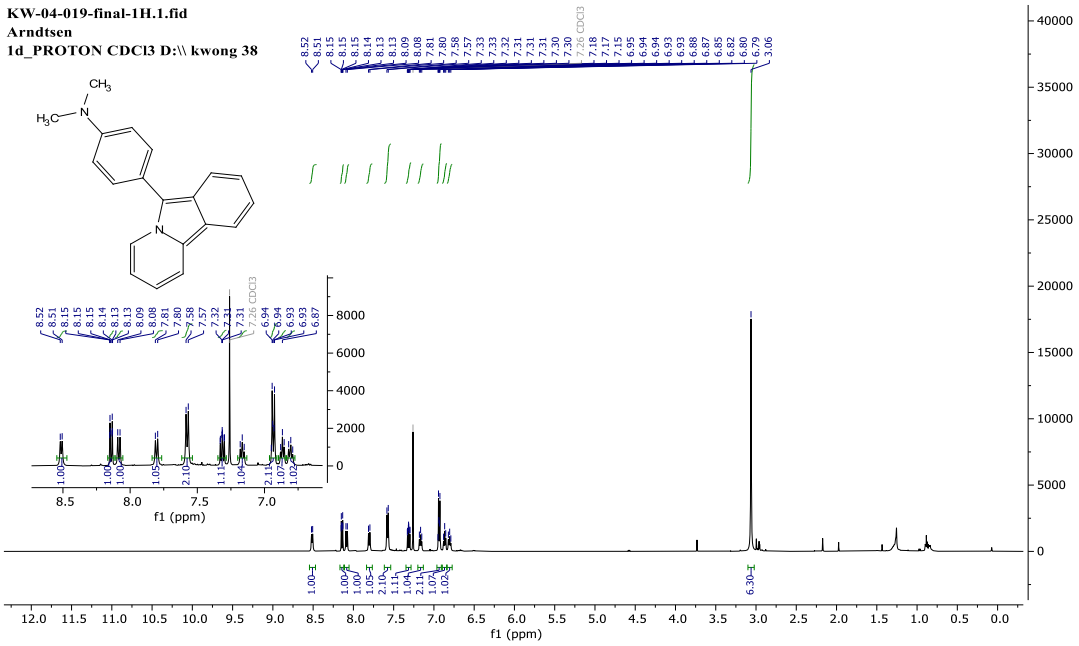

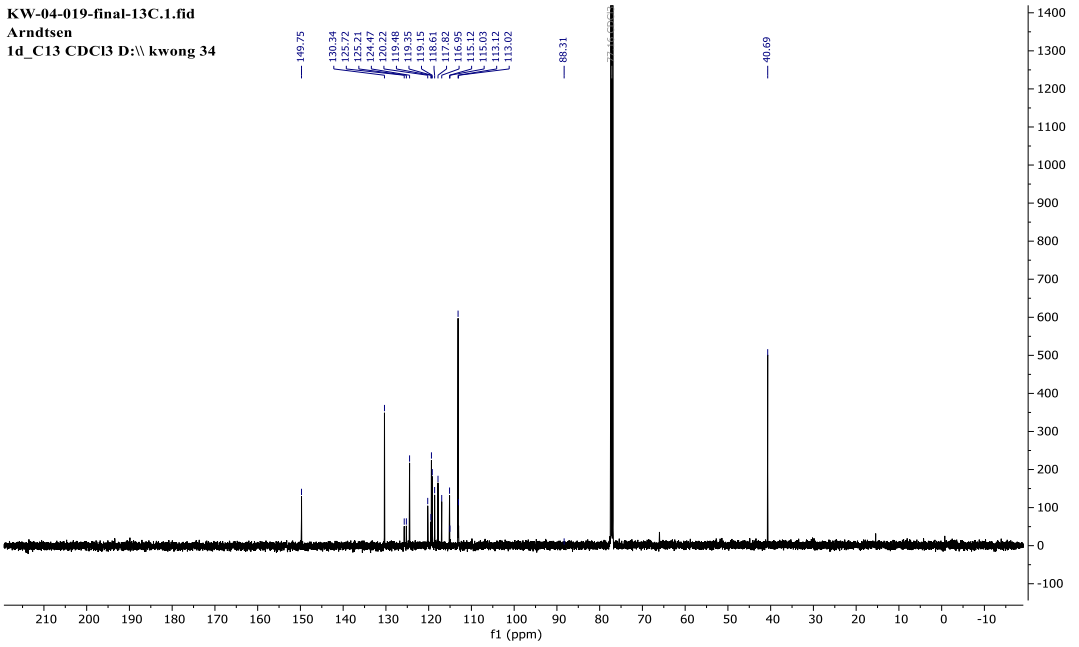

6-(4-methoxyphenyl)pyrido[2,1-α]isoindole (**2c**)

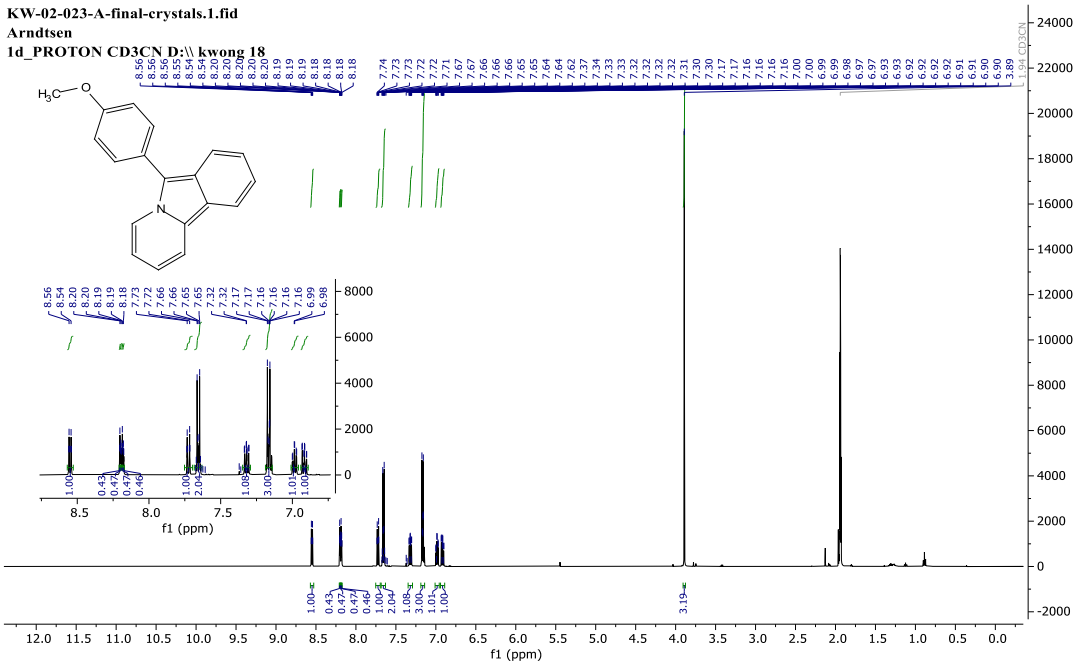

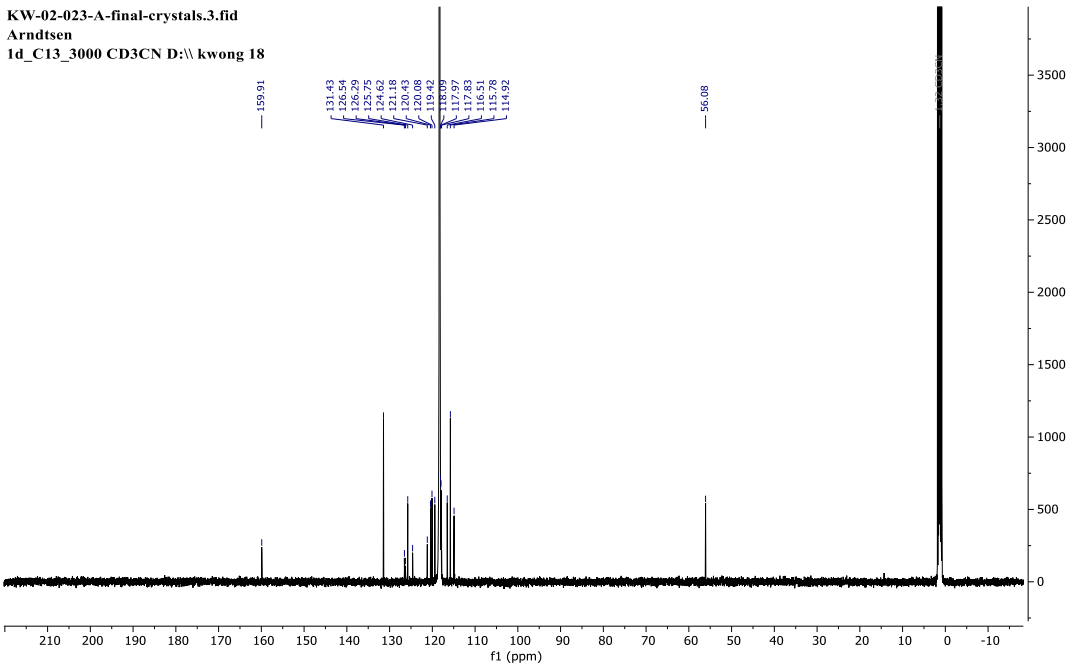

6-(4-(methylthio)phenyl)pyrido[2,1-α]isoindole (**2d**)

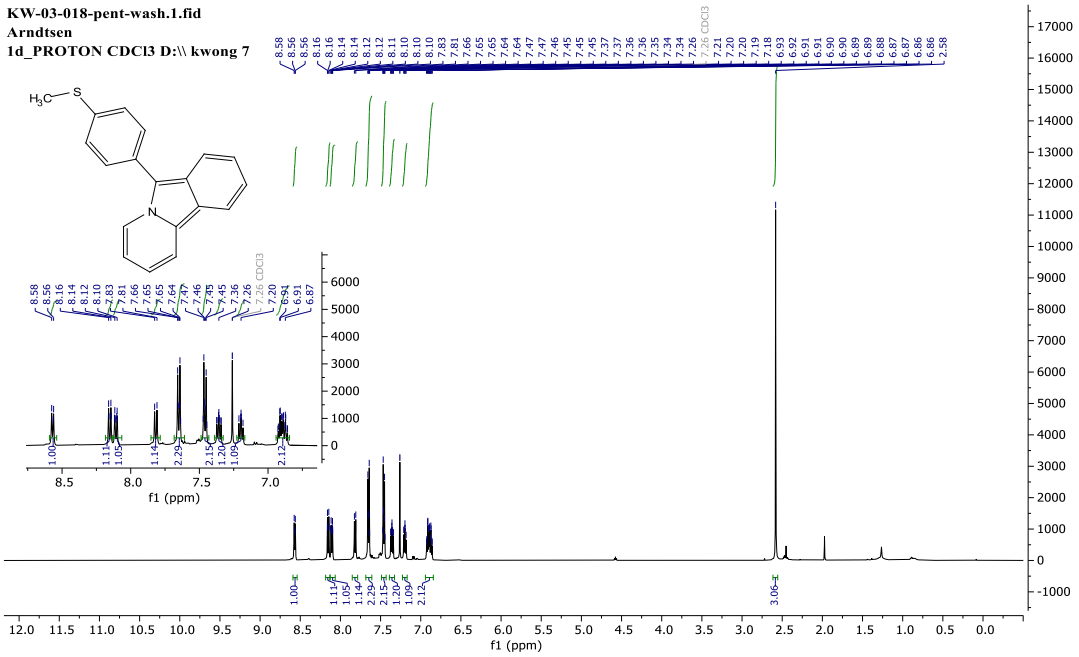

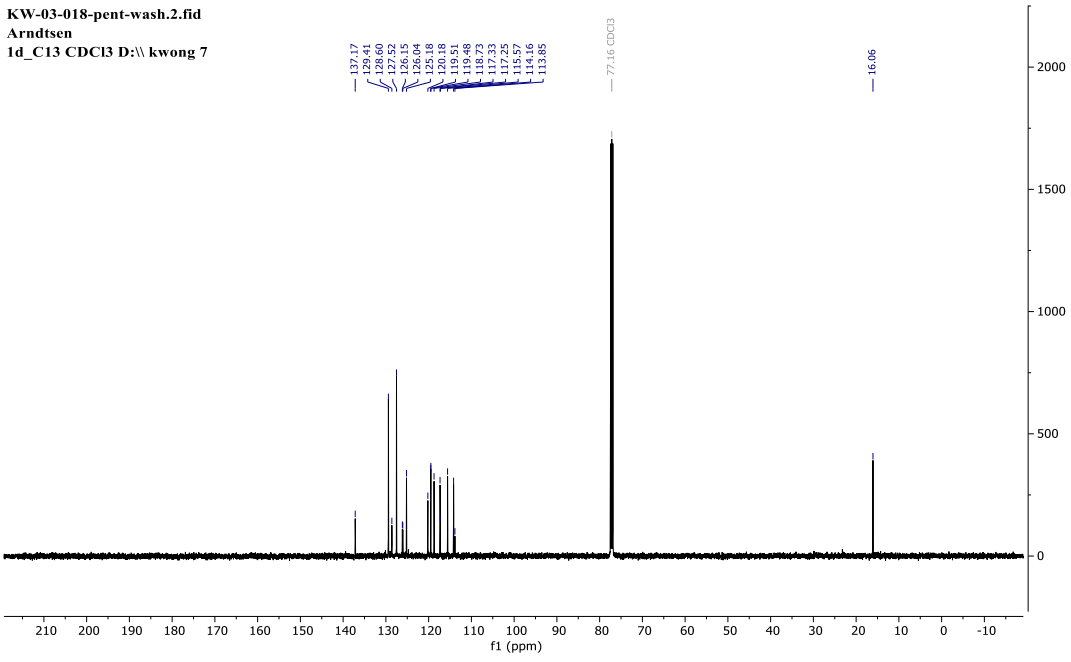

6-(o-tolyl)pyrido[2,1-α]isoindole (**2e**)

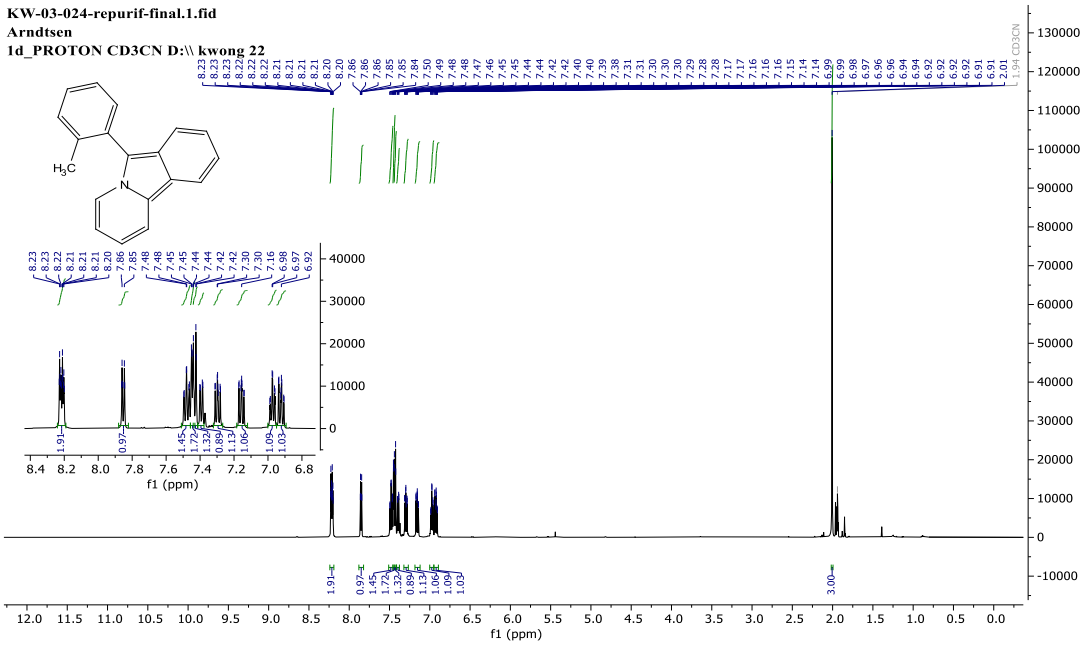

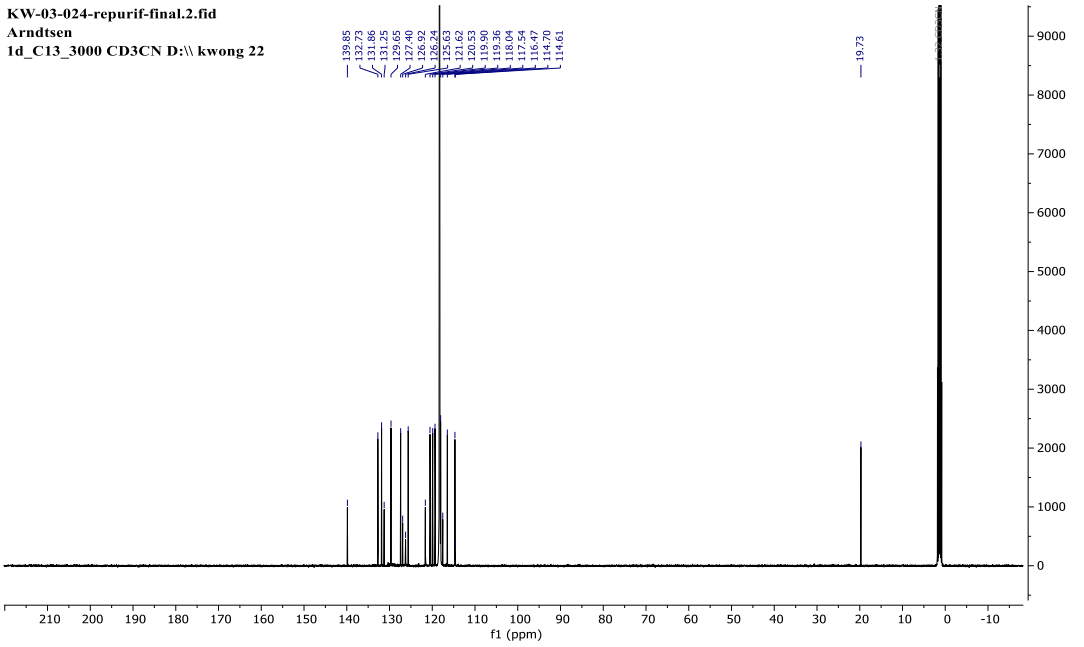

6-(pyridin-2-yl)pyrido[2,1-α]isoindole (**2f**)

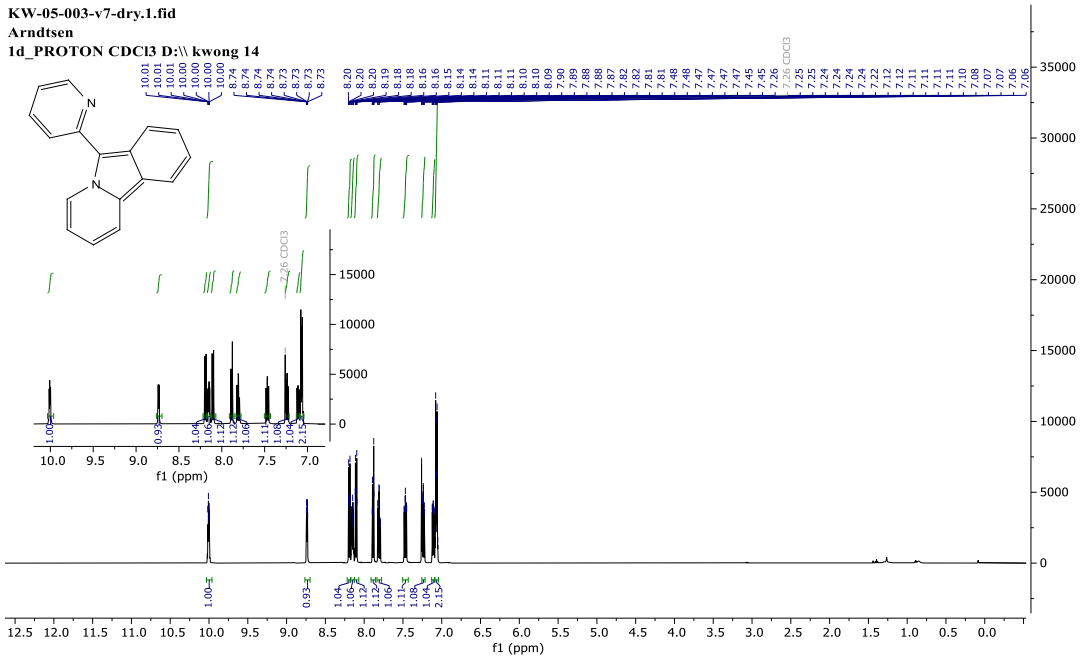

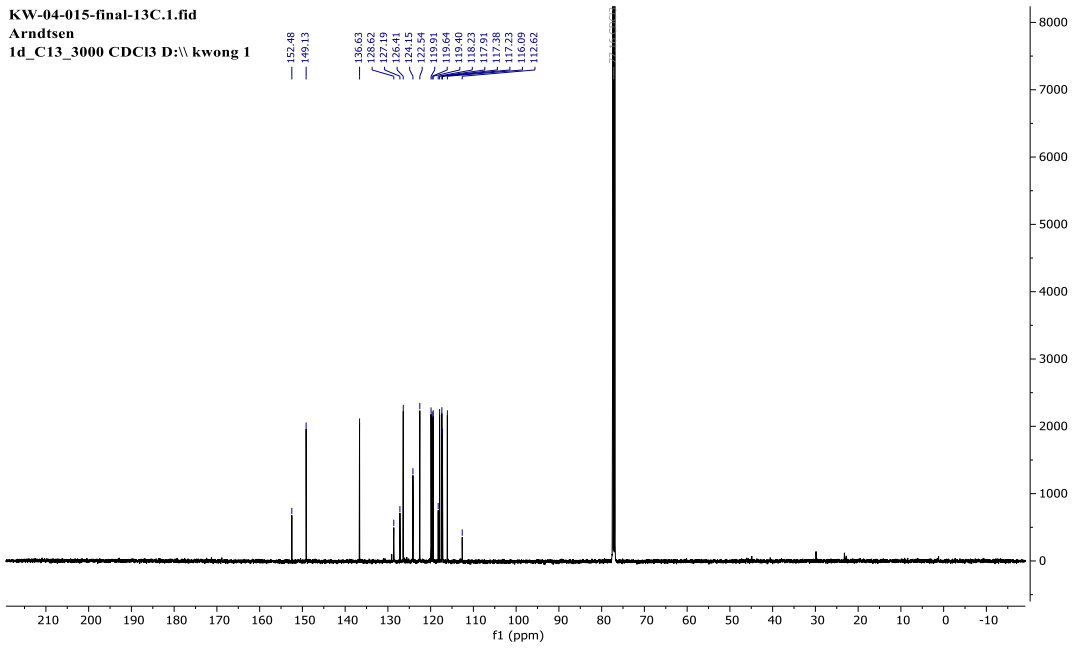

6-(thiophen-2-yl)pyrido[2,1-α]isoindole (**2g**)

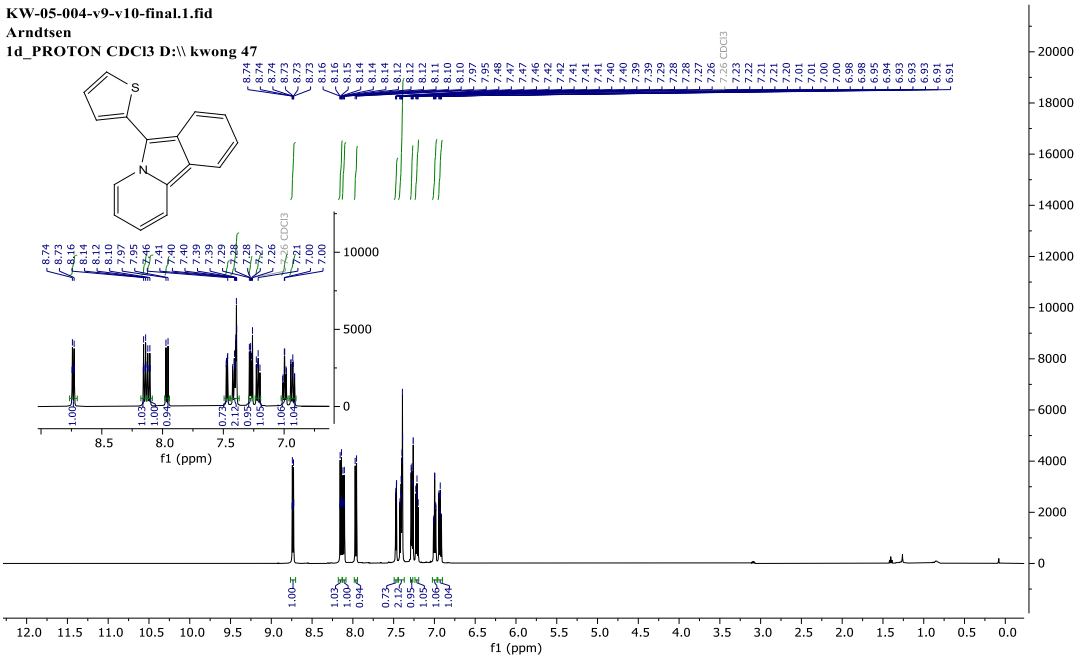

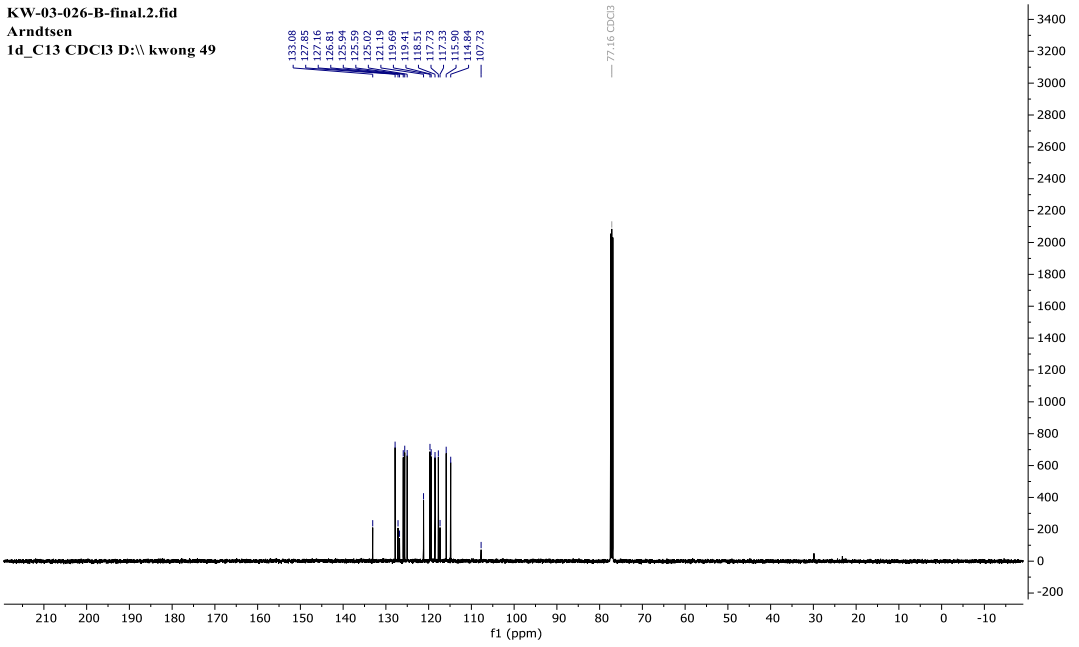

6-(4-nitrophenyl)pyrido[2,1-α]isoindole (**2h**)

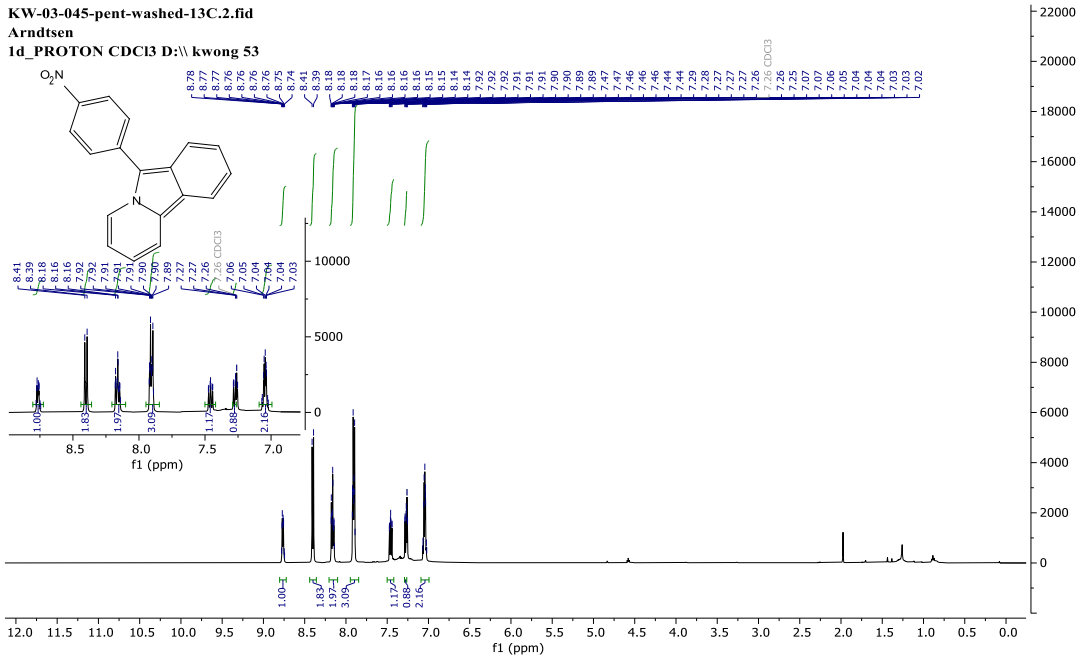

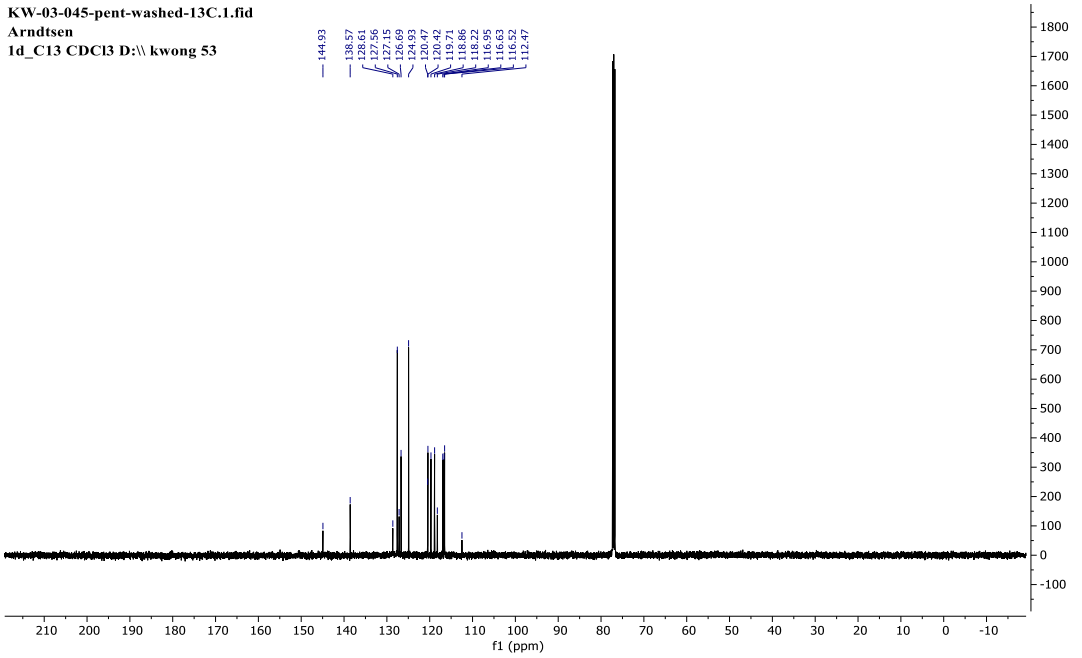

6-(phenanthren-9-yl)pyrido[2,1-α]isoindole (**2i**)

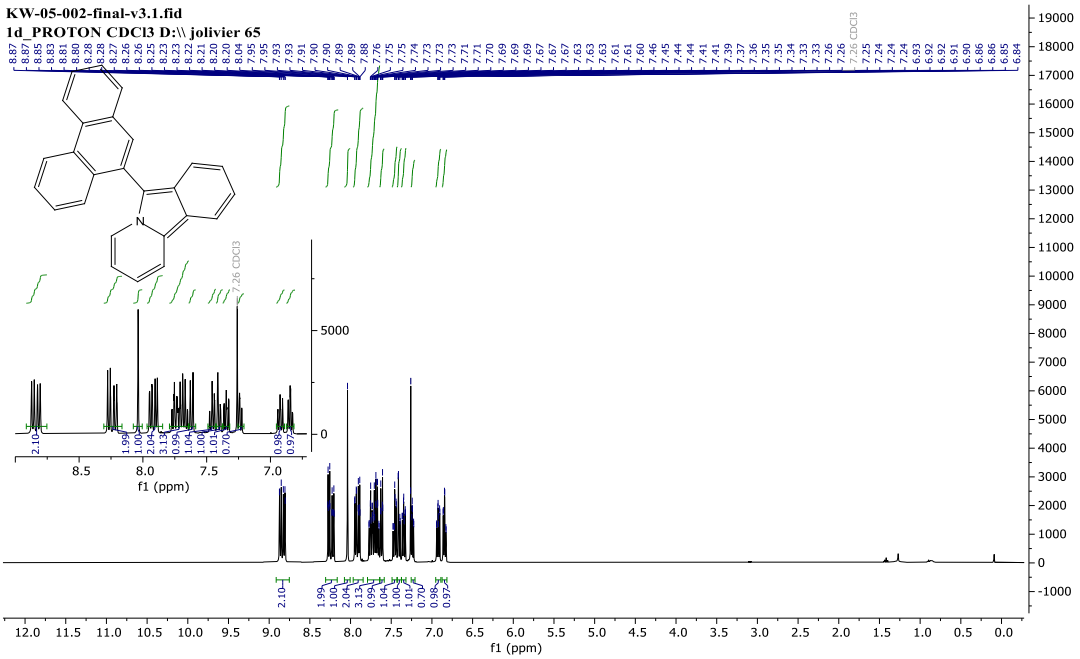

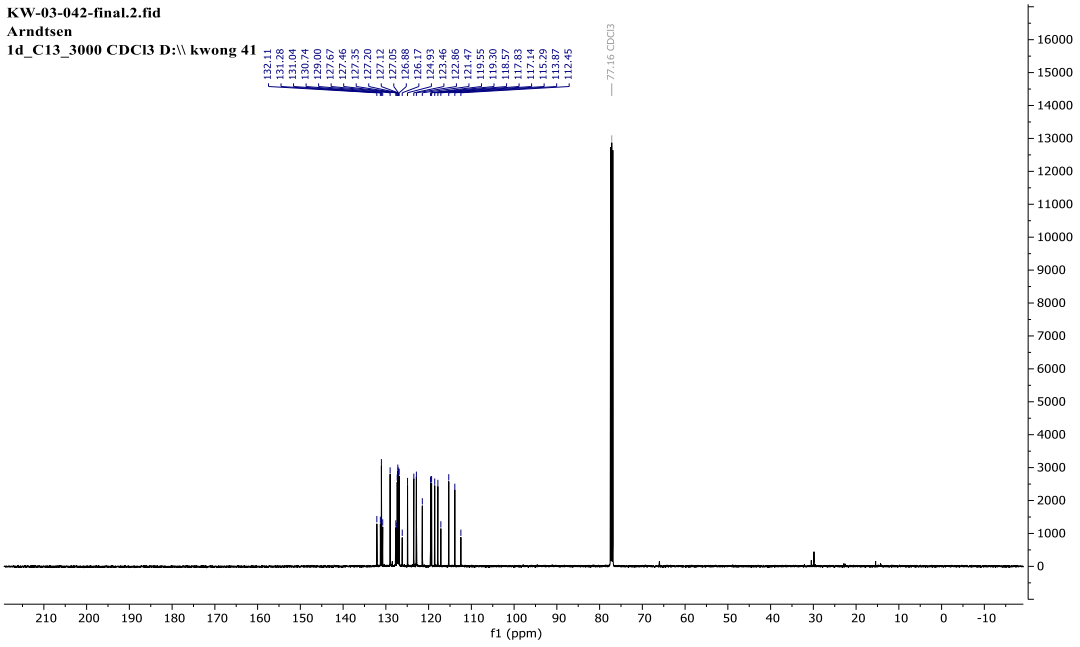

6-(anthracen-9-yl)pyrido[2,1-α]isoindole (**2j**)

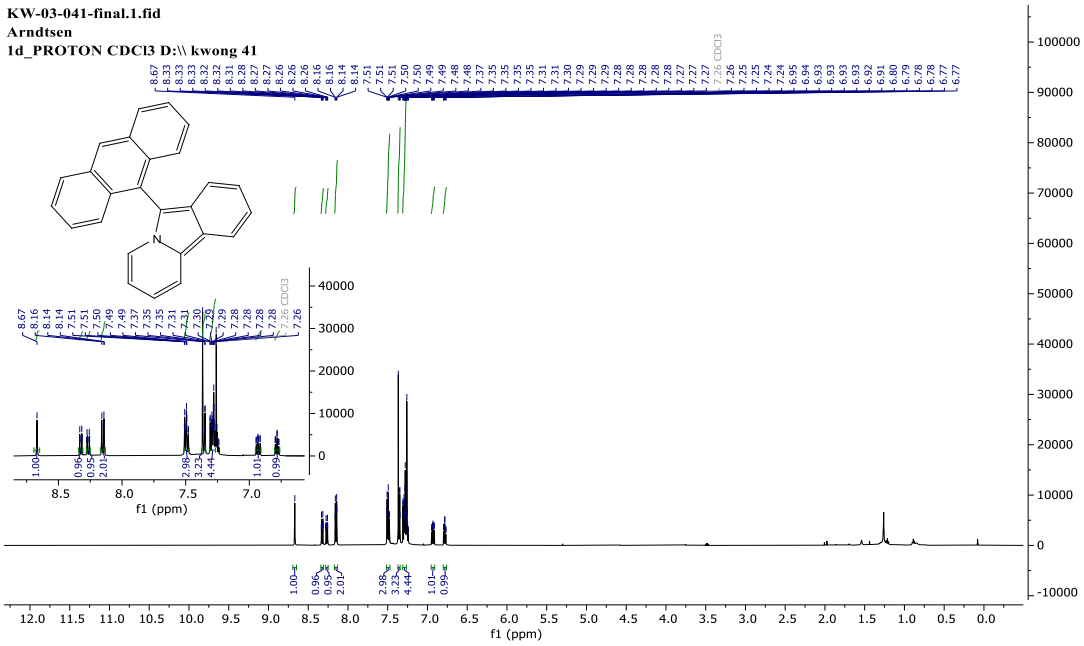

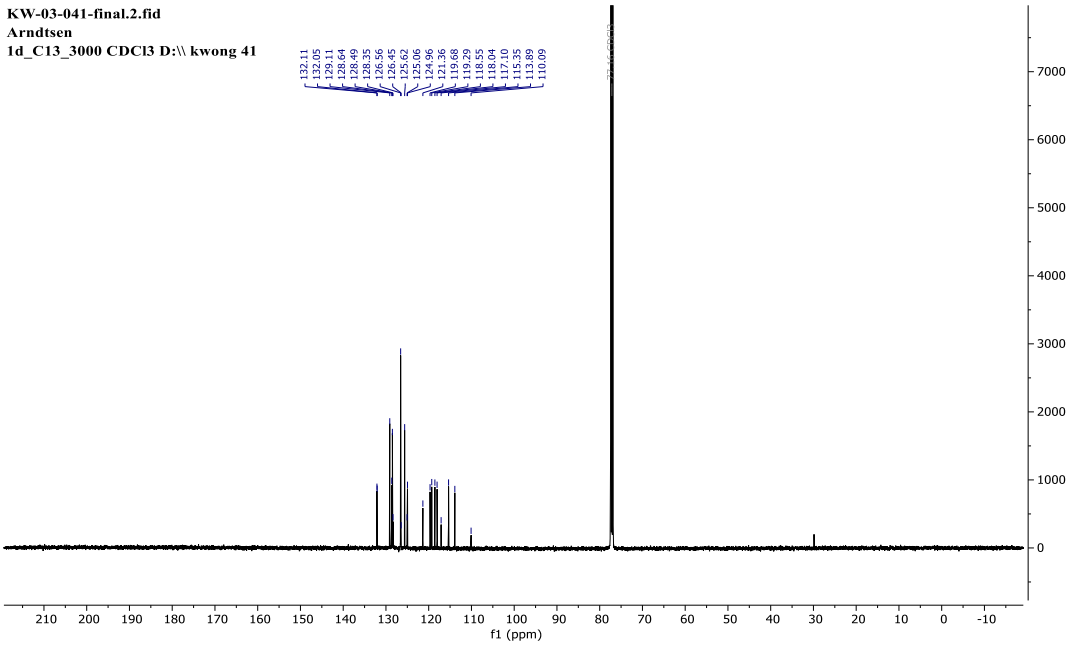

6-isopropylpyrido[2,1-α]isoindole (**2k**)

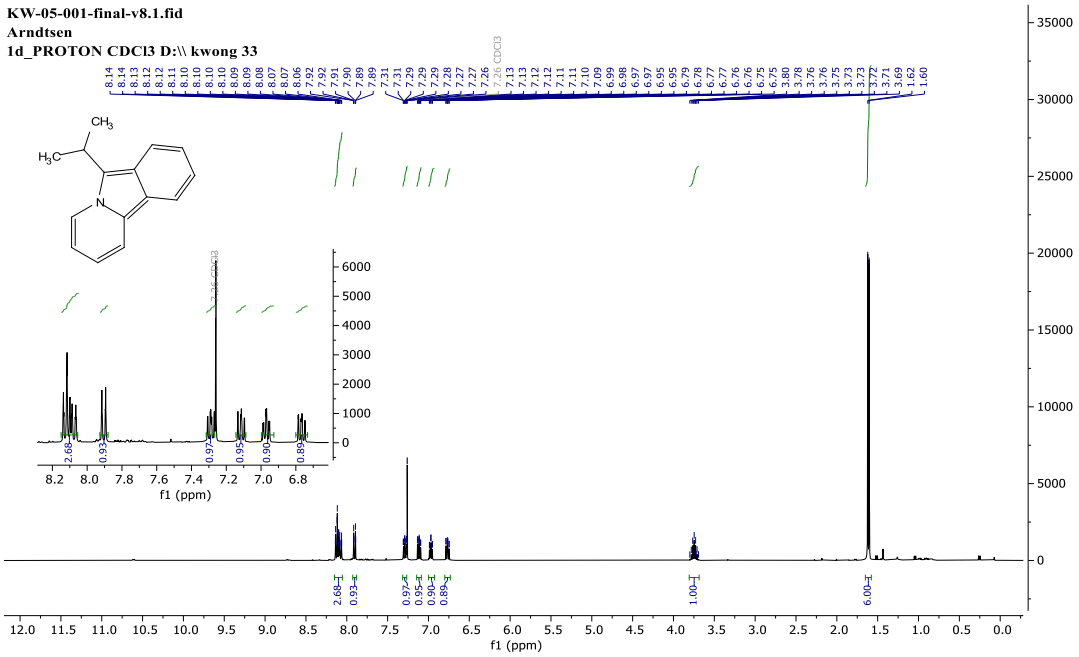

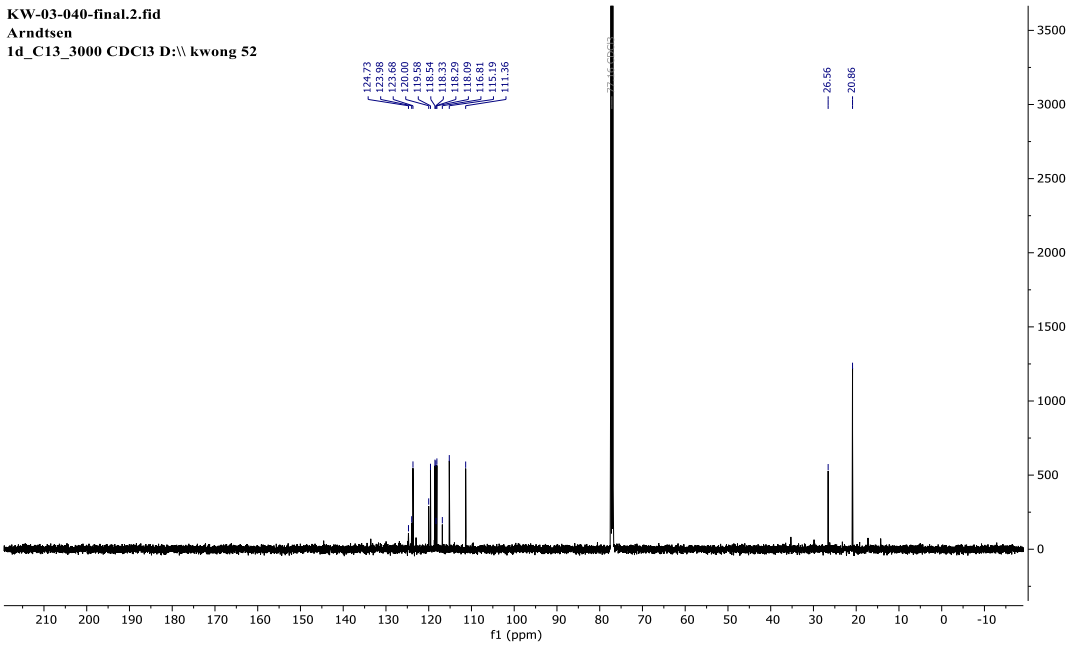

6-cyclohexylpyrido[2,1-α]isoindole (**2l**)

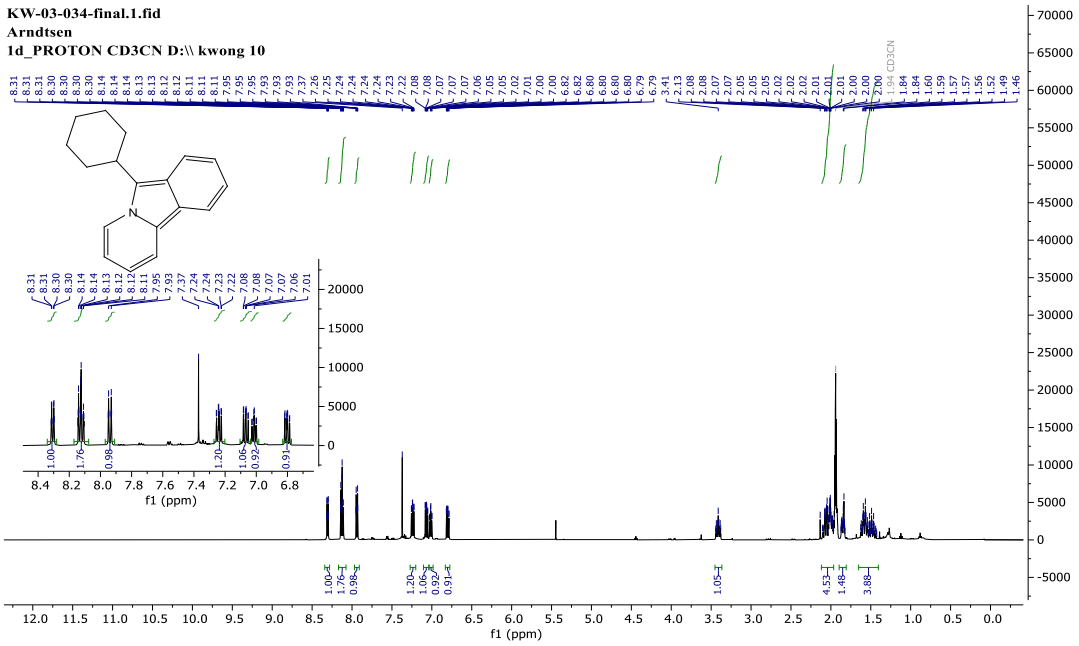

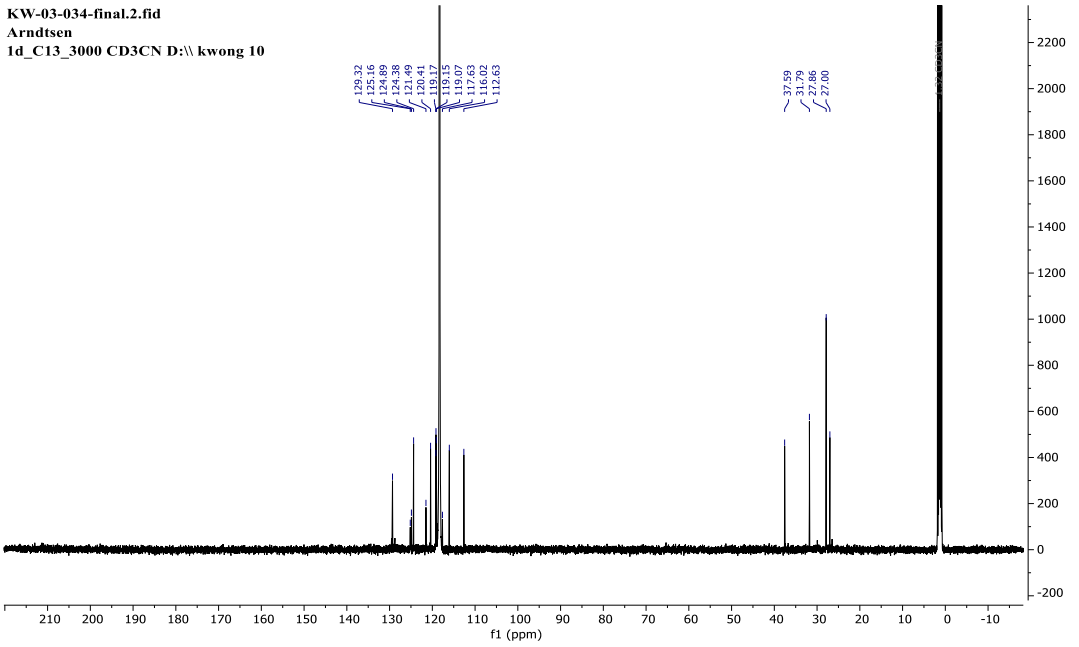

3-methyl-6-(o-tolyl)pyrido[2,1-α]isoindole (**2m**)

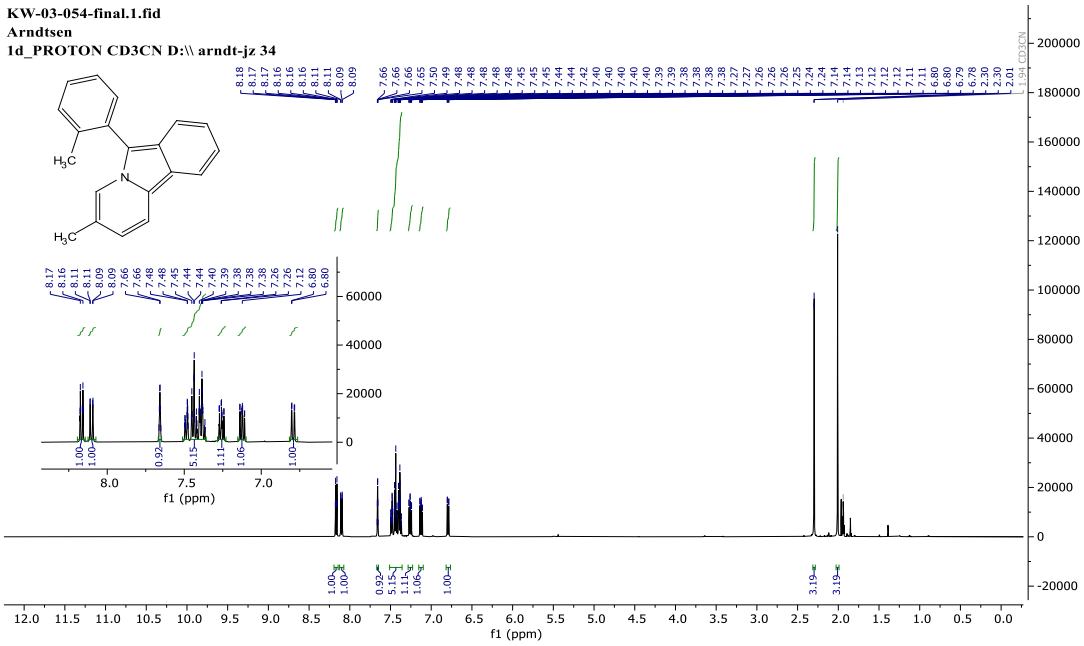

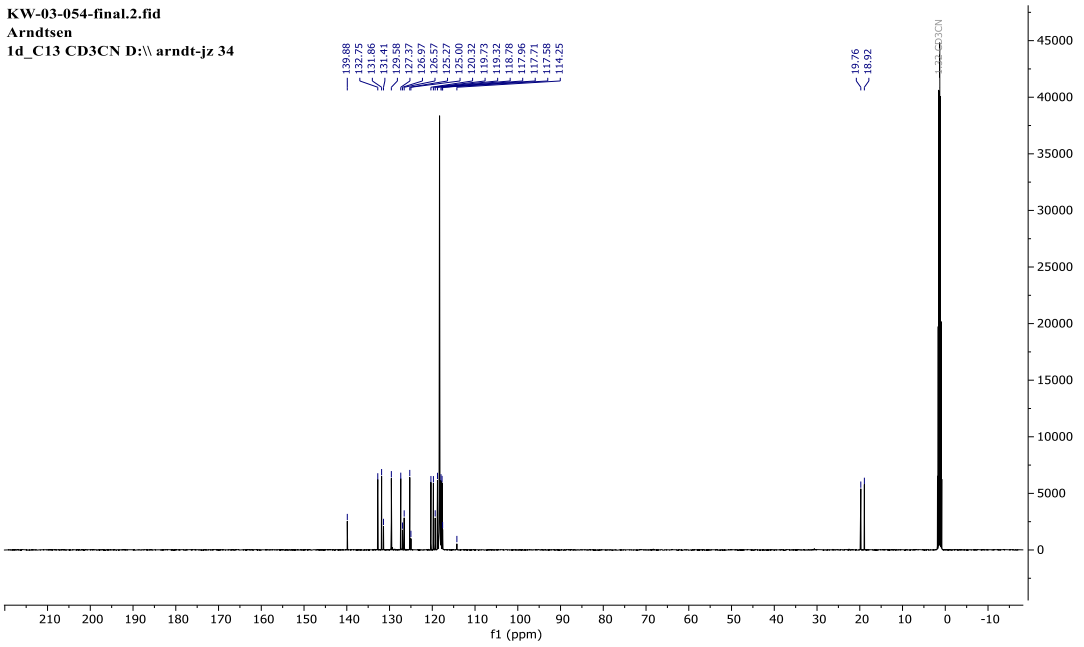

Methyl 6-(o-tolyl)pyrido[2,1-α]isoindole-3-carboxylate (**2n**)

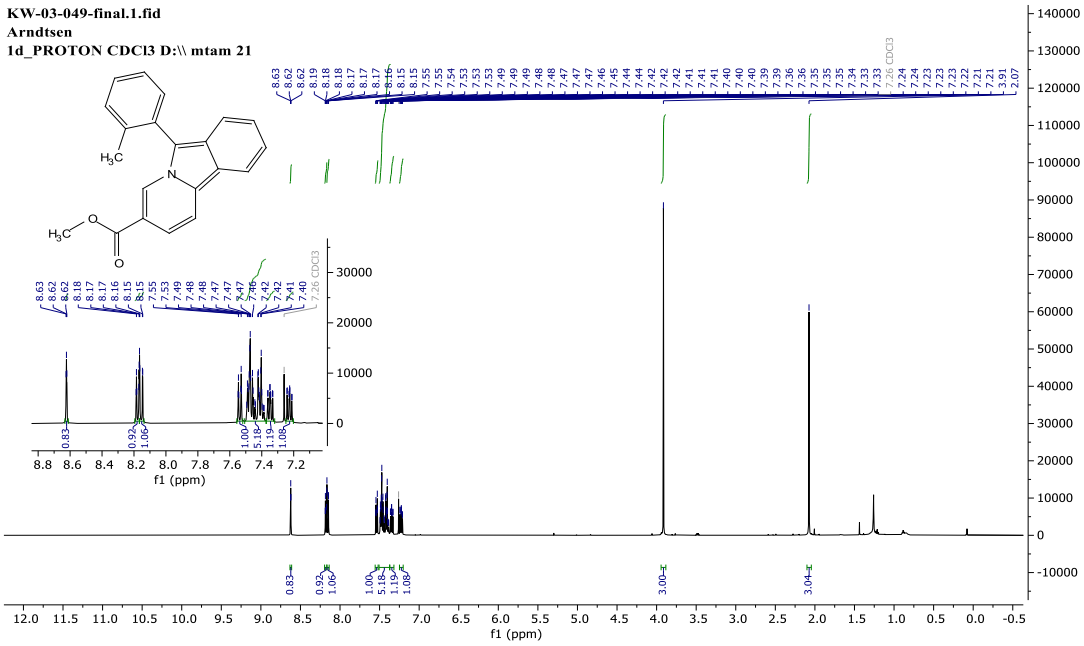

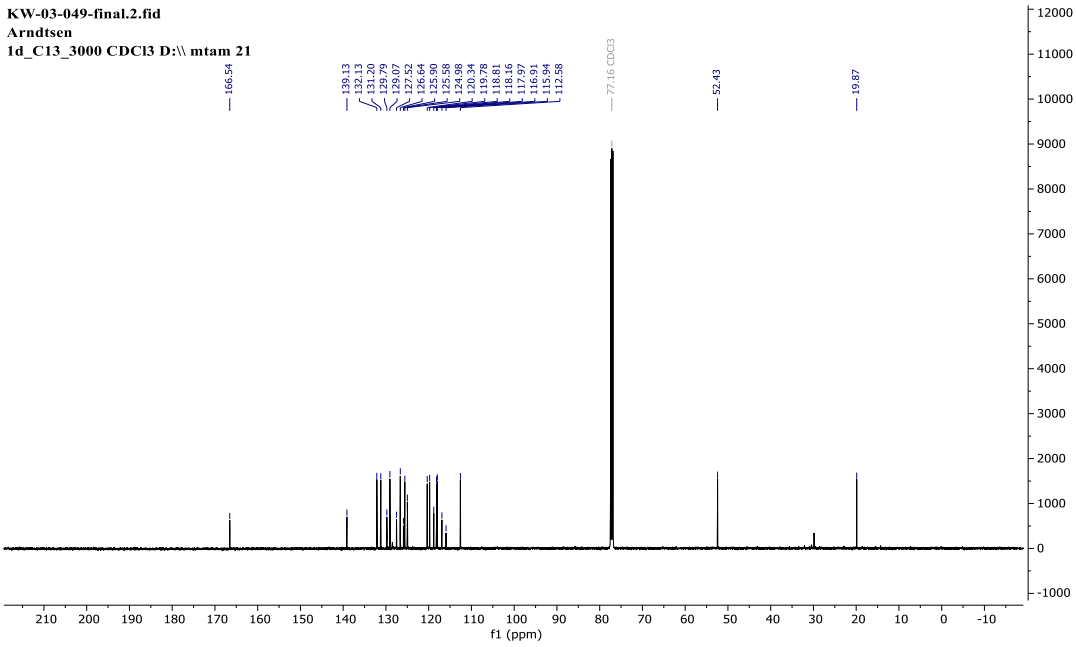

6-(o-tolyl)-3-(trifluoromethyl)pyrido[2,1-α]isoindole (**2o**)

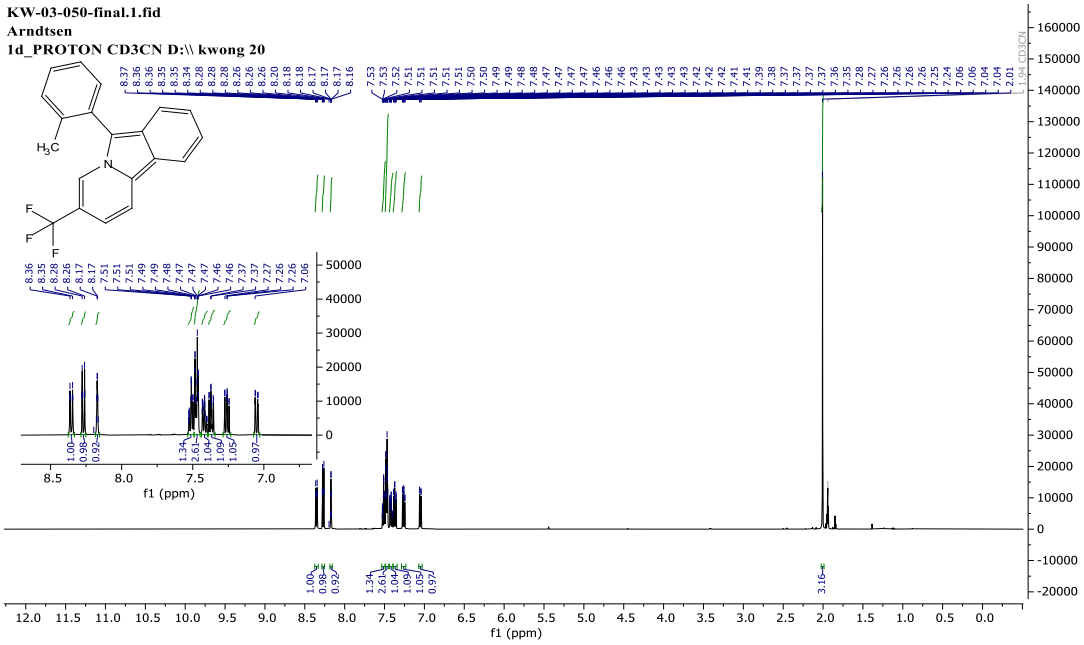

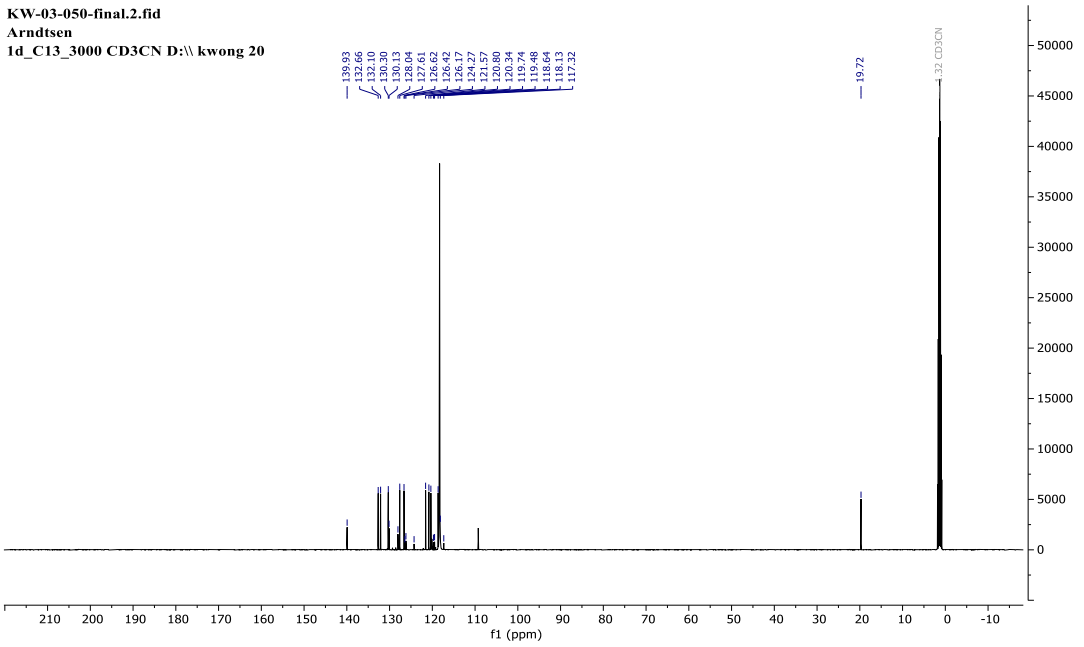

1-methoxy-6-(o-tolyl)pyrido[2,1-α]isoindole (**2p**)

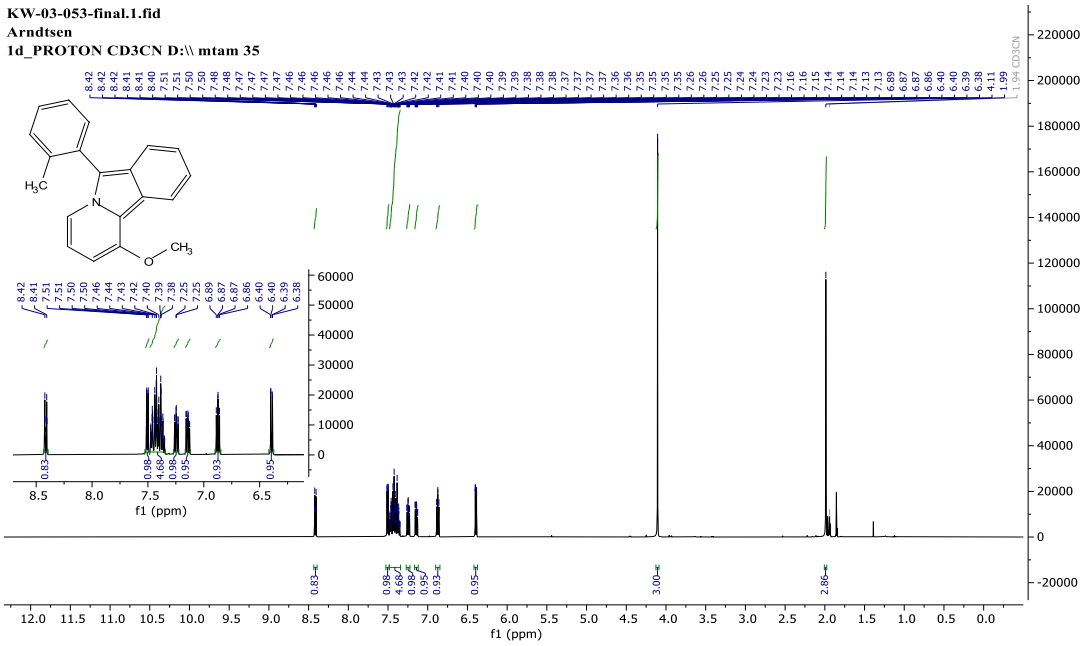

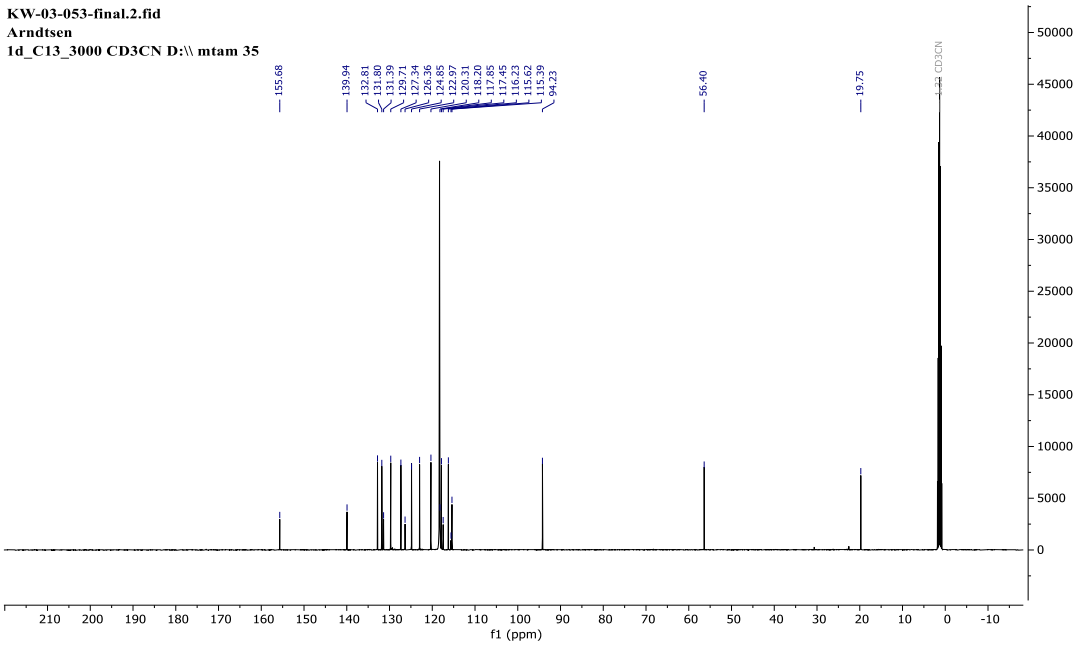

11-(o-tolyl)isoindolo[2,1-α]quinoline (**2q**)

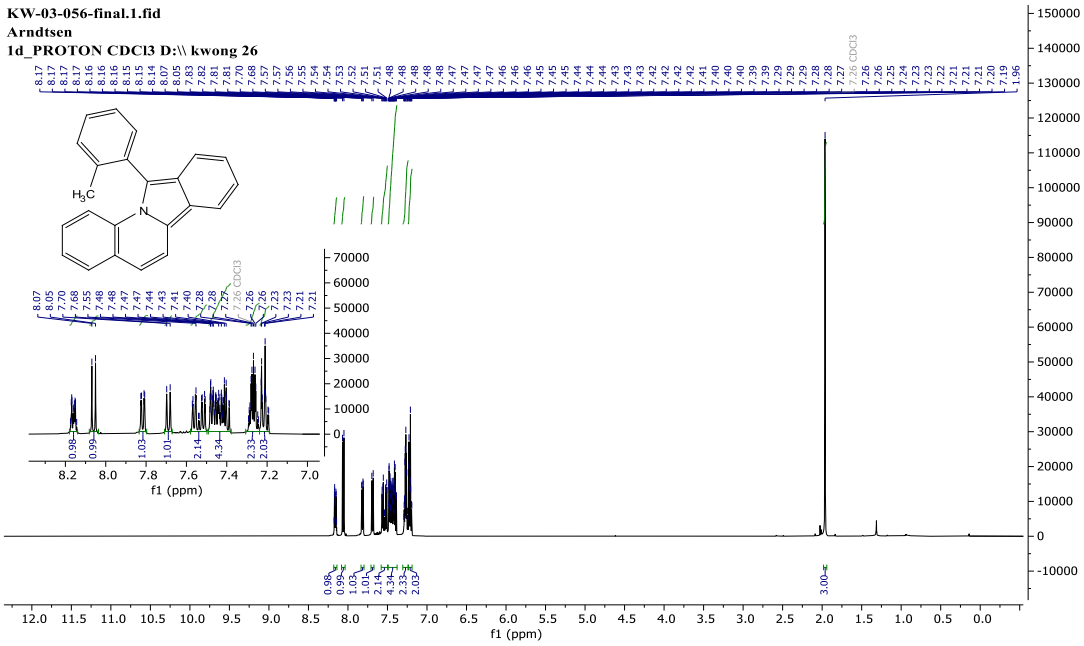

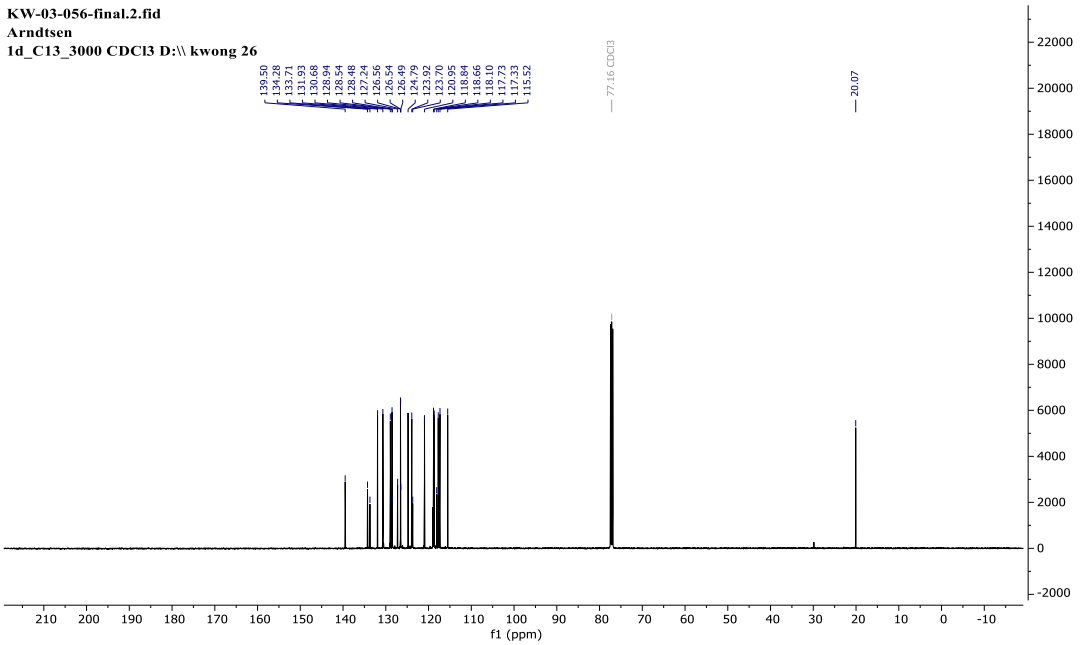

Methyl 4-(isoindolo[2,1-α]quinolin-11-yl)benzoate (**2r**)

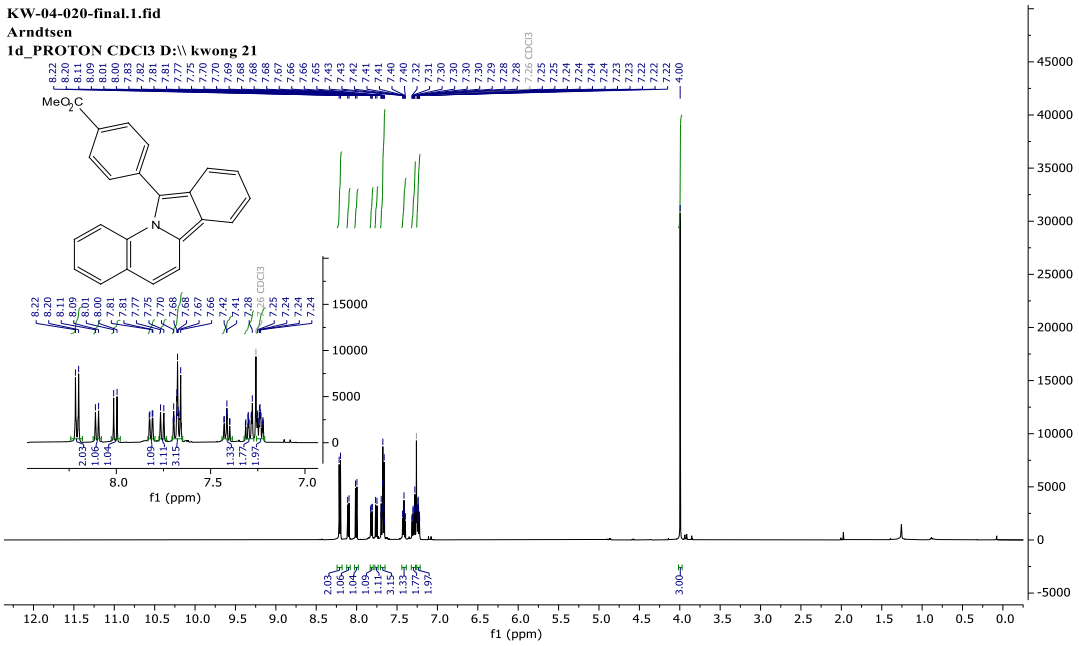

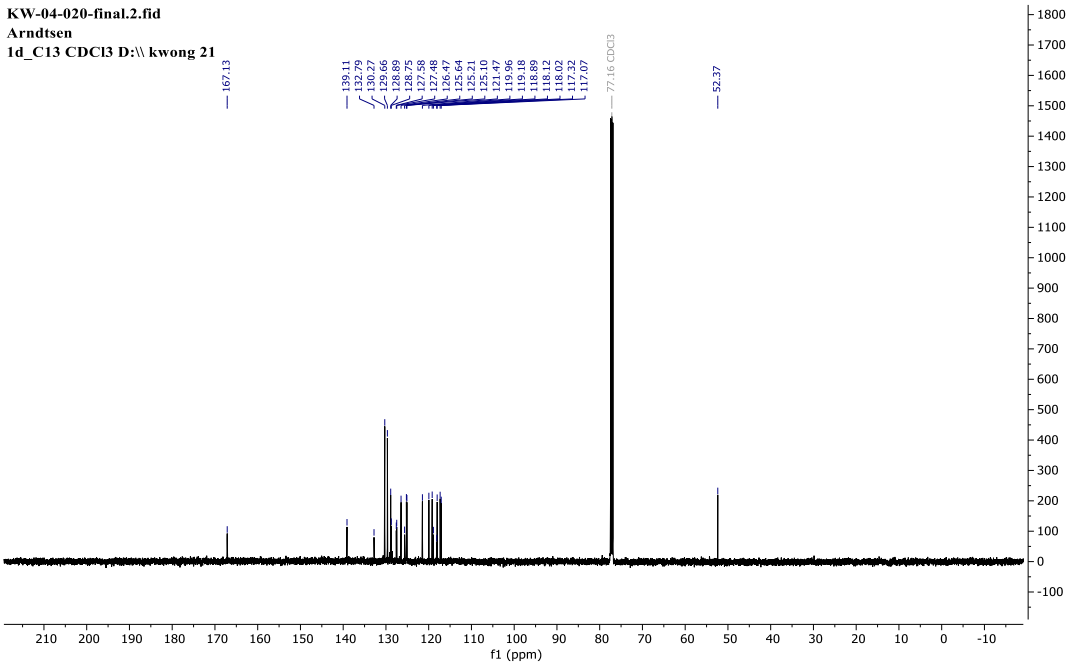

8,9-dimethyl-6-(o-tolyl)pyrido[2,1-α]isoindole (**2s**)

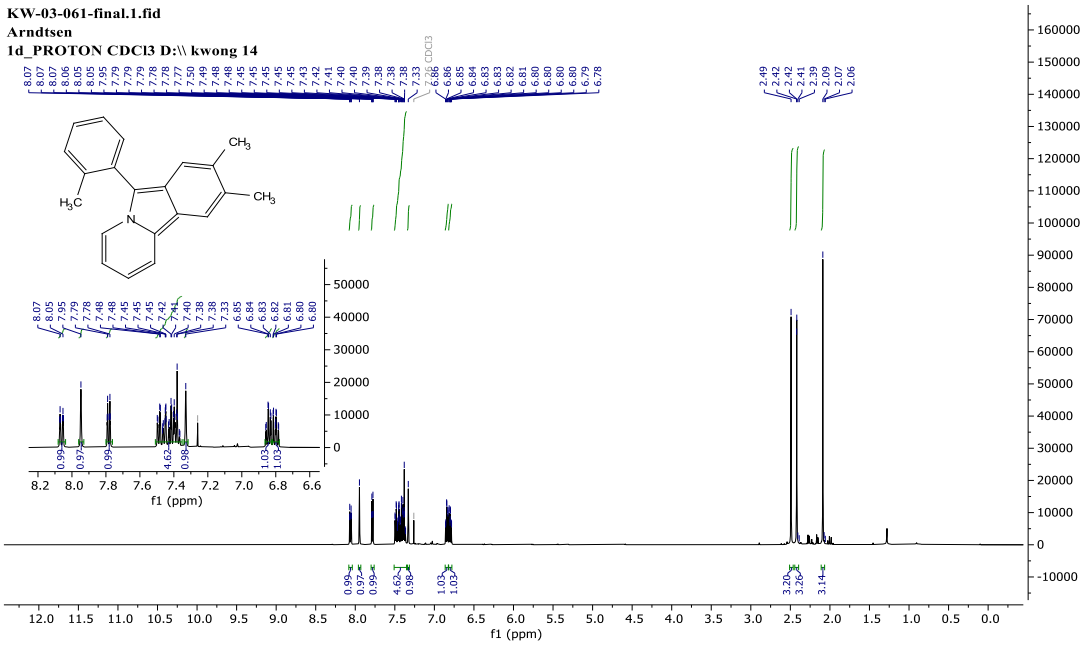

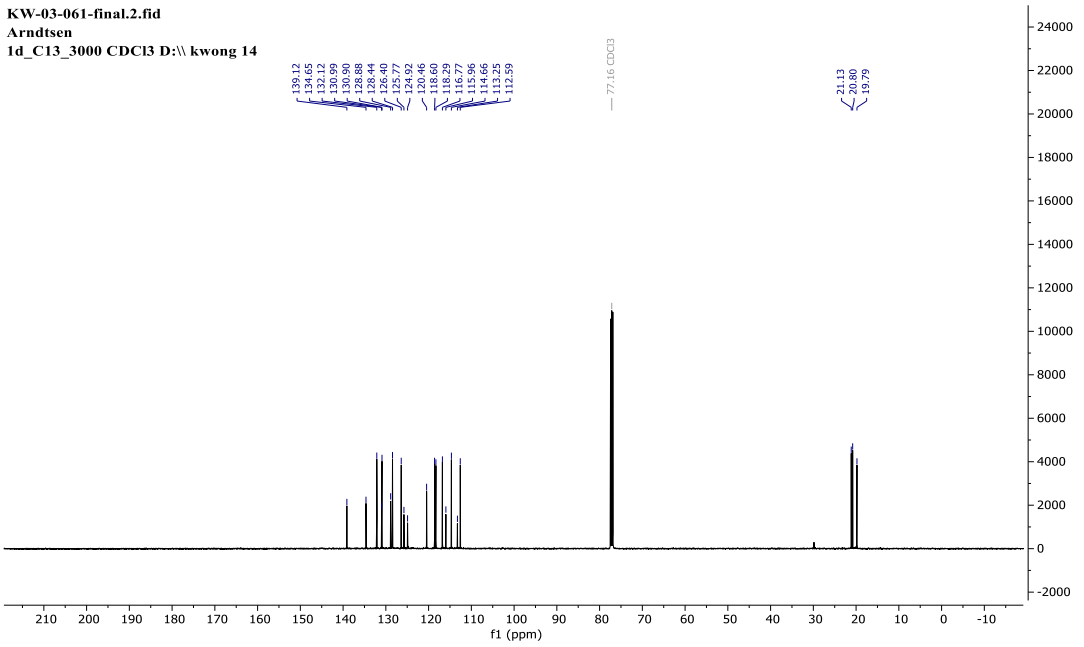

6-(o-tolyl)benzo[f]pyrido[2,1-α]isoindole (**2t**)

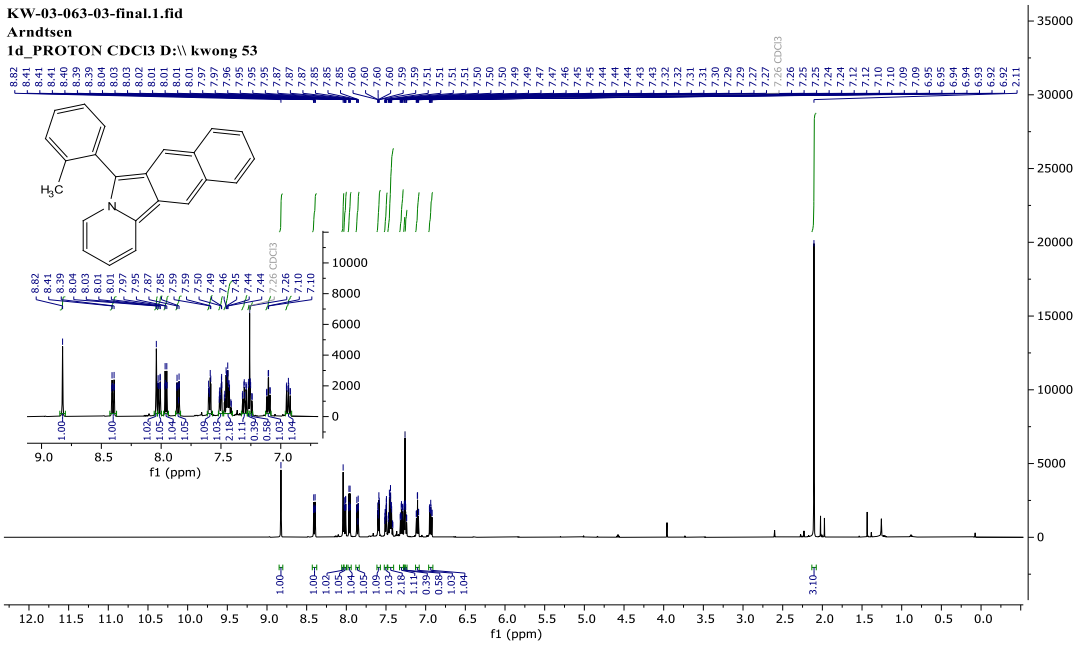

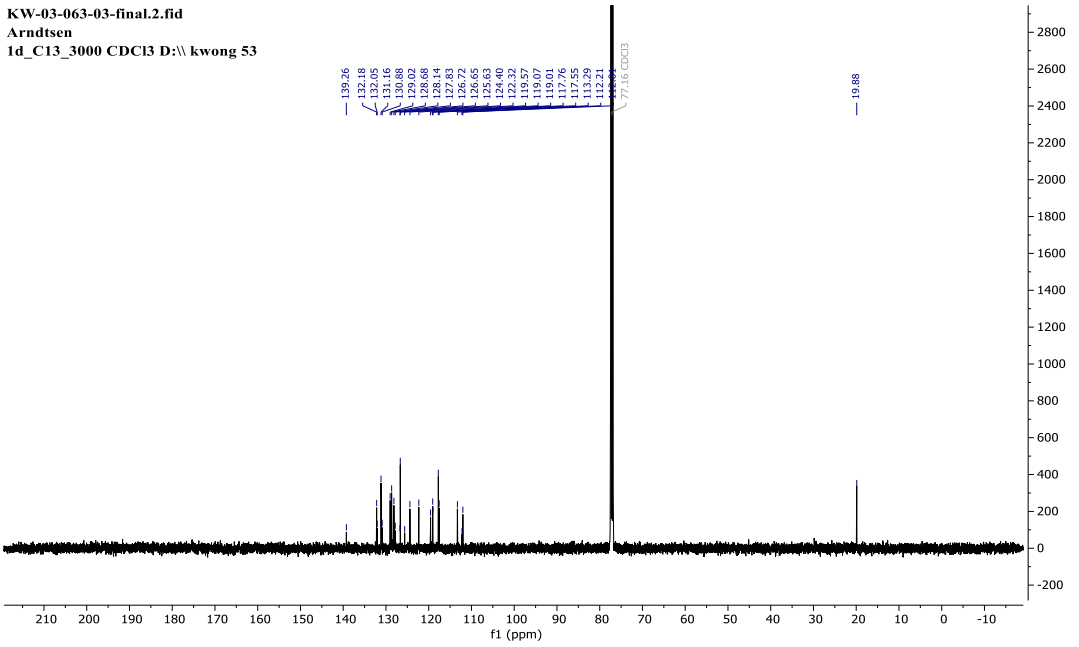

8-methoxy-6-(o-tolyl)-3-(trifluoromethyl)pyrido[2,1-α]isoindole and 9-methoxy-6-(o-tolyl)-3-(trifluoromethyl)pyrido[2,1-α]isoindole (**2u**)

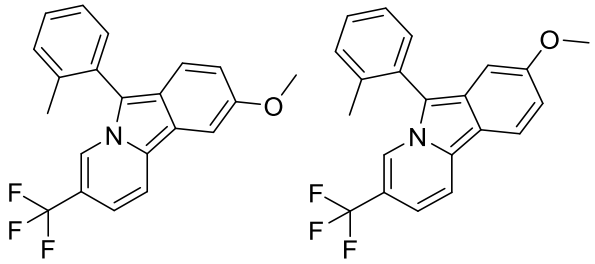

Isomer 1:

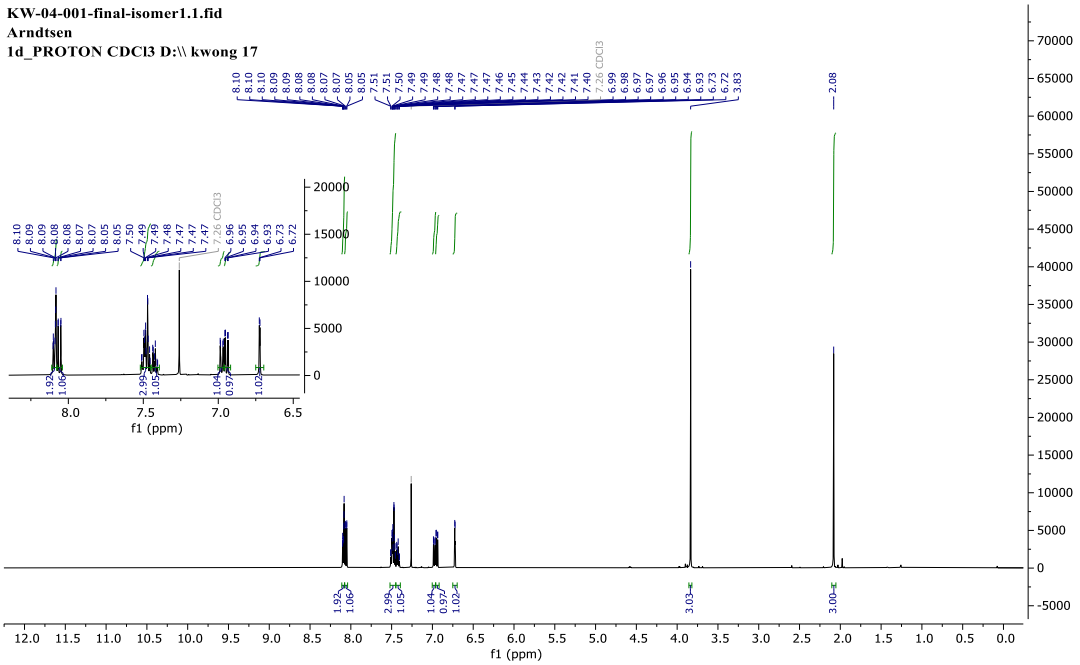

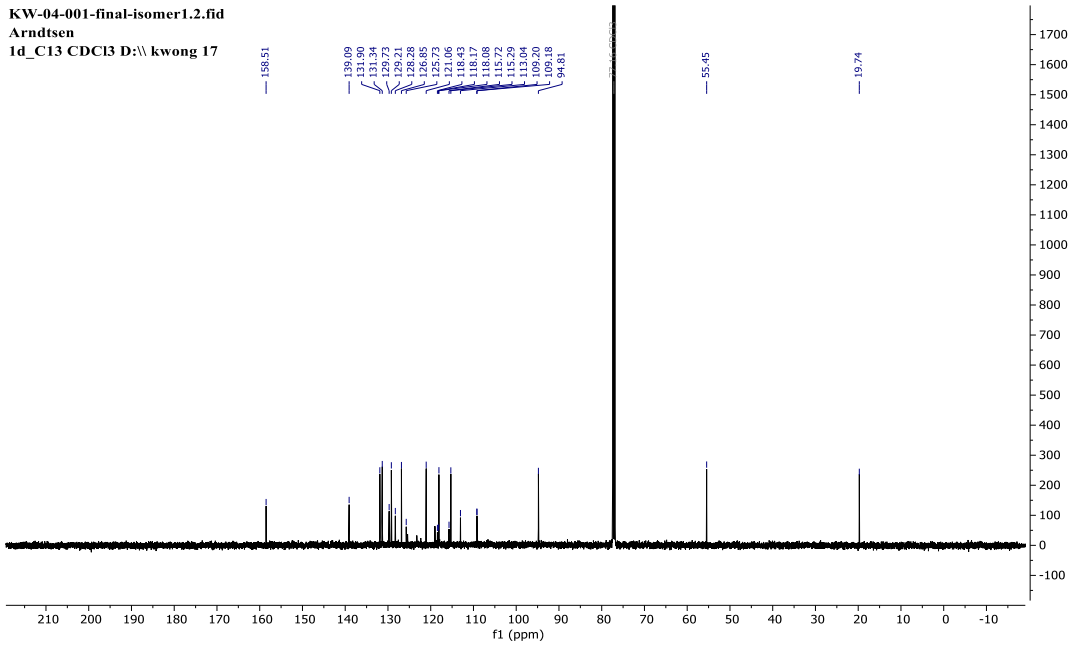
KW-04-001-final-isomer1.2.fid
Arndtsen
1d_C13 CDCl3 D:\\ kwong 17
158.51
139.09
131.90
131.34
129.73
129.21
128.28
126.85
125.73
121.06
118.43
118.17
118.08
115.72
115.29
113.04
109.20
109.18
94.81
77.40 CDCl3
55.45
19.74
f1 (ppm)

Isomer 2:

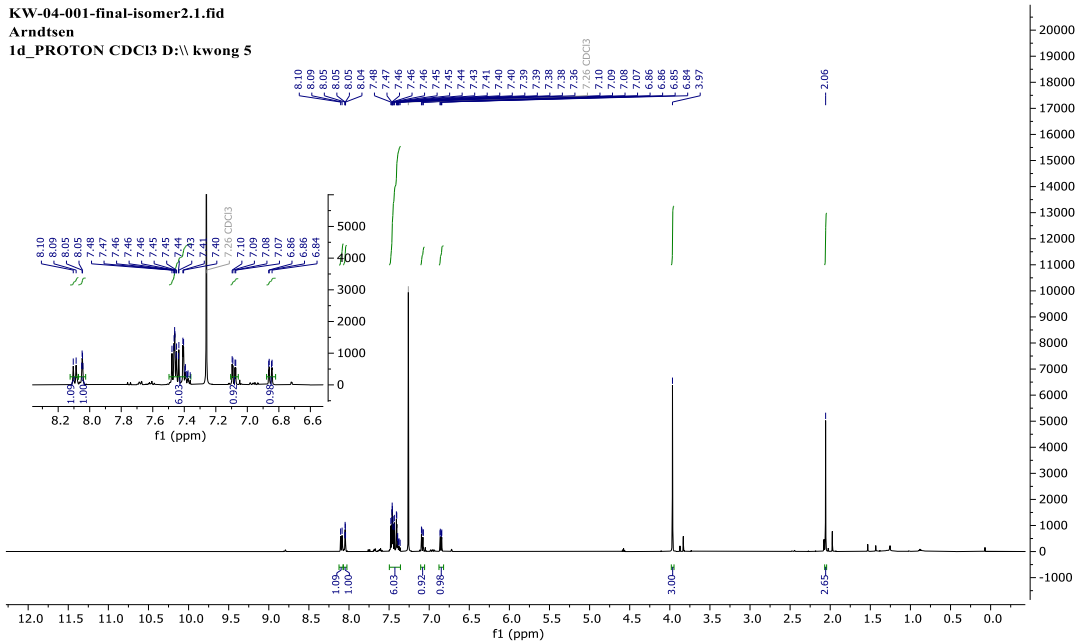
KW-04-001-final-isomer2.1.fid
Arndtsen
1d_PROTON CDCl3 D:\\ kwong 5
8.10
8.09
8.05
8.05
8.04
7.48
7.47
7.46
7.46
7.46
7.45
7.45
7.44
7.43
7.41
7.40
7.40
7.39
7.39
7.38
7.36
7.26 CDCl3
7.10
7.09
7.08
7.07
6.86
6.86
6.85
6.84
3.97
2.06
1.09
1.00
6.03
0.92
0.98
3.00
2.65
f1 (ppm)

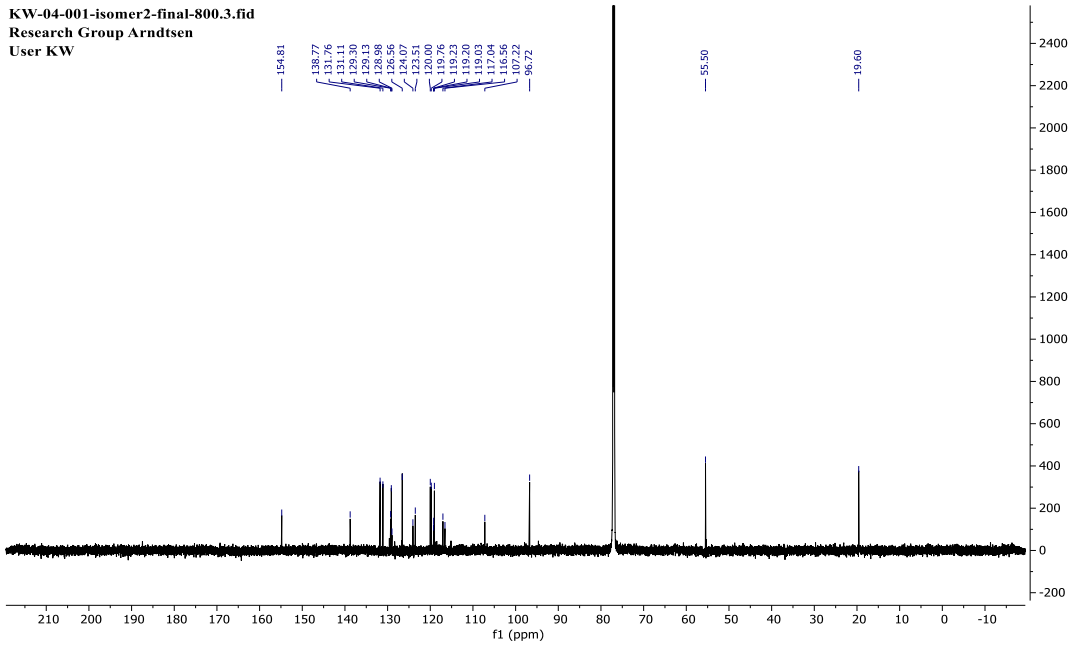
KW-04-001-isomer2-final-800.3.fid
Research Group Arndtsen
User KW
154.81
138.77
131.76
131.11
129.30
128.13
128.98
126.56
124.07
123.51
120.00
119.76
119.23
119.20
117.03
117.04
116.56
107.22
96.72
55.50
19.60
f1 (ppm)